Whole genome approaches to identify genes involved in early meiosis

by

Wayne Matthew Crismani

B. Biotech. (Honours), The University of Adelaide

A thesis submitted for the degree of

Doctor of Philosophy

at

The University of Adelaide

Faculty of Sciences

School of Agriculture, Food and Wine

The Discipline of Plant and Food Science

Waite Campus

November 2008

Table of Contents

List of Figures

List of Tables

Abstract

Meiosis is a process which occurs in sexually reproducing organisms to halve the genetic complement prior to fertilisation. During meiosis a single round of DNA replication is followed by two successive rounds of chromosome segregation and cell division. The meiotic pathway in plants is complex from multiple perspectives. From a mechanical view; prior to the first meiotic division the chromosomes must replicate during meiotic interphase, then while retaining sister chromatid cohesion the homologous chromosomes must align, physically synapse and also concomitantly recombine (with the majority of sites being non-randomly positioned). Further complexities arise in allopolyploids such as bread wheat, which contains three very similar genomes from slightly diverged progenitors. Despite having homoeologous chromosomes present in the same nucleus, bread wheat displays diploid-like behaviour during meiosis I. Such an involved physical process as meiosis also has complexity reflected in the transcriptome and proteome, whether the organism be a simple eukaryote such as yeast, or a more complex eukaryote such as bread wheat.

Initially, this study utilised whole genome approaches to identify novel genes that could be involved in early meiosis, focusing on bread wheat in particular. Analysis of the wheat meiotic transcriptome over seven stages of anther development identified at least 1,350 transcripts which displayed meiotic regulation. The expression profiles of a subset of selected transcripts were analysed with Q-PCR and found to correlate strongly to those obtained in the microarray. Available meiotic transcriptome data from rice was compared to the wheat data, which enabled the identification of similar sequences, many previously unidentified, which also displayed meiotic regulation. Selected candidate genes from the

microarray study were also mapped in bread wheat. This data was combined with available literature and approximately 70% of candidate meiotic loci were located on chromosome group 3 or 5, which historically has been shown to contain multiple loci involved in chromosome pairing control.

One of the candidates located on chromosome group 3, a plant-specific mismatch repair gene, *Triticum aestivum MSH7* (*TaMSH7*), has previously been speculated to suppress homoeologous chromosome associations. Independent transgenic wheat plants produced using RNA interference (RNAi) were functionally characterised to ascertain a greater understanding of the role *TaMSH7* has during early meiosis in bread wheat. Localisation of a synaptonemal complex-associated protein (*Ta*ASY1) displayed subtle abnormalities in these mutants when compared to wild-type. Feulgen staining of meiotic chromosomes at metaphase I in these mutants revealed some interlocking and multivalent associations. These results suggest that *Ta*MSH7 may be linked to the mechanism underlying the phenotype that is observed in the *ph2a/ph2b* mutant, however further research still needs to be conducted to conclusively demonstrate that this is the case.

A component of the research presented in this study was performed in the model plant *Arabidopsis thaliana* due to the limitations of bread wheat. Extensive mutant banks and a sequenced genome have aided a decade of meiotic research in Arabidopsis and the identification of close to 50 meiotic genes. One of these, *AtMER3*, has been shown to control the non-random location of well above half of the recombination events that occur in many species. *At*MER3 was localised in meiotic nuclei in wild-type Arabidopsis and found to form foci on freshly synapsed regions of chromosomes in quantities far in excess of the average number of crossovers, indicating that *At*MER3 does not localise exclusively to sites of crossovers. *At*MER3 localisation was also analysed in several mutant

backgrounds and found to act in an *At*SPO11-dependent manner. However, *At*MER3 loading onto meiotic chromosomes was not affected in *Atrad51*, *Atdmc1* or *Atmsh5* mutant backgrounds.

Declaration

I declare that the work presented in this thesis contains no material which has been accepted for the award of any other degree or diploma in any University or other tertiary institution. To the best of my knowledge and belief, this thesis does not contain any material previously written or published by another person, except where due reference is made in the text.

I give consent to this copy of my thesis when deposited in the University Library, being available for loan and photocopying, subject to the provisions of the copyright Act 1968.

The author acknowledges that copyright of the published works contained within this thesis resides with the copyright holder(s) of those works.

Wayne Crismani

November 2008

Acknowledgements

So many people have contributed to the contents of this thesis and my education in the past. I have done my best to thank you all but I acknowledge that these are just the top few and I wish I had the space to write out all the stories about how you have helped me get to what certainly feels like the pinnacle. Thank you.

First and foremost: Jason Able my principal supervisor. You have pushed me so hard to get the absolute best out of me and I will never be able to put in words how grateful I am for your colossal contribution to my education and the quality of the rest of my life. As I have told you before, you are an excellent supervisor who truly prioritises your students and fights for them. Your students' achievements are a reflection of your virtue. Someone said that "you are a success if you get up, do what you want to do and go to bed". You are extremely successful mate. Last but certainly not least, thank you for your friendship. I look forward to many more years of good times.

Thank you also to my co-supervisors and all of the other people who have guided me or provided a service: Ute Baumann, Tim Sutton, Peter Langridge, Neil Shirley, Amanda Able and her lab members, Andy Milligan, Ursula Langridge, Carolyn Schultz, Andrew Jacobs, Melissa Pickering, the MPBCRC education team past and present but particularly, Heather Bray and Michael McLean. Very special thanks also go to Margaret Pallotta for allowing me to use her fantastic nulli-tetra membranes.

I am eternally grateful to all of the wonderful people in France who made my time there nothing short of surreal. Thank you to Mathilde Grelon and Raphaël Mercier for your supervision, taking a chance on someone you didn't know, teaching me so much about meiosis, good cytology and good science and of course the wonderful friendship you

Glossary of Abbreviations

Abbreviation	Full term
3′	three prime
5′	five prime
9 mer	9 base pair nucleotide
α-dCTP	alpha-deoxycytidine triphosphate
ºC	degrees Celsius
ASY1	*ASYnapsis 1*
At	*Arabidopsis thaliana*
BAC	bacterial artificial chromosome
bar	bialaphos resistance gene
BLAST	Basic Local Alignment and Search Tool
bp	base pair
BSA	Bovine Serum Albumin
BW26	Bob White 26 cultivar of bread wheat
CDK	*Cyclin Dependent Kinase*
cDNA	complimentary deoxyribonucleic acid
cv.	cultivar
CO	crossover
DABCO	diazabicyclo-[2,2,2] octane
DAPI	4',6-diamidino-2-phenylindole
DMC1	*Disrupted Meiotic cDNA 1*
dHJ	double Holliday Junction

DNA	deoxyribonucleic acid
DPSS	diode-pumped solid state (laser)
dNTP	deoxynucleotide triphosphate
DSBR	double-strand break repair
DTT	dithiothreitol
E	Expect value
EDTA	ethylene diamine tetra-acetic acid
EFA	*Elongation Factor 1 Alpha*
eFP	electronic fluorescent pictograph
EGTA	ethylene glycol tetra-acetic acid
EST	expressed sequence tag
g	gram
GAPDH	*GlycerAldehyde-3-Phosphate DeHydrogenase*
gDNA	genomic deoxyribonucleic acid
HOP1	*HOmologous Pairing 1*
Hv	*Hordeum vulgare*
kb	kilobase
LASER	Light Amplification by Stimulated Emission of Radiation
M	molar
mCi/mL	milli Curie per millilitre
mg	milligram
mM	millimolar
MER3	*MEiotic Recombination 3*
MLH1/3	*Mut L Homologue 1/3*

XX

MMR	mismatch repair
mRNA	messenger ribonucleic acid
MPBCRC	Molecular Plant Breeding Co-operative Research Centre
MRE11	*Meiotic REcombination 11*
MSH2/3/4/5/6/7	*Mut S Homologue 2/3/4/5/6/7*
NCBI	National Center of Biotechnology Information
NCO	non-crossover
ng	nanogram
nm	nanometre
NT	nullisomic-tetrasomic
P	probability
PBS	phosphate buffered saline
PCR	polymerase chain reaction
Ph	*Pairing homoeologous*
PHS1	*Poor Homologous Synapsis 1*
PMC	pollen mother cell
PRD1	*Putative Recombination initiation Defect 1*
PVP	polyvinyl pyrrolidone
Q-PCR	quantitative real-time PCR
RAD51	*RADiation sensitive 51*
RMA	robust multichip analysis
RNA	ribonucleic acid
RNAi	RNA interference
rRNA	ribosomal ribonucleic acid

SC	synaptonemal complex
SDS	sodium dodecyl sulphate
SNP	single nucleotide polymorphism
SSC	standard saline citrate
ssDNA	single-stranded deoxyribonucleic acid
SPO11	*SPOrulation-deficient 11*
Ta	*Triticum aestivum*
Taq	*Thermus aquaticus*
T-DNA	transfer DNA
TILLING	targeted induced local lesions in genomes
U	units
μL	microlitre
μg	microgram
μm	micrometre
μM	micromolar
v/v	volume per volume
w/v	weight per volume

Chapter 1 – Literature review

1.1 – Meiosis

Meiosis from a Greek root meaning "to diminish" is an essential process in the majority of sexually reproducing organisms, resulting in the production of gametes containing half the normal cellular chromosome complement. Meiosis also enables the generation of diversity, assists the maintenance of genome integrity through generations, and defines the 'species barrier'. Meiosis consists of a round of DNA replication followed by two successive rounds of cell division. The first division is considered a reductional segregation pattern because a replicated pair of maternal and paternal chromosomes containing a pair of sister chromatids move to opposite poles after a re-shuffling of genetic material. Sisters are held together by cohesion, analogous to that which occurs during S-phase in mitosis. Shortly after the first division has commenced at anaphase I, cohesion is lost between the sister arms but cohesion of centromeric regions remains (Figure 1.1H). At the second division the connected sisters of a single chromosome now lose the centromeric attachment and segregate equationally to opposite poles (Figure 1.1M).

1.1.1 – Prophase I and meiotic recombination

Many of the most interesting events of meiosis occur during early prophase I. These events are all linked and to a great extent occur at the same time or at least have considerable overlap. This can complicate studying these events as it is very difficult to disrupt one component of prophase I progression without drastically affecting the others. Prophase I

can be roughly divided into five sub-stages: leptotene, zygotene, pachytene, diplotene and diakinesis.

During prophase I the chromatin condenses at leptotene (Greek "leptos" = thin) and homologous chromosomes undergo a rough alignment (Figure 1.1A). Both of these events commence prior to leptotene during pre-meiosis. In budding yeast (*Saccharomyces cerevisiae*) double-strand break (DSB) formation occurs at leptotene in addition to axial element formation. At zygotene (Greek "zygos" = pair), synapsis initiates and chromosomes condense further while the homologous chromosomes reduce the distance that separates them (Figure 1.1B). A meiotic feature known as the telomere bouquet forms after DSB formation in *S. cerevisiae* (Joseph & Lustig, 2007). The telomere bouquet is believed to provide a site at which homologous chromosomes may pair correctly in addition to lending itself to synapsis initiating from sub-telomeric sites (Zickler & Kleckner, 1998). Furthermore it is the one site where all of the equivalent regions of chromosomes have the same conformation in addition to being specifically and intimately located near the cytosol and may potentially receive any necessary signal (an extensive discussion of the telomere bouquet can be found in Zickler & Kleckner (1998)).

By pachytene (Greek "pakhus" = thick) synapsis has occurred (Figure 1.1C). Synapsis is an intimate association between homologous chromosomes which is achieved using a transient proteinaceous structure called the synaptonemal complex (SC). The axial elements of the SC which appeared in leptotene have become lateral elements and are joined by transverse filaments and a central region which polymerised along the length of the homologous chromosome pairs. The exact purpose of the SC is not known because while it often promotes the successful completion of the first meiotic division, it can also be uncoupled from various aspects of recombination (Chelysheva *et al.*, 2007; Higgins *et al.*,

2005; Jantsch *et al.*, 2004). However some species have undergone an evolutionary change which uses an alternative strategy/(ies) to promote the correct segregation of chromosomes. Fission yeast (*Schizosaccharomyces pombe*), the fungus, *Aspergillus nidulans*, and fruit fly (*Drosophila melanogaster*) males undergo meiosis, yet have no synaptonemal complex (Egel-mitani *et al.*, 1982; Meyer, 1960; Olson *et al.*, 1978; Rasmussen, 1973).

At diplotene (Greek "diploos" = double) the SC disassembles and bivalents can be observed which are held together at chiasmata (Greek "chiasma", plural "chiasmata" = beams arranged in a cross in the framework of a roof) (Figure 1.1D). The chromosomes still continue to condense in diakinesis (Greek "kinesis" = movement) (Figure 1.1E, F) as the bivalents continue a dynamic motion which results in their alignment on the metaphase plate during metaphase I (Figure 1.1G) still held together by chiasmata.
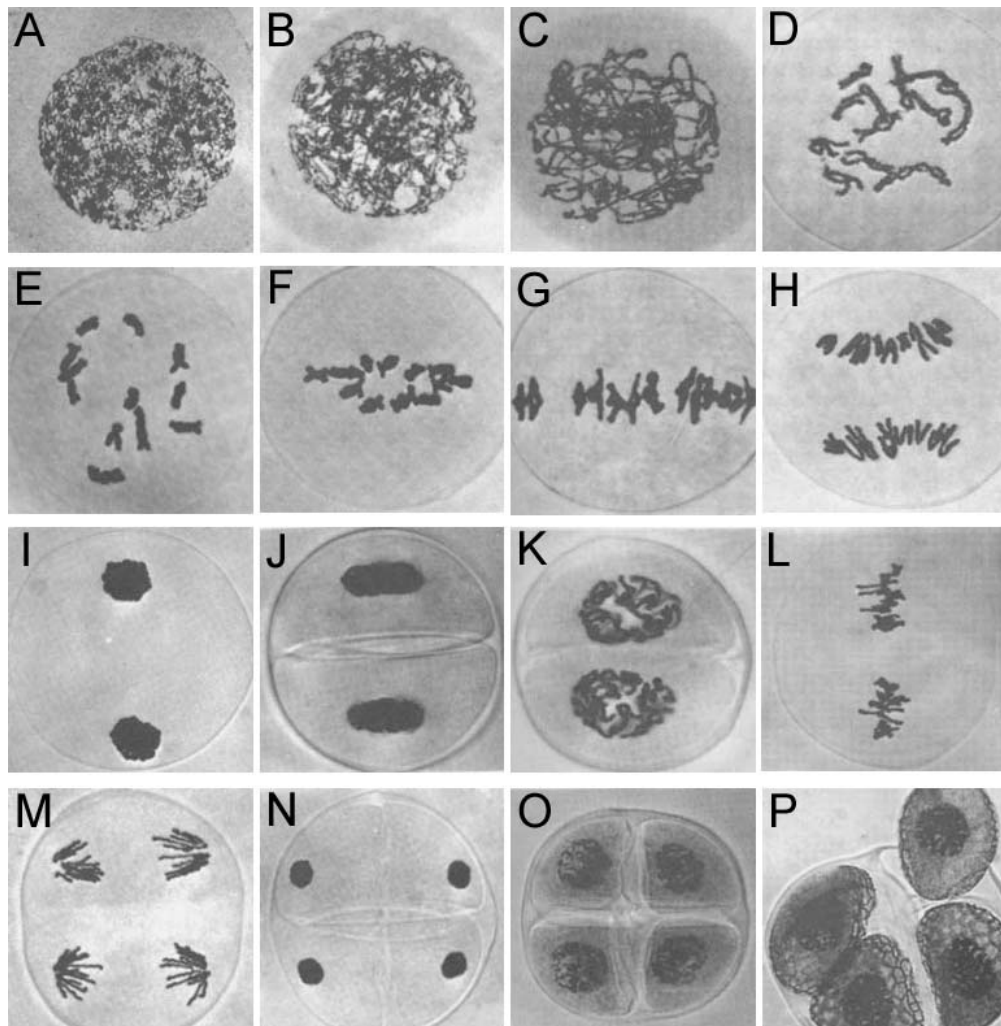
Figure 1.1 – The first and second meiotic divisions in regal lily (*Lilium regale*). Chromosomes condense at leptotene (A). Homologue alignment at zygotene (B). Synapsis is complete at pachytene (C). Disassembly of SC at diplotene and chiasmata bind homologous chromosomes (D). Bivalents aligned at metaphase I as predominantly ring bivalents (G). Anaphase I, telophase I, interphase II, prophase II, metaphase II, anaphase II, telophase II, tetrads and immature pollen (H, I, J, K, L, M, N, O and P respectively). This figure has been adapted from; McLeish and Snoad, Looking at chromosomes, 1958, Macmillan and company limited, reproduced with permission of Palgrave Macmillan. This material may not be copied or reproduced without permission from Palgrave Macmillan.

1.1.2 – Homologous recombination *via* the double strand break repair pathway

Most recombination events which occur during meiosis in wild-type species occur through the action of what is known as the double-stand break repair (DSBR) pathway. Much of the early and current research on the DSBR pathway was performed in *S. cerevisiae* which led to the first model of this process (Szostak *et al.*, 1983). This model has not only been updated as further discoveries have been made but has also been "overlaid" onto other organisms as a framework to begin research with putative homologues in the species of interest. The DSBR pathway in plants is best characterised in *Arabidopsis thaliana.*

In yeast, SPO11 (SPOrulation-deficient 11) requires nine other proteins to produce double-strand breaks (DSBs) (Keeney, 2001). However until recently, the only protein directly implicated in DSB formation in Arabidopsis was SPO11-1 (Grelon *et al.*, 2001), until Stacey and colleagues (2006) identified a similar phenotype to that of *Atspo11-1* mutant plants in *Atspo11-2* mutants; that is, a severe reduction in synapsis and recombination. *Putative Recombination initiation Defect 1* (*PRD1*) has also recently been shown to be essential for DSB formation in Arabidopsis by De Muyt *et al.* (2007), who also demonstrated that *At*SPO11-1 and *At*PRD1 form a heterodimer using a yeast 2-hybrid assay. Other direct interactions have not yet been shown between these three proteins.

The double-strand breaks produced by SPO11 in yeast are resected by a multi function heterotrimeric complex containing MRE11, RAD50 and XRS2/NBS1 (MRX) to leave 3′ single-stranded DNA (ssDNA) overhangs. MRE11 and RAD50 have also been shown to be required for the processing of DSBs in Arabidopsis (Bleuyard *et al.*, 2004; Puizina *et al.*, 2004). The 3′ ssDNA overhangs form a substrate to which additional proteins

bind creating a nucleoprotein filament that facilitates meiotic recombination. Two of the best characterised proteins that play roles in recombination downstream of the MRX complex at the stage of nucleoprotein function are the RecA homologues, RAD51 and DMC1. During meiosis in Arabidopsis, *At*RAD51 is required for repair of double-strand breaks, as the loss of RAD51 function leads to SPO11-dependent chromosome fragmentation (Li *et al.*, 2004). *Atdmc1* mutants on the other hand do not display fragmentation, rather univalents. This suggests that loss of DMC1 allows sister chromatid selection as a template for repair (Couteau *et al.*, 1999; Siaud *et al.*, 2004). However over-expression of yeast *RAD51* in *dmc1* mutants restores inter-homologue recombination, suggesting that DMC1 is not exclusively required for selecting homologous chromsomes as repair templates during yeast meiosis (Bishop *et al.*, 1999; Tsubouchi & Roeder, 2003).

Once the nucleoprotein filament has invaded a homologous chromosome, branch migration can occur. Conversion of recombination intermediates to either non-crossovers or crossovers is a tightly controlled process. Classical models of the DSBR pathway in *S. cerevisiae* have been refined to show that non-crossover (NCO, also known as gene conversion) intermediates are unstable and quickly rejected, whereas the intermediates destined to form crossovers (COs) are designated as such prior to heteroduplex molecule formation in what is termed the early crossover decision model (Allers & Lichten, 2001; Bishop & Zickler, 2004).

1.1.3 – Crossover interference

In *S. cerevisiae* there are two classes of crossovers that occur *via* distinct mechanisms. Class I COs occur in a distance-dependent manner to other COs on the same pair of homologous chromosomes, and this phenomenon is known as crossover interference (Lynn

et al., 2007). Class II COs are those which do not occur in a distance-dependent manner to other COs on the same chromosome and are therefore more likely to occur at an interval adjacent to another CO compared to class I COs (Lynn *et al.*, 2007). Interestingly, organisms also exist with only one class of CO at meiosis. Only class I COs occur in *Caenorhabditis elegans* and only class II COs occur in *S. pombe* (Hollingsworth & Brill, 2004). Both class I and II COs occur in Arabidopsis as shown in studies using both genetic and cytological data (Chelysheva *et al.*, 2007; Copenhaver *et al.*, 2002; Drouaud *et al.*, 2006; Higgins *et al.*, 2004; Higgins *et al.*, 2008; Macaisne *et al.*, 2008; Mercier *et al.*, 2005). In *S. cerevisiae* all members of the ZMM epistasis group (ZIP1, ZIP2, ZIP3, ZIP4, MER3, MSH4 and MSH5) are essential for the formation of class I COs (Borner *et al.*, 2004). Analysis of the ZMM homologues in Arabidopsis T-DNA mutants has produced similar results, with *Atmer3*, *Atzip4*, *Atmsh4* and *Atmsh5* mutants all showing an absence of interfering crossovers (Chelysheva *et al.*, 2007; Higgins *et al.*, 2004; Higgins *et al.*, 2008; Mercier *et al.*, 2005). However, an RNAi-induced *Atzyp1* mutant maintained near wild-type levels of crossovers and a distribution suggestive that crossover interference was still present, albeit between both homologous and non-homologous chromosome pairs (Higgins *et al.*, 2005). Interestingly a recent study has identified a novel member of the ZMM epistatic group: SHOrtage in Chiasmata (SHOC1) which is annotated as being related to the XPF endonuclease family and is therefore speculated to directly lead to the resolution of recombination intermediates (Macaisne *et al.*, 2008). The SHOC1 protein is well conserved in plants and also extends to humans and mice. Interestingly, no SHOC1 homologue was detected in *C. elegans* in which only class I COs occur.

Further intriguing CO data in Arabidopsis has been generated showing that double *Atmsh4mus81* mutants, which have no class I COs or class II COs, resulted in only an 80%

reduction in genetic distance of an interval on chromosome 3 when compared to the same genomic region in wild-type. The genetic distance in the double mutant was smaller than both of the single mutants, although crossovers still remained, therefore suggesting that in addition to class I and class II COs, at least one more CO pathway exists in Arabidopsis (Berchowitz *et al.*, 2007).

1.1.4 – Mismatch repair

Another genetic process which is well conserved throughout most organisms is the mismatch repair (MMR) system which has both meiotic and somatic functions. This is especially important in plants for maintaining genomic integrity as a reserved germline is absent. In prokaryotes, MutS and MutL form homodimers which undertake MMR (Ban & Yang, 1998; Lamers *et al.*, 2000; Obmolova *et al.*, 2000). Eukaryotes have functional MutS and MutL Homologues, MSH and MLH respectively (Culligan *et al.*, 2000). However most eukaryotes have six MSH proteins encoded within their genomes. In plants, there is an additional MSH protein which is an MSH6 paralogue referred to as MSH7 (sometimes termed MSH6-2) (Ade *et al.*, 1999; Culligan & Hays, 2000).

Studies in Arabidopsis have shown that MSH2 forms three distinct heterodimers: MSH2/MSH3, MSH2/MSH6 and MSH2/MSH7, all of which have varying affinities for different types of mismatches (Culligan & Hays, 2000; Wu *et al.*, 2003). *At*MSH2 is therefore a central component of the mismatch repair system. This biochemical data is consistent with genetic data in Arabidopsis and the moss *Physcomitrella patens*. *AtMSH2* and *PpMSH2* have been shown to maintain genomic integrity by suppressing recombination between diverged/homoeologous sequences (Emmanuel et al, 2006; Li et al, 2006; Trouiller et al, 2006). A recent study in barley (*Hordeum vulgare*) has also shown

that MSH7 plays a role in fertility (Lloyd *et al.*, 2007), and in bread wheat (*Triticum aestivum*) it has been reported that *TaMSH7* maps to a locus (*Pairing homoeologous 2 – Ph2*) which is responsible for the suppression of homoeologous recombination (Dong *et al.*, 2002) (also see section 1.2.3.1).

1.2 – Tools for meiotic research

1.2.1 – Model organisms

It is not always possible to study the biological process of interest in the relevant species. Humans (*Homo sapiens*) are a good example of this and consequently mice (*Mus musculus*) or rats (*Rattus rattus*) are used due to shorter life cycles, a smaller size, and also the ethical issues involved, while still being relatively similar in the context of evolution. In studying meiosis, plants are favoured by many research groups due to their often large chromosomes, lack of meiotic arrest in prophase I mutants and ease of access to material (which can also be synchronous with respect to the meiotic stage).

1.2.2 – *Arabidopsis thaliana*

In the plant kingdom, the favoured model organism is Arabidopsis because of its short life cycle, small size and small genome (Arabidopsis Genome Initiative, 2000; Boyes *et al.*, 2001). These reasons contributed to Arabidopsis being the first plant to have its genome sequenced. This genomic sequence resource in addition to the extensive T-DNA mutant collections with flanking sequence tags (Alonso *et al.*, 2003; Samson *et al.*, 2002; Sessions *et al.*, 2002) has already enabled extensive research in Arabidopsis to be completed.

Despite the small size of Arabidopsis chromosomes, researchers have developed techniques to visualise and track the proteins and genetic material that play roles during

meiosis (Armstrong *et al.*, 2002; Ross *et al.*, 1996) in addition to considering various approaches to study genes with meiotic functions (Mercier *et al.*, 2001). Ten years of research in Arabidopsis has seen the identification of approximately 50 genes with roles in meiosis which is comprised of a mixture of novel genes and those with homologues in other taxonomic kingdoms (Mercier & Grelon, 2008).

1.2.3 – Chromosome dynamics in allopolyploid plant species

It is estimated that approximately 70% of plant species have experienced at least one polyploidisation event during their evolution (Masterson, 1994). Although polyploids contain more than two sets of genomes per cell, such species frequently behave as cytological diploids during meiosis with only homologous chromosomes pairing with one another. This suggests that there are mechanisms in place that control chromosome pairing in these species. The meiotic behaviour from a number of allopolyploid plant species have been studied, including bread wheat (Boden *et al.*, 2008; Colas *et al.*, 2008; Griffiths *et al.*, 2006; Martinez-Perez *et al.*, 2001; Martinez *et al.*, 2001; Riley & Chapman, 1958; Sears & Okamoto, 1958; Sears, 1982), oilseed rape (*Brassica napus*) (Attia & Robbelen, 1986; Jenczewski *et al.*, 2003; Leflon *et al.*, 2006; Liu *et al.*, 2006; Nicolas *et al.*, 2008; Udall *et al.*, 2005), oats (*Avena sativa*) (Gauthier & McGinnis, 1968; Rajhathy & Thomas, 1972), cotton (*Gossypium hirsutum*) (Brown, 1954; Ji *et al.*, 2007; Reyesvaldes & Stelly, 1995; Vafaie-Tabar & Chandrashekaran, 2007) and tobacco (*Nicotiana tabacum*) (Trojak-Goluch & Berbeć, 2003; Trojak-Goluch & Berbeć, 2007). Given the focus of this dissertation, bread wheat is discussed further here.

1.2.3.1 − Allohexaploid bread wheat

Bread wheat is an allohexaploid with three genomes (AABBDD; 2n = 6x = 42) derived from related progenitors. The A, B and D genomes exhibit a syntenic relationship with respect to the gene order and content and are believed to originate from *Triticum uratu*, *Aegilops speltoides* and *Triticum tauschii* respectively (Dvorak, 1988). The progenitor of the B genome is extinct and *A. speltoides* (SS; 2n = 14) is the closest living relative (Feldman & Levy, 2005). The cytological diploidisation of bread wheat is known to be controlled by multiple loci. The locus with the strongest effect is referred to as *Pairing homoeologous 1* (*Ph1*), which is located on the long arm of chromosome 5B (Riley *et al.*, 1960; Riley & Chapman, 1958; Sears & Okamoto, 1958). Another locus, *Ph2*, is located on the short arm of chromosome 3D (3DS) and has a weaker effect on controlling homoeologous chromosome pairing than *Ph1* (Sears, 1982). Even so, an effect similar to the loss of *Ph1* can be created by removing the *Ph2* locus and the short arm of chromosome 3A (3AS) (Driscoll, 1972; Mello-Sampayo, 1971; Mello-Sampayo & Canas, 1973). These earlier studies used mutant plants missing entire chromosomes or chromosome arms. Mutations of the *Ph* loci that are used to study chromosome pairing in wheat were acquired with X-ray induced deletions (some upwards of 70 Mbp in size; *ph1b*, *ph1c*, *ph2a*) (Giorgi, 1978; Sears, 1977; Sears, 1982)) or EMS-induced mutagenesis (*ph2b*) (Wall *et al.*, 1971b)), which often results in point mutations. Interestingly and perhaps highlighting the complexity of the interactions involved, the *ph1* mutant phenotype has never been successfully re-created with EMS mutagenesis.

During early synapsis hexaploid and tetraploid wheat (*T. turgidum*) have multiple interactions between chromosomes but these are corrected as synapsis progresses (Holm,

1986; Martinez *et al.*, 2001). In fact when wheat chromosomes synapse during meiosis, half do so as bivalents and the other half as multivalents (Holm, 1986; Holm, 1988). An inability to correct these multiple associations leads to karyotypic instability in *ph1b*, and to a far lesser extent in *ph2b*, nulli-3D lines and the *ph1c* mutant from allotetraploid wheat (Sanchez-Moran *et al.*, 2001).

Fifty years of research on the *Ph1* locus has led to a basic understanding of one mechanism which creates a cytogenetic diploid of bread wheat. It was shown using wheat-rye hybrids (a nuclear environment with only homoeologues and no homologues) that in both the presence and absence of *Ph1*, pairing and synapsis could occur (Gillies, 1987). Additional information about the mechanical function of *Ph1* has also been obtained by numerous studies of telomeres and centromeres. In wild-type bread wheat the telomeres and centromeres are arranged in a Rabl configuration beginning during pre-meiosis (Abranches *et al.*, 1998) with the centromeres and telomeres polarised to opposing regions of the inner nuclear membrane. The telomere behaviour that was observed in this study is consistent with other species (an exception being Arabidopsis which has telomeres that associate with the nucleolus and no true telomere bouquet (Armstrong *et al.*, 2001)). Bread wheat centromeres associate prior to the onset of meiosis in a haploid number (21). Upon telomere clustering, sister chromatids join through cohesion which is followed by the sub-telomeric regions of homologous chromosomes, which are in rough alignment, becoming progressively synapsed as chromatid cohesion is achieved.

The *Ph1* locus was reduced from 70 Mbp to approximately 2.5 Mbp almost 50 years after the discovery of the promoter of homologous pairing that lied on 5BL (Griffiths *et al.*, 2006). The putative sequence annotations within this region suggested that the genetic material was a tandem repeat of four *CDC2-like* genes with a sub-telomeric insertion of

heterochromatin from chromosome 3A. However, additional sequencing since has revised this to seven *CDK-like* genes with the sub-telomeric insertion between the sixth and seventh *CDK-like* genes (Al-Kaff *et al.*, 2007). Through expression analysis of the *CDK-like* genes it became apparent that they were altered in the absence of *Ph1*, suggesting that these genes co-ordinate chromatin remodelling of homologues to ensure that they are in the same conformation at the onset of pairing (Al-Kaff *et al.*, 2007).

Subsequently, *Asynapsis1 1* (ASY1) localisation was shown to be perturbed in *ph1b* mutants (Boden *et al.*, 2008). This is interesting given that ASY1 localisation often progresses normally in Arabidopsis meiotic mutants. However, *Ph1* plays a major role pre-meiotically and therefore perhaps this is not unexpected as it is presumably upstream of the DSBR pathway, the stage where many Arabidopsis meiotic mutants are studied. It was also found that expression of *TaASY1* is dramatically up-regulated in the *ph1b* background over a meiotic time course but still shows the same pattern of expression. So it is only the amplitude of the transcript level that is affected which implicates *Ph1* in the rate of lateral element formation, which is a theory consistent with all of the *Ph1*-related research discussed above.

Less research has focussed on the *Ph2* locus, presumably due to its less dramatic role in chromosome pairing when compared to *Ph1*. However research has identified differences between the underlying mechanisms of the two loci. A *ph1/ph2* double mutant showed even higher levels of abnormalities at metaphase I highlighting that *Ph2* is responsible for correcting errors that are independent of the function of *Ph1* (Ceoloni & Donini, 1993). More recently it was shown that the behaviour of sub-telomeric regions in the absence of *Ph1* or *Ph2* in wheat-rye hybrids is different (Prieto *et al.*, 2005). A signal which polymerises away from the telomeres in the *ph1b* mutant background that "pushes"

chromosomes together does not occur in the *ph2b* background, similar to the behaviour that is seen in the presence of both *Ph1* and *Ph2*. Even though this signal does not polymerise in the *ph2* background, there is a significant increase in homoeologous associations at metaphase I in the *ph2* mutants compared to wild-type. As different synaptic behaviours are seen when the *Ph1* and *Ph2* loci are absent/disrupted (respectively), this suggests that while *Ph1* leads to a diploid-like behaviour in meiocytes, *Ph2* has a role later in synapsis rather than homologue recognition (Martinez *et al.*, 2001; Prieto *et al.*, 2005). It would be at this point where *Ph2* resolves the relatively minimal number of incorrect associations that arise in the presence of *Ph1*.

1.2.4 – Comparative genetics

Sequencing of a complete genome, irrespective of how small the genome is, requires significant time and resources. Fortunately many genomes have already been sequenced and assembled and can therefore provide a framework on which to base the structure of other genomes (Gale & Devos, 1998). This is typically referred to as comparative genetics and a common example is the relationship that exists between the genomes of bread wheat and rice (*Oryza sativa*) (Sorrells *et al.*, 2003). Rice has a smaller genome (420-466 Mbp (Goff *et al.*, 2002; Yu *et al.*, 2002)) than bread wheat (17-billion-base-pairs (Paux *et al.*, 2008)) and was one of the earlier plant species to be completely sequenced (Goff *et al.*, 2002; Yu *et al.*, 2002).

Due to the complexity of the bread wheat genome, sequencing and assembly of this is still in its infancy (Moolhuijzen *et al.*, 2007). Nonetheless, several studies have used the sequenced genome of rice in order to compare it to comparative regions of the wheat genome (Griffiths *et al.*, 2006; Huang *et al.*, 2008; Jardim, 2007; Paux *et al.*, 2006; Quarrie

et al., 2005; Sutton *et al.*, 2003). One of the most appropriate studies to discuss here is the comparative genetics research that has been conducted with the *Ph1* locus. The similarity between bread wheat, rice and *Brachypodium sylvaticum* (approximately 160 Mbp genome size) genomes were used to create the framework for the bacterial artificial chromosomes (BACs) that contained sequence from the *Ph1* locus and also the homoeologous regions on the long arms of chromosomes 5A and 5D (Griffiths *et al.*, 2006). This enabled the original fast-neutron irradiation-induced 70 Mbp deletion to be refined to a 2.5 Mbp region, and the identification of genes believed to be responsible for the action of *Ph1*.

A similar approach was also used between wheat and rice to gain a greater understanding of the gene content of the *Ph2* locus (Sutton *et al.*, 2003). That research identified 280 ESTs which resided within the 6.58 Mbp region of rice chromosome 1 syntenic to the *Ph2* locus. Subsequent mapping of a subset of these revealed that 78% mapped to *Ph2* and provided additional information about putative genes which may encode the action of *Ph2*. These two studies highlighted above demonstrate the utility of comparative genetics as a tool for when there is limited sequence information available in the species of interest. However as the diversity of technologies used for meiotic research increase, there will also be comparisons made between biological processes such as the transcriptomes of organisms and the biochemical pathways that they control.

1.2.5 – Microarrays

Typically, functional genomics research in the past has been limited to experiments with individual genes. However the current point in time is being referred to by many as the post-genomic era, due to having obtained the complete genome sequences of a number of organisms including but not limited to; human, rice, *S. cerevisiae*, *C. elegans* and

Arabidopsis (Arabidopsis Genome Initiative, 2000; Goff *et al.*, 2002; Lander *et al.*, 2001; Levy, 1994; The *C. elegans* Sequencing Consortium, 1998; Yu *et al.*, 2002). In having all of this data available, systems now need to be established to use this information meaningfully and efficiently. While the data is of significance, the value must still be uncovered as it is buried in genetic code (Eisen *et al.*, 1998).

One approach used to extract meaningful outcomes from such vast amounts of data involves the constantly evolving microarray technology which was initially designed as a high throughput platform to quantify gene expression (Schena *et al.*, 1995). Since this time microarray-based research has grown exponentially, with respect to popularity and scientific application (Schena, 2003). Applications of microarray experiments can include analysing differences between expression profiles from various tissue types, the developmental stages of a tissue type (Schmid *et al.*, 2005), diseased compared to non-diseased tissue (for example, the expression profile of healthy tissue specimens compared to an expression profile of the same tissue that has been infected with a disease (Kononen *et al.*, 1998; van't Veer *et al.*, 2002; van de Vijver *et al.*, 2002)), and/or genotyping (which is becoming increasingly popular) (Pastinen *et al.*, 1997; Pastinen *et al.*, 2000; Redon *et al.*, 2006).

Interpretation of the microarray data requires implementing many types of statistical analyses upon completion of the 'laboratory' component of the experiment. The data quality is interrogated in addition to being normalised. Normalising microarray data adjusts the data for any effects arising from variation in the technology, as opposed to biological variation (Smyth & Speed, 2003). The statistical methods used for microarray analysis have been the subject of great discussion as it is not uncommon for microarray experiments to face issues of undesirable levels of specificity, sensitivity and reproducibility (Rockett &

Hellmann, 2004). These problems arise through the use of many discrete technical variables being used in a long experimental process. This can then affect the biological variability which is being studied (Rockett & Hellmann, 2004).

Validating the expression of selected probe sets and their respective genes from large microarray datasets is a desirable component of microarray experiments. Confirmation experiments are typically an independent measure of gene expression patterns/levels, using the same RNA from the microarray experiment, for a selected group of transcripts that are represented on the microarray chips (Chuaqui *et al.*, 2002). A validation technique commonly employed is Q-PCR in parallel with analysis of the literature. Recently there have been a number of publications addressing the topic of microarray data validation, with particular emphasis on investigating the choice of genes used for normalising Q-PCR data (Canales *et al.*, 2006; Chuaqui *et al.*, 2002; Shippy *et al.*, 2004; Tan *et al.*, 2003). One study found a strong correlation between the majority of their two data sets, however 13 to 16% of the data generated did not correlate well (Dallas *et al.*, 2005). This therefore leaves room for refining some of the experimental variables. Another study also produced microarray and Q-PCR results with correlation coefficients ranging from -0.48 to 0.93 (0 being no correlation, and +1 being a perfect correlation) (Etienne *et al.*, 2004). Not only can microarrays provide experimental evidence for genes, but they have also been shown to assist in the optimisation of other techniques, simply through the vast amount of data they generate. Using the Affymetrix ATH-1 whole genome GeneChip with diverse stages of developmental and environmental conditions, "superior" genes for normalising Arabidopsis Q-PCR data were identified when compared to traditional reference/housekeeping genes such as 18S rRNA, *GAPDH* and *β-tubulin* (Czechowski *et al.*, 2005).

Microarray experimental design and the analysis of the resulting data have not always been consistent in the past, yet they have still produced valuable results. Individual microarray experiments have implicated thousands of genes in biological processes under study that may have taken decades to identify using classical methods (Kim *et al.*, 2001; Maleck *et al.*, 2000; Primig *et al.*, 2000; Schena *et al.*, 1996). In more recent years, microarray experiments have also been designed specifically to infer genetic regulatory networks. This typically involves perturbing the expression of a single gene and monitoring the effect exerted on other genes, thereby allowing the eventual dissection of complex pathways (de la Fuente *et al.*, 2002).

1.2.5.1 – Meiosis and microarrays

Through microarray technology, a number of studies have investigated reproductive processes including; stages of meiosis, differences in germline and somatic tissues, and differences in male and female germlines. Much of the research has been completed in model species including; *S. cerevisiae*, *S. pombe*, *C. elegans*, fruit fly, rats, and Arabidopsis (Andrews *et al.*, 2000; Chu *et al.*, 1998; Mata *et al.*, 2002; Primig *et al.*, 2000; Reinke *et al.*, 2000; Schlecht *et al.*, 2004).

Some of the earliest meiotic microarray work investigated the transcriptional program of *S. cerevisiae* (Chu *et al.*, 1998). cDNA microarrays containing 97% of the known *S. cerevisiae* genes were used to increase the number of genes meiotically-regulated from approximately 150 which were identified using conventional methods (Chu *et al.*, 1998, and references therein), to over 1,000 using a microarray approach. Subsequently the two *S. cerevisiae* strains, SK1 and W303, which show different sporulation efficiencies, were compared. This revealed gene deletions, polymorphisms and approximately 1,600

temporally-regulated genes in both strains (Primig *et al.*, 2000). The majority of the transcripts (60%) displayed similar expression patterns between strains. The 1,600 genes identified that were temporally regulated were assigned into seven broad expression clusters. Some of the genes represented in these clusters have roles in DNA synthesis, recombination, synaptonemal complex and asci formation.

Approximately 650 meiotically-regulated genes identified in the Primig *et al.* (2000) study were not previously reported. Particular attention was paid to the genes expressed specifically in meiosis, as it is possible that amongst these genes are those responsible for 'reprogramming' mitotically-dividing cells to meiotic cells. Prior to the research of Primig *et al.* (2000), classical techniques had identified approximately 200 genes essential for meiosis from a diverse range of organisms. The studies by Primig *et al.* (2000) and Chu *et al.* (1998), whilst similar, report different numbers of meiotically-regulated transcripts. This difference may be accounted for due to the sensitivity of the microarray technology, the experimental design between the two research groups or possibly the interpretation of data.

Another microarray-based meiotic study by Reinke *et al.* (2000) studied the hermaphrodite germline of *C. elegans* to detect germline-enriched genes by using mutant strains unable to produce male or female gametes. In total, 650 sperm-enriched genes, 258 oocyte-enriched genes and 508 germline-intrinsic genes were identified. In addition to the genes identified, it was noted that the sperm-enriched and germline-intrinsic genes were rarely found on the X chromosome, while oocyte-enriched genes were spread throughout the genome evenly.

Other meiotic studies in animals, such as those by Andrews *et al.* (2000) found that fruit fly testes have a highly specialised gene expression profile, differentially expressing a

number of genes when compared to other tissue types. Fruit fly testes were also shown to be almost as different from ovaries as they are from the soma, despite the fact that testes and ovaries are analogous organs. Further animal reports have included a large scale investigation of male meiosis in rats, where Schlecht and colleagues (2004) identified 1,268 meiotically-regulated transcripts, of which 231 had no significant similarities to sequences in databases at that time (Schlecht *et al.*, 2004). These novel transcripts represent possible targets for novel contraceptives targeted at a male market. The results also show that expression data obtained using conventional molecular biology techniques was successfully reproduced with microarrays.

It has been shown that many genes are conserved, as are processes such as the cell cycle, between species as distantly related as yeast and humans (Schlecht & Primig, 2003). Comparative expression profiling to identify important meiotic genes is therefore an approach that might yield useful information between similar and/or divergent species. However, one study comparing the distantly related *S. pombe* and *S. cerevisiae*, revealed less than 100 commonly induced genes between the two species (Mata *et al.*, 2002). This could be interpreted in at least four ways: 1) comparative expression profiling is not always going to be a useful approach; 2) the core meiotic transcriptome in eukaryotes may contain less than 100 genes; 3) meiosis was very simple or absent in the common ancestor of the two yeast species; 4) meiosis to some extent is a mechanical process which conserves ultra-structural features and/or amino acid sequences of proteins. In identifying gene targets (whether novel or otherwise) using microarrays, analysis of candidate genes using a reverse genetics approach can then be undertaken.

1.2.6 – Reverse genetics

Reverse genetics makes use of a candidate gene approach where a gene is targeted, often by mutation, to then study the effect that has on the biological process of interest. Tools that currently exist in the reverse genetics field are numerous ranging from T-DNA insertions, RNA interference (RNAi), ethylmethane sulphonate (EMS) mutagenesis and Targeting Induced Local Lesions in Genomes (TILLING) populations.

1.2.6.1 – T-DNA

Meiotic mutant studies in Arabidopsis often use T-DNA insertion lines. To generate these lines, T-DNA disrupts the expression of the gene and therefore the protein that would normally be translated. Due to the abundance of inexpensive mutants which have flanking sequence tags detailing their position in the genome, T-DNA insertions are a logical choice in reverse genetic studies. However T-DNA insertions are not available for every gene in Arabidopsis. For example, the gene *AtZYP1* is duplicated and *AtZYP1a* and *AtZYP1b* cover a 13 kb region on chromosome 1. The start codons are separated by 2 kb and transcribe in opposite directions. Given the small genetic distance between the paralogues, the chance of obtaining a recombination event in F_1 hybrids of *Atzyp1a* and *Atzyp1b* is minimal. To overcome this, another reverse genetics approach known as RNA interference (RNAi) was used to study this gene (Higgins *et al.*, 2005).

1.2.6.2 – RNA interference (RNAi)

RNAi has been widely exploited in functional genomics since its serendipitous discovery in *Petunia* (Napoli *et al.*, 1990) where it was first coined as co-suppression. This phenomenon

is an endogenous process that occurs in many organisms, and which has arisen over the course of evolution with multiple functions including defence response and the normal regulation of endogenous protein-coding genes (Bartel, 2004; Hannon, 2002; Holmes & Cohen, 2007; Tolia & Joshua-Tor, 2007). In an attempt to increase a dark pigment in *Petunia hybrida* petals, anti-sense constructs for chalcone synthase were expressed with the resulting petal pigmentation actually being reduced (Napoli *et al.*, 1990). With this knowledge many research groups have since 'silenced' individual gene targets, enabling function(s) to be assigned to the gene of interest by studying the resulting phenotype of the species under study (Boden *et al.*, 2008; Higgins *et al.*, 2005; Lloyd *et al.*, 2007; Namekawa *et al.*, 2005; Siaud *et al.*, 2004).

The RNAi pathway begins with the introduction of dsRNA (typically 200-500 bp) into a cell, where the Dicer enzyme cleaves dsRNA into fragments approximately 21-26 bp in length, referred to as short interfering RNA (siRNA) or micro RNA (miRNA) (Tolia & Joshua-Tor, 2007). An endonuclease, RNA-induced silencing complex (RISC), uses the siRNA as a guide to locate complementary sequences which will be degraded, thus resulting in the inhibition or significantly lowered rate of mRNA translation (Hannon, 2002). Plants are capable of amplifying this signal which can lead to gene silencing by mechanisms such as histone methylation (Mette *et al.*, 2000; Thomas *et al.*, 2001; Wassenegger *et al.*, 1994; Zilberman *et al.*, 2003).

T-DNA mutant banks such as those for Arabidopsis do not exist for many organisms. Bread wheat is such an example with the problem being two-fold. Firstly, the genome is not sequenced, and therefore the position of insertions would not be known. Secondly and more importantly, the lack of understanding of cross-talk between homoeologous genes, at the level of expression, means that creating triple mutants (one for each of the copies on the A,

B and D genomes) would make analysis extremely difficult and be in any case, a substantial investment of time and resources. Even so, RNAi has been studied in bread wheat where the reduction of the *TaASY1* transcript level was achieved using RNAi (Boden *et al.*, 2008). This resulted in phenotypes which have not been seen with *Atasy1* mutants (Armstrong *et al.*, 2001; Caryl *et al.*, 2000; Ross *et al.*, 1997). The variation of *TaASY1* transcript detected between independent lines reported by Boden *et al.* (2008) suggests one of two things: 1) the RNAi pathway is not completely understood with respect to how the affected transcript levels lead to altered protein levels (especially in germ-line tissue (Holmes & Cohen, 2007)), and 2) Q-PCR (which was used in this study) is not a flawless methodology for determining quantitative transcript-based mutations.

1.3 – Rationale of current study

Meiotic biochemical pathways operate through an integrated and complicated array of networks. Certain aspects of these genetic and biochemical networks are better understood than others. Using both model organisms and a food staple, bread wheat, this study seeks to achieve multiple goals:

The first component aims to create a freely available resource to complement meiotic studies by generating a microarray dataset from a high resolution tissue series and then compare the meiotic transcriptomes of multiple plant species. This could lead to the discovery of new genes involved in meiosis, subsequently filling knowledge gaps with our current understanding of how meiosis works at the genetic and biochemical level.

The second half of this dissertation then investigates in detail two key genes/proteins that are involved in early meiosis (specifically prophase I). The first

candidate, *TaMSH7*, will be studied and assessed for what role the mismatch repair gene may play in the suppression of homoeologous chromosome interactions (utilising RNAi-induced knock-down bread wheat mutants that were produced). The second candidate, *At*MER3 will be investigated and localised in the meiotic pathway that leads to interfering crossovers.

Broadly, the research presented aims to generate knowledge which will further the altruistic goal of accelerating agriculture-based plant breeding programmes. It will be through the results of such studies that will enable the introgression of new traits rapidly between species that would not naturally produce fertile offspring.

Chapter 2 – Comparative transcriptomics of bread wheat and rice gametophyte development

2.1 – Introduction

Microarray technologies have increased in their applications and popularity since their creation over a decade ago (Schena *et al.*, 1995). Initially microarrays were developed to measure expression levels of given transcripts, however SNP arrays now also form a common component of genotyping projects. This has led to a large increase in using the technology and seen the creation of various "-omics" technologies. Microarrays can provide a snap-shot of the dynamic cellular transcriptomes which have been extracted from an isolated tissue type. A common application is comparing the same tissue type at the same stage of development between an experimental treatment or a diseased tissue compared to a wild-type control. Data from tissue time-courses/developmental series can also be generated with microarrays. The outcomes of these experiments can provide many advantages including; a freely available public resource, and eliminating the need to perform thousands of northern blot analyses or Q-PCR experiments which would otherwise be unrealistic. One of the goals in using microarrays is to answer biological questions and create solutions for a given problem. Various studies have now studied meiotic transcriptomes (often time-course experiments) in a variety of kingdoms. Examples include yeast, rat, mouse, *Drosophila*, *Caenorhabiditis elegans* and wheat (Chapter 3) (Andrews *et al.*, 2000; Chu *et al.*, 1998; Crismani *et al.*, 2006; Pang *et al.*, 2006; Primig *et al.*, 2000; Reinke *et al.*, 2000; Schlecht *et al.*, 2004).

The objective of the work presented in this chapter was to identify genes in both wheat and rice that may play roles during meiosis that were previously unidentified or not identified as having a meiotic role. This was achieved by using a comparative approach between the wheat and rice meiotic transcriptomes over a time-course. Given the accessibility to rice mutant stocks and also putative homologues in Arabidopsis, this makes for an attractive approach in identifying the phenotype resulting from gene knock-outs which would otherwise be a significant investment of time and money to achieve in bread wheat.

2.2 – Materials and methods

Two microarray datasets exist which both represent a time-course of male gametophyte development. The production of the wheat dataset is described in depth in chapter three (Crismani *et al.*, 2006). The rice dataset (Deveshwar, Bovill, Able & Kapoor, *unpublished data*) obtained using the GeneChip® Rice Genome Array was less detailed than the dataset from the wheat time-course. Particular stages of the wheat dataset were therefore excluded from the analysis or pooled, where appropriate.

The four stages of male gametophyte development available for rice were; pre-meiosis (PM), meiosis (M), immature pollen (IP) and mature anthers (MAN). Seven stages were available for wheat: pre-meiosis, leptotene to pachytene (LP), diplotene to anaphase I (DA), telophase I to telophase II (TT), tetrads (T) immature pollen and mature pollen (Crismani *et al.*, 2006).

2.2.1 – Data reduction

The two datasets were very large, containing 60,703 and 57,194 for wheat and rice respectively. To create a subset of transcripts enriched for potential meiotic transcripts, the two datasets were reduced significantly.

2.2.1.1 – Rice

T-tests were performed between PM and M from the rice microarray data to identify transcripts that were regulated by anther progression through meiosis. Probe sets were selected that had a corrected p-value smaller than 0.05 between PM and M in addition to a log base 2 RMA-normalised value greater than 5 in at least one of the PM or M microarrays.

2.2.1.2 – Wheat

The wheat microarray experiment separated meiotic stages specifically. Therefore, data from a pool of material as broad as "meiotic" did not exist for the wheat dataset. In order to create a subset of data comparable to the rice PM v M subset, t-tests were performed individually between the three PM replicates and the three replicates from the meiotic stages: LP, DA and TT. Then the transcripts were refined to only include those with a log base 2 RMA-normalised intensity greater than 5 in at least one of the microarrays hybridised with cRNA from the meiotic stages; PM, LP, DA or TT. The results were pooled. Therefore transcripts which were expressed significantly different in more than one of the wheat t-tests were only included in the dataset once, thus creating a non-redundant dataset.

2.2.2 – Sequence retrieval, further data filtration and transcript annotation

The program – Fast tricks with FASTA – a useful Bioinformatics tool developed in-house (Baumann, *unpublished data*) was used to retrieve the subset of sequences for the rice and wheat meiotically-regulated transcripts from whole chip sequences. A database was created with the rice and the wheat subset sequences. To identify the transcripts within the wheat and rice subsets that shared strong sequence similarity (E value $< e^{-30}$) in addition to being meiotically regulated, Basic Local Alignment Search Tool (BLAST) analyses were performed between the two subsets of transcripts. The wheat and rice reduced datasets were reciprocally BLASTed against one another using both nucleotide BLAST (BLASTn) and a translated nucleotide BLAST (tBLASTx). The most similar hit was added to the further refined subsets of data for each query, given that they had occurred at a significance level below the set threshold. Transcripts which appeared as the most similar hit for more than one query were only included once. Annotations for the transcripts were retrieved from the NCBI database by using a batch BLAST program with a translated nucleotide database search using a translated nucleotide query (BLASTx) and tBLASTx to simultaneously identify annotated sequences (cut off E value $< e^{-20}$).

2.2.3 – Comparative expression profiling

The meiotically-regulated data from the wheat and rice datasets was then centred by removing the average expression intensity value for a given transcript across their respective time-course. This removes the absolute values and replaces them with a movement about their average expression over the time-course with respect to doubling or

halving their expression levels as the RMA-normalised data is presented as log base 2. This analysis places more emphasis on expression trends across the time-course rather than absolute values. Hierarchical clustering was performed using a Euclidean squared similarity metric and an average linkage method (Acuity 4.0, Axon Instruments, U.S.A.).

The expression profiles of 12 randomly selected transcripts from the final subset of 129 identified meiotically-regulated and sequentially-related transcripts were compared with respect to their expression profiles. In creating the pooled meiosis stage for wheat, the centred values for LP, DA, TT stages were averaged.

2.3 – Results

2.3.1 – Data filtration and transcript annotation

For the wheat analysis, PM versus LP resulted in zero transcripts with a corrected p-value equal to or smaller than 0.05. PM versus DA resulted in identifying 415 transcripts while PM versus TT resulted in 181 transcripts. The union of these three sets of results returned 497 non-redundant probe sets, indicating there were multiple probe sets appearing in both t-test results that met the selection criteria (Figure 2.1). The t-test between the rice PM and M stages resulted in the identification of 7,410 transcripts which were regulated by the progression of anthers from PM to M. The reciprocal use of tBLASTx and BLASTn between the two transcript subsets identified 83 sequences with BLASTn and 129 sequences with tBLASTx (Figure 2.1). The annotation retrieval of the 129 transcripts returned annotations for 104 of the sequences (Batch BLAST results are shown in Appendix A). 25 sequences were either not functionally annotated or returned hits below the accepted threshold.

These 129 transcripts were then assigned to a functional category. The highest representations were meiosis/cell division candidates which accounted for 13.2% of the 129 transcripts (Table 2.1). Examples of these meiotic functions included a protein essential for synapsis of homologous chromosomes (ASY1) (Armstrong *et al.*, 2002), a protein involved in signal transduction during the entry into meiosis in yeast (RIM11) (Rubin-Bejerano *et al.*, 2004), a cross-over formation gene (MLH3) (Jackson *et al.*, 2006), cell-cycle proteins and chromosome morphogenesis genes (for example, multiple CDCs, a cyclin and SPO76) (Francis, 2007; Grasser, 2000; van Heemst *et al.*, 2001). The next highest group was annotated as binding smaller nucleic acid structures (as opposed to chromosomes). This included many proteins broadly defined as zinc fingers. Transcripts which had no hits found (8) within the set threshold or simply no functions annotated (17), collectively represented 19.4% of the 129 transcripts.
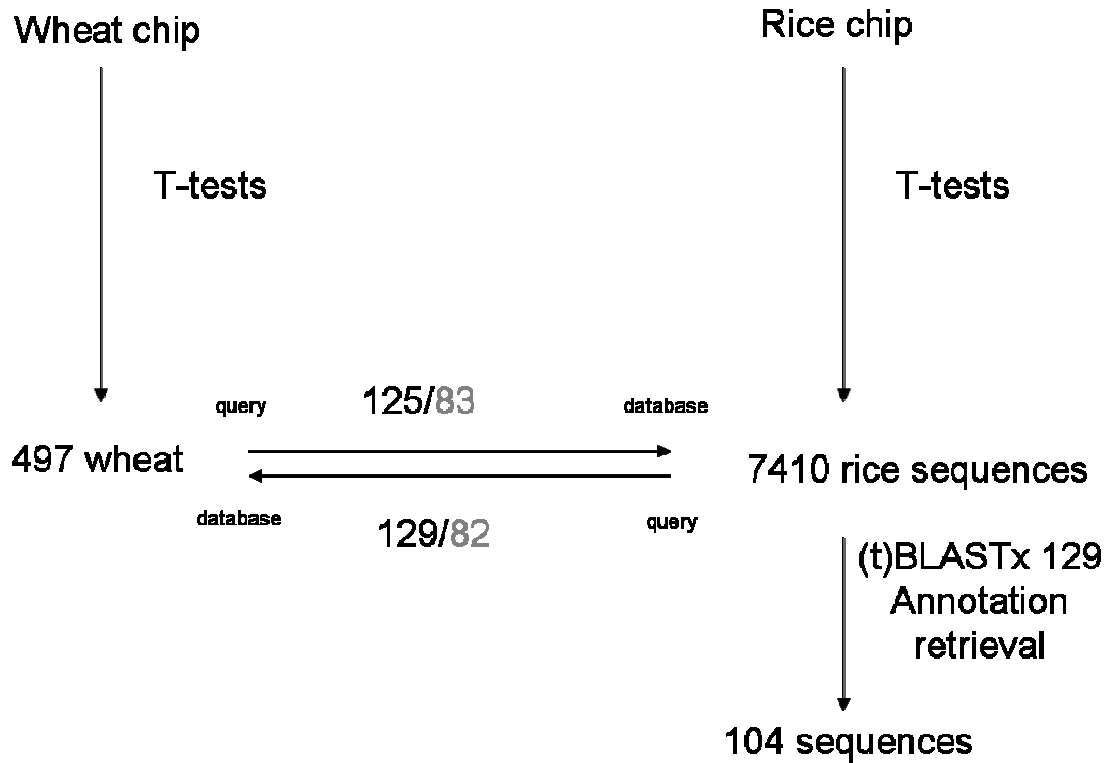
Figure 2.1 – Diagrammatic representation of the data filtration leading to a subset of 129 meiotic transcripts from bread wheat and rice. T-tests identified transcripts which showed transient regulation during meiotic anther development. Reciprocal BLASTs were then performed between the wheat and rice subsets. tBLASTx results (black) and BLASTn results (grey) are shown. Functional annotations were retrieved from pubic databases using the 129 rice transcripts as the query. A total of 104 annotations were retrieved.

Table 2.1 – Biological classification for 129 meiotically-regulated wheat and rice transcripts. Annotations retrieved from NCBI were functionally categorised by manually searching available literature. Numbers in parentheses correspond to the percentage representation within the 129 transcripts. No hits found implies so for a threshold E-value $< e^{-20}$.

Category	Representations (%)
Meiosis/cell cycle	17 (13.2)
Transcription factors and nucleic acid binding	13 (10.1)
Cellular metabolism	12 (9.3)
Organelle activity	10 (7.8)
Biotic stress-related	9 (7.0)
Signal transduction	8 (6.2)
Secondary metabolism	6 (4.7)
Protein metabolism	6 (4.7)
Membrane transport	5 (3.9)
Hormone regulation	4 (3.1)
Protein transport	3 (2.3)
Abiotic stress response	2 (1.6)
Cell wall-related	2 (1.6)
Lipid metabolism	2 (1.6)
Tapetal function	1 (0.8)
Protein folding	1 (0.8)
Embryonic development	1 (0.8)
Ribosomal	1 (0.8)
Development	1 (0.8)
Function not annotated	17 (13.2)
No hits found	8 (6.2)

2.3.2 – Comparative expression profiling

Transcripts with similar expression profiles were clustered together using hierarchical clustering. This resulted in the identification of a number of interesting clusters (Figure 2.2). A group of 28 transcripts from the wheat dataset were expressed at higher levels during the meiotic stages (Figure 2.2B). Some of these transcripts showed strong sequence similarities to histones and chromatin remodelling factors, proteins controlling cell cycle, recombination and synapsis. Another cluster of interest with 20 transcripts was also expressed preferentially in pre-meiosis but was down-regulated at a greater rate than the

cluster mentioned above (Figure 2.2C). This cluster contained putative homologues of proteins involved in crossover formation, cell division, microtubule function and chromatin remodelling. A similar methodology with the rice dataset resulted in the identification of a cluster where 39 transcripts showed higher levels of expression during the pre-meiotic and meiotic stage, and then lower transcript levels in the remaining two stages (Figure 2.3C). Annotations of the 39 transcripts from rice identified less transcripts that can be easily associated with meiotic functions when compared to the wheat transcripts. The rice transcripts did however include similarity to genes that have roles in chromatin remodelling. A cluster which was represented by only seven transcripts contained *OsPAIR2* (essential for synapsis in rice (Nonomura *et al.*, 2006)), putative homologues of a PIWI domain containing protein (germline specific RNAi components) and a cyclin (Figure 2.3B).
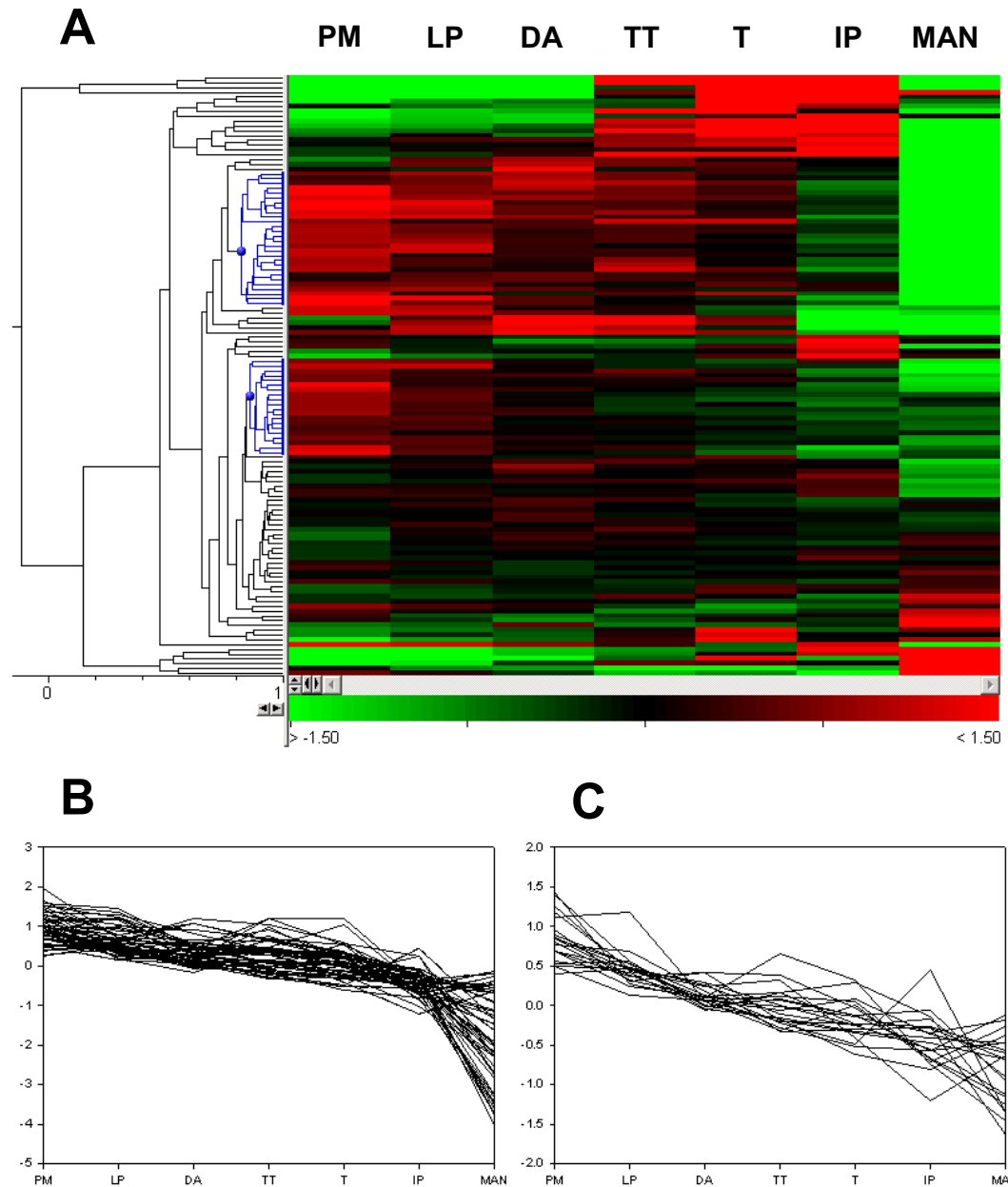
Figure 2.2 – Hierarchical clustering of 125 wheat transcripts that are regulated over the progression of meiosis. The expression profiles of 125 transcripts (rows) were grouped across seven anther stages (columns) in a heat map (A). Similar expression profiles are clustered together as indicated by the dendrogram. The expression profiles of two clusters that are preferentially expressed in early meiosis which display similar expression profiles are highlighted in blue on the dendrogram. These clusters representing 28 and 20 transcripts are also shown separately in (B) and (C), respectively. Pre-meiosis **(**PM), leptotene – pachytene (LP), diplotene – anaphase I (DA), telophase I – telophase II (TT), tetrads (T), immature pollen (IP), mature anthers (MAN). Expression values (indicated by green through to red in colour) are centred, log base 2, RMA-normalised values.
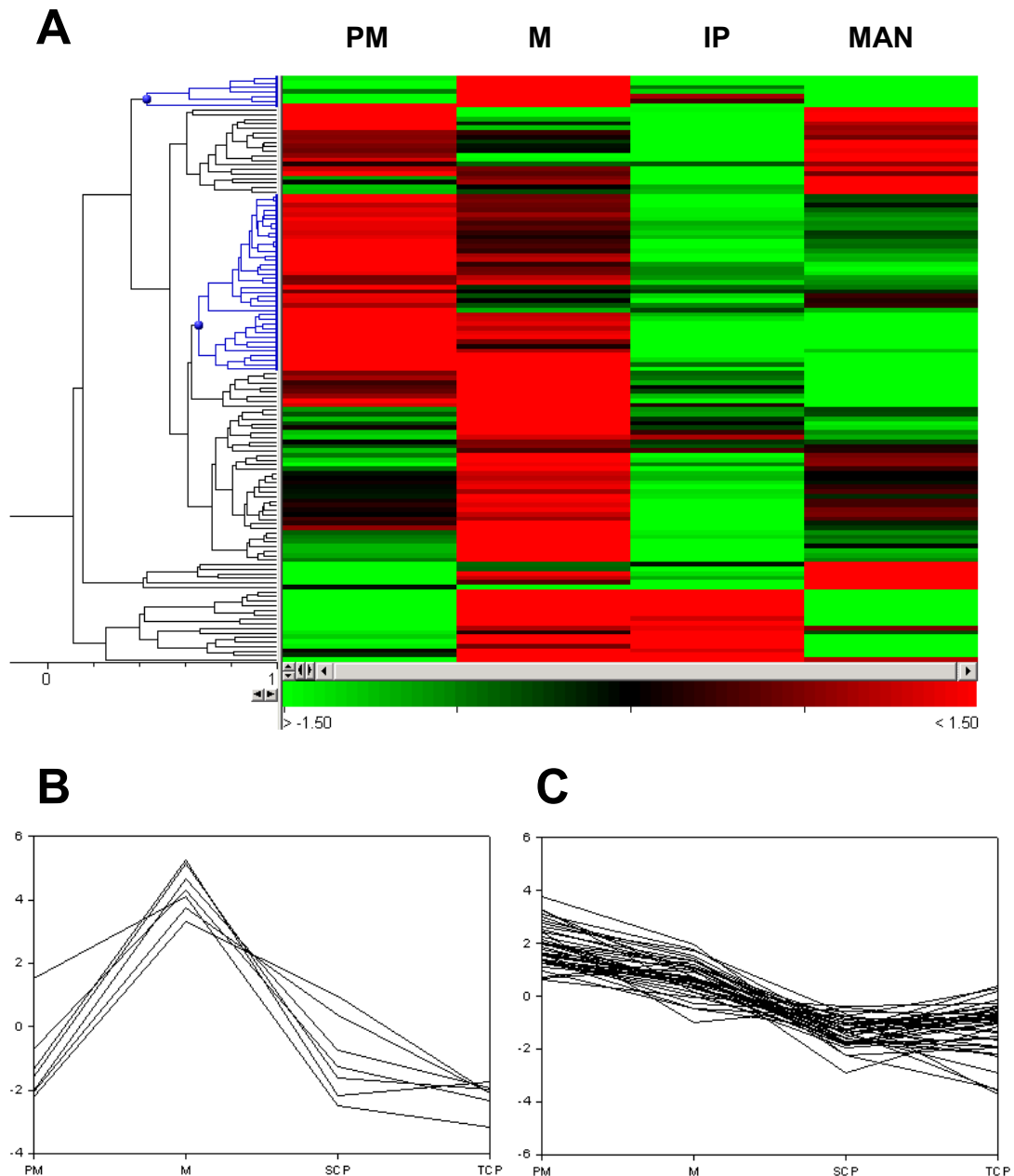
Figure 2.3 – Hierarchical clustering of 129 rice transcripts that are regulated over the progression of meiosis. The expression profiles of 129 transcripts (rows) were grouped across four anther stages (columns) in a heat map (A). Similar expression profiles are sorted together as indicated by the dendrogram. The expression profiles of two clusters that are preferentially expressed in pre-meiotic and/or meiotic stages which display similar expression profiles are highlighted in blue on the dendrogram. These clusters representing 7 and 39 transcripts are also shown separately in (B) and (C), respectively. Pre-meiosis (PM), meiosis (M), immature pollen (IP), mature anthers (MAN). Expression values (indicated by green through to red in colour) are centred, log base 2, RMA-normalised values.

12 randomly selected transcripts from the 129 meiotically-regulated and sequentially-related transcripts were compared between wheat and rice with respect to their expression profiles (Figure 2.4). Correlation co-efficients between the wheat and rice expression profiles varied, with a positive correlation as high as 0.91 being observed, while a moderate-high negative correlation of -0.79 was also recorded. In total, seven out of 12 transcripts shared a correlation co-efficient stronger than 0.6.
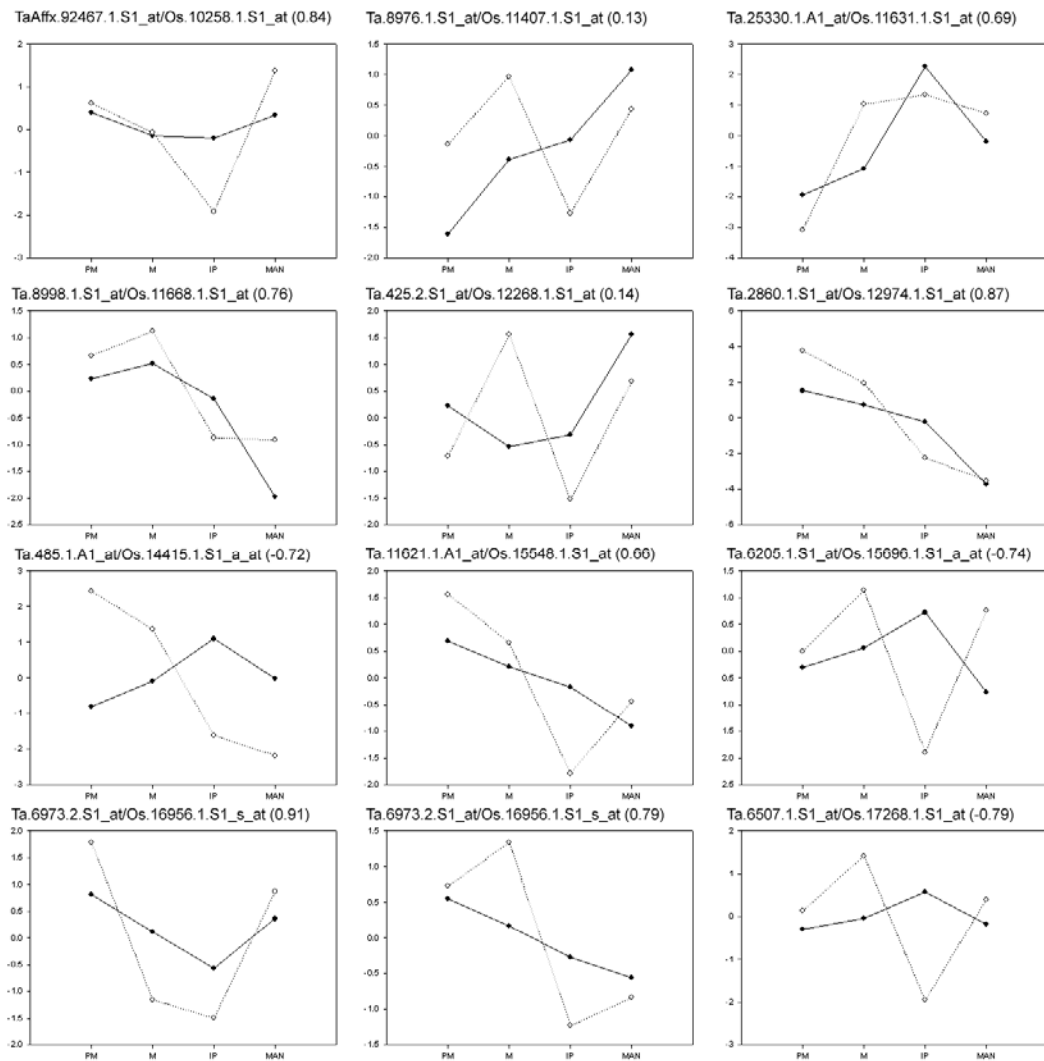
Figure 2.4 – Correlation of 12 meiotically-regulated expression profiles identified from the wheat and rice datasets. Closed and open circles represent the wheat and rice transcripts respectively. Numbers in parentheses represent the correlation co-efficient between the two expression profiles. Expression values on the X axes are centred, log base 2, RMA-normalised values. Stages of anther development are displayed on the Y axes: pre-meiosis (PM), meiosis (M), immature pollen (IP), mature anthers (MAN).

Putative homologues in Arabidopsis and Poplar (*Populus sp.*) for a select number of transcripts from wheat and rice were also identified. An Electronic Fluorescent Pictograph (eFP) browser was then used to provide an indication as to whether the transcripts showed preferential expression in meiotic material in either of these additional plant species. Many transcripts (including *ASY1*) showed preferential expression in meiotic tissue (buds in Arabidopsis and catkins in Poplar) (Figure 2.5A, B, D). Numerous transcripts also showed patterns with stronger expression in vegetative tissues (Figure 2.5C).
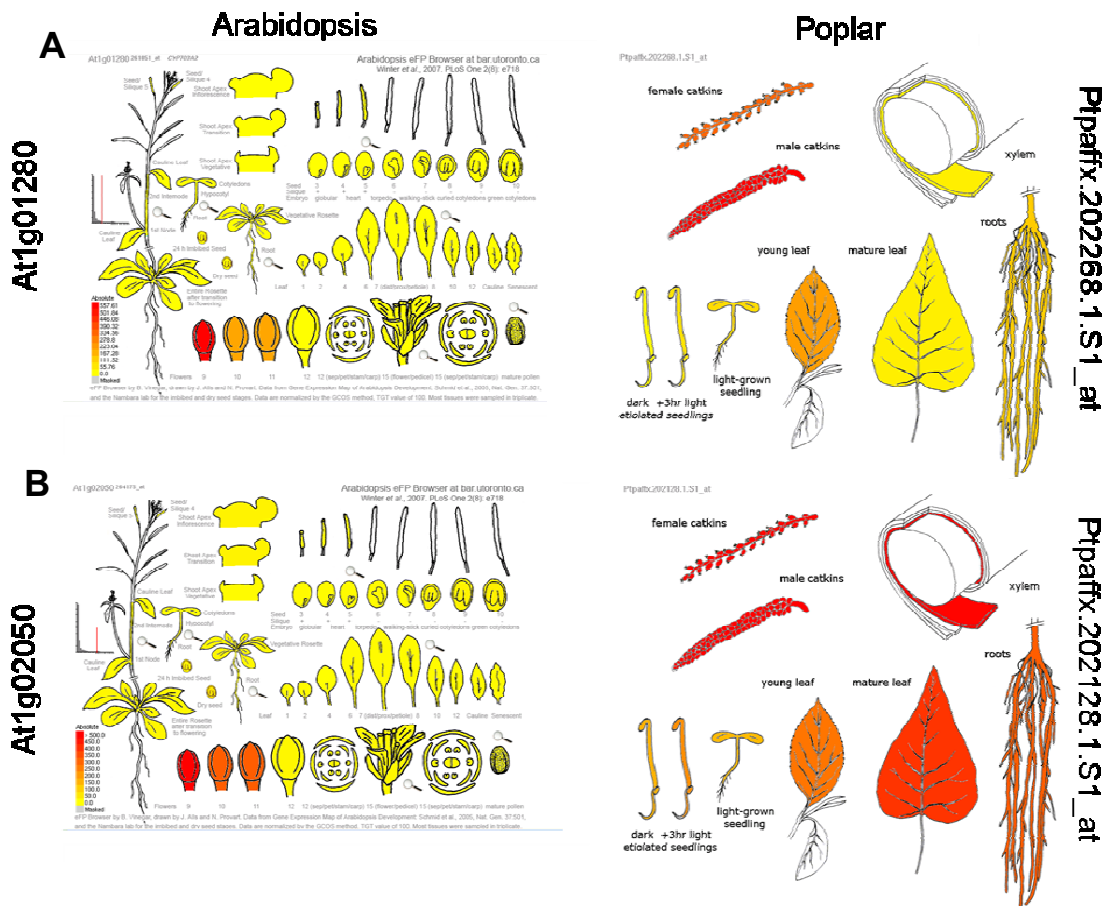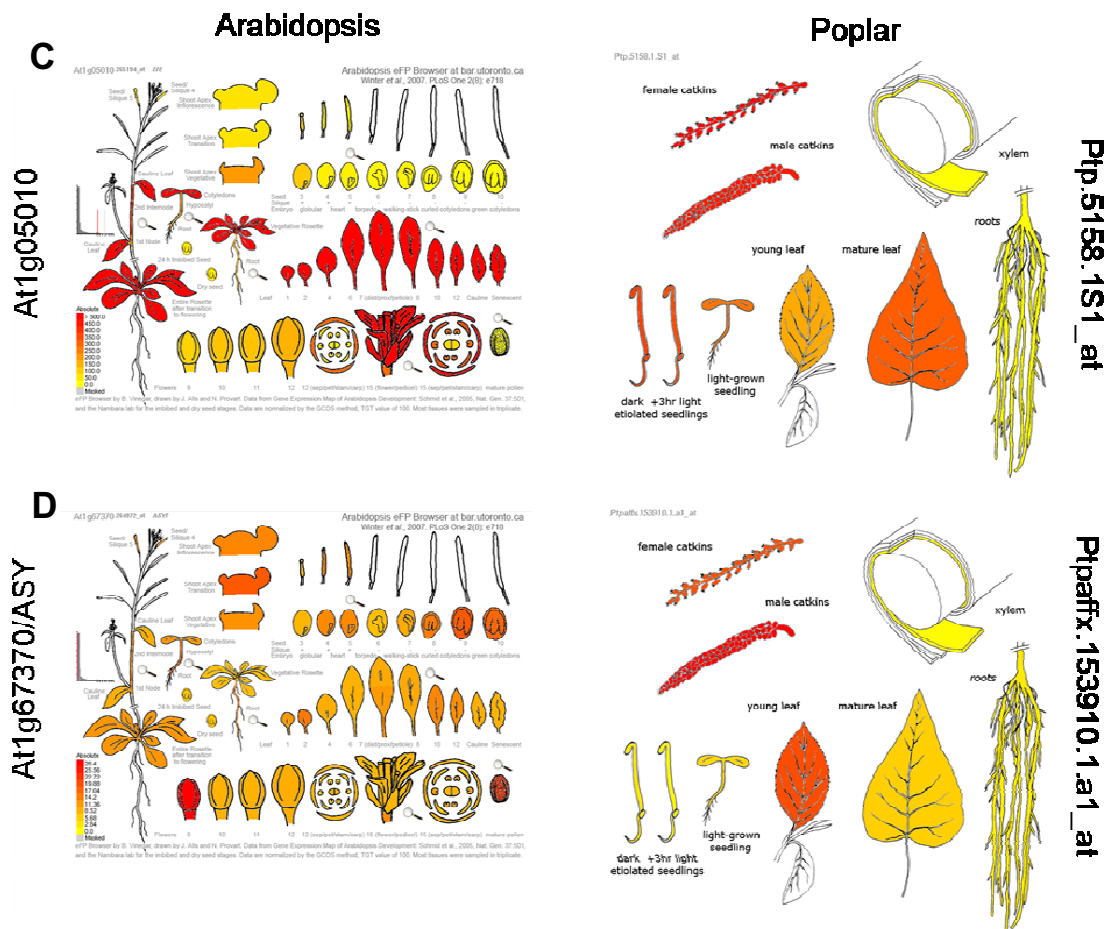
Figure 2.5 – Electronic Fluorescent Pictographs comparing candidate meiotic transcript expression levels between tissue types of Arabidopsis in addition to the putative Poplar homologues. Transcripts At1g01280 (A) and At1g02050 (B) show preferential expression in Arabidopsis buds at approximately prophase I. Similar results are seen in male meiotic tissue (male catkins) of the respective putative Poplar homologues. Transcript At1g05010 (C) does not show preferential expression in meiotic tissue. The transcript representative of *AtASY1* (D) is included as an indication of what genes with specific meiotic roles frequently look like using the eFP browser. Greater expression levels are indicated in red and low (if any) expression is indicated in yellow. Information is derived from Winter *et al.* (2007) and can be viewed in greater detail at http://bbc.botany.utoronto.ca/efp/cgi-bin/efpWeb.cgi.

2.4 – Discussion

2.4.1 – Data filtration

The wheat and rice data filtration method used to identify transcripts putatively having meiotic roles yielded very different numbers, 497 and 7,410 respectively. While there are a different number of genes (represented by transcripts) in the wheat and rice genomes, in addition to the wheat genome having not yet been completely sequenced, the difference must be accounted to something else. This is most likely due to the staging of the material collected as the wheat and rice datasets were produced by different research groups. T-tests between the meiotic tissues and IP or MAN were excluded from the analysis as IP and MAN have very different profiles at the transcript level with the vast majority of the genome being temporally-regulated during these stages. Including these stages would have resulted in an over-estimation of probe sets that are involved in meiosis during the development of the male gametophyte.

The reciprocal BLASTs between the 497 and 7,410 were expected to return approximately the same numbers as the majority of genes in rice would have a wheat homologue based on both sequence and function. This was found to be the case with 125/83 returned for wheat to rice, while 129/82 were returned for rice to wheat. However, as the microarrays are made of many probe sets which can represent fragments of transcripts (for example, non-overlapping ESTs derived from opposite ends and of the same mRNA transcripts), they are not always complete. Therefore, if a homologous sequence exists between wheat and rice but the probe sets are designed to opposite ends of the transcript, this can cause discrepancies in the numbers returned in reciprocal BLASTs. This becomes increasingly likely given that the wheat chip was designed as a "discovery chip"

from the wheat ESTs which were present in the public databases in 2004. The rice chip is a much closer representation of what is the entire transcriptome in this plant species. Generally however, there was only a discrepancy of one significant hit using BLASTn or four significant hits when using the tBLASTx program (Figure 2.1).

104 transcripts shared similarity with previously annotated sequences. As anticipated, the most common annotation was meiosis/cell cycle. The two processes were pooled since they are very difficult to uncouple as meiosis is a specialised type of cell cycle division. There are close to 50 meiotic genes in plants that have been identified and characterised to date (Mercier & Grelon, 2008) and the categorical data presented here included only two of these 50 or so meiotic genes, *ASY1* and *MLH3*, in addition to various proteins related to more generalised cell cycle and chromatin remodelling. The inability to detect a higher percentage of the 50 known meiotic genes suggests that in wheat and rice at least, 1) the remaining known genes not identified by this method have a more static expression profile than the transcripts that matched the selection criteria used in this chapter; 2) they were not present on the wheat chip and therefore were not detected; 3) some of the sequences have not been conserved across species.

From a gene discovery perspective it is exciting to note that there were 25 transcripts with no similarity to functionally characterised genes which potentially have roles as important as *ASY1*, *MLH3* and chromatin remodelling. Other annotations such as roles in embryo development and tapetal-specific roles are consistent with the type of background expression profiles detected in a meiotic time-course, especially as whole anthers were used.

2.4.2 – Comparative expression profiling

Hierarchical clustering of the wheat and rice data subsets grouped transcripts with similar expression profiles adjacent to one another in the dendrogram. There were similarities between the results produced in the heat map clusters for wheat and rice. However, given less information (stages) was available for rice the clusters have less resolution than those in wheat. Analysis of the clusters which contain transcripts and are preferentially expressed did reveal an enrichment of meiotic/cell cycle transcripts. Given that there are approximately 50 known meiotic genes in plants and approximately 30,000 genes predicted to be in the rice genome, this represents 0.17% of the genome. The identification of *ASY1*, *MLH3* and *SPO76* alone, is approximately a 14-fold increase in meiotic transcripts than the genomic average.

The comparison of 12 randomly wheat/rice selected transcripts from the subset of 129 revealed that the expression profiles between more than half of these shared a correlation co-efficient greater than 0.6. This suggests that while not all putative homologues are expressed identically from the time they diverged over the course of evolution, there are still common themes in the grass meiome. Another point which must be taken into consideration is human error/variation in staging given that the two datasets originate from different laboratories.

The cross-species expression analysis was also extended to Arabidopsis and Poplar by using the eFP browser tool. Analysis of putative Arabidopsis and Poplar homologues from selected wheat and rice transcripts in the eFP browser revealed some commonalities between all four plant species. Such a finding suggests that the information generated from wheat and rice is transferrable not only reciprocally but also into Arabidopsis and other

plant species (where sequence and expression data exists). This infers that the results of whole genome screens in one plant species can be used as a starting point for screening meiotic mutants in other plant species.

Chapter 3 – Microarray expression analysis of meiosis and microsporogenesis in hexaploid bread wheat

In the electronic version of this thesis a separate PDF file named Crismani *et al.*, (2006) is attached. A signed declaration by all authors allowing the inclusion of this manuscript is presented in Appendix C.

BMC Genomics

Research article

Microarray expression analysis of meiosis and microsporogenesis in hexaploid bread wheat

Wayne Crismani[1], Ute Baumann[2], Tim Sutton[2], Neil Shirley[2], Tracie Webster[3], German Spangenberg[3], Peter Langridge[2] and Jason A Able*[1]

Address: [1]Molecular Plant Breeding Cooperative Research Centre, School of Agriculture, Food and Wine, The University of Adelaide, Waite Campus, PMB1, Glen Osmond, South Australia, 5064, Australia, [2]Australian Centre for Plant Functional Genomics, School of Agriculture, Food and Wine, The University of Adelaide, Waite Campus, PMB1, Glen Osmond, South Australia, 5064, Australia and [3]Molecular Plant Breeding Cooperative Research Centre and Australian Centre for Plant Functional Genomics, Victorian AgriBiosciences Centre, La Trobe University, 1 Park Drive, Bundoora, Victoria, 3083, Australia

Email: Wayne Crismani - wayne.crismani@adelaide.edu.au; Ute Baumann - ute.baumann@acpfg.com.au; Tim Sutton - tim.sutton@acpfg.com.au; Neil Shirley - neil.shirley@acpfg.com.au; Tracie Webster - tracie.webster@dpi.vic.gov.au; German Spangenberg - german.spangenberg@dpi.vic.gov.au; Peter Langridge - peter.langridge@acpfg.com.au; Jason A Able* - jason.able@adelaide.edu.au

* Corresponding author

Abstract

Background: Our understanding of the mechanisms that govern the cellular process of meiosis is limited in higher plants with polyploid genomes. Bread wheat is an allohexaploid that behaves as a diploid during meiosis. Chromosome pairing is restricted to homologous chromosomes despite the presence of homoeologues in the nucleus. The importance of wheat as a crop and the extensive use of wild wheat relatives in breeding programs has prompted many years of cytogenetic and genetic research to develop an understanding of the control of chromosome pairing and recombination. The rapid advance of biochemical and molecular information on meiosis in model organisms such as yeast provides new opportunities to investigate the molecular basis of chromosome pairing control in wheat. However, building the link between the model and wheat requires points of data contact.

Results: We report here a large-scale transcriptomics study using the Affymetrix wheat GeneChip® aimed at providing this link between wheat and model systems and at identifying early meiotic genes. Analysis of the microarray data identified 1,350 transcripts temporally-regulated during the early stages of meiosis. Expression profiles with annotated transcript functions including chromatin condensation, synaptonemal complex formation, recombination and fertility were identified. From the 1,350 transcripts, 30 displayed at least an eight-fold expression change between and including pre-meiosis and telophase II, with more than 50% of these having no similarities to known sequences in NCBI and TIGR databases.

Conclusion: This resource is now available to support research into the molecular basis of pairing and recombination control in the complex polyploid, wheat.

Background

Bread wheat (*Triticum aestivum* L.) is an allohexaploid (2n = 6x = 42) containing three related genomes: A, B and D, with significant conservation of gene order between the chromosomes of the respective genomes. Early mapping studies including those conducted by Chao *et al.* [1] using RFLPs to map markers on chromosome group 7 confirmed strong conservation of gene order between chromosomes of each genome. Indeed, this conservation is also seen when comparing wheat with other grasses. While several papers have been published reporting synteny between the Poaceae genomes at the macro level [2,3], microsynteny appears to be perturbed frequently [4,5]. The current comparative genomics model reported by Devos [3] segregates nine major monocotyledonous genomes into 25 'rice linkage blocks' and provides a valuable base for gene discovery and genome structural analysis in grass species leading out from the sequenced rice genome.

While comparative genomics has enabled the identification of putative orthologues in many cereals, there are processes or characteristics that are either species specific, such as quality, or for which wheat provides a good model, such as the control of chromosome pairing during meiosis. During meiosis, DNA undergoes a round of replication, chromatin is condensed and the genetic content is halved twice after two rounds of chromosome segregation and cell division. Classical cytogenetic techniques suggest that the fundamental events and processes of meiosis are conserved amongst higher eukaryotes. The production of viable gametes at the conclusion of meiosis requires completion of several critical processes during prophase I that include chromosome pairing, synapsis and recombination.

During meiosis in bread wheat, strict regulation of homologous chromosome pairing is maintained, despite the presence of homoeologous chromosomes. This maintains the stability of the complex wheat genome but is also a limitation in utilizing the extensive variation available in wild relatives of wheat. Several hundred wild grasses can be crossed to wheat but introgression of desirable alleles from these species is dependent upon the induction of pairing and recombination with the wheat chromosomes. Several genes, particularly *Ph1*, are known to block or enhance homoeologous pairing; with removal of this locus shown to induce novel pairing and recombinational behaviour. An understanding and ability to modify the mechanisms that control pairing, synaptonemal complex formation and recombination would be of great benefit to crop improvement programs. Such information would also enhance our understanding of complex polyploidy genomes and factors influencing fertility.

While functional studies of individual genes have been useful for advancing our knowledge of meiosis, very few resources are available to examine whole genome expression changes during meiotic development. A broad resource base will be important to help identify conserved processes between organisms, and conversely, highlight processes that have diverged. Microarray studies have provided valuable data on meiosis and related cellular processes in several species. An early study in *Saccharomyces cerevisiae* used a microarray chip with 97% of the then known budding yeast genes [6], which increased the number of known meiotically-regulated genes from approximately 150 to over 1,000. A more recent experiment with budding yeast compared the meiotic transcriptomes of two strains with different sporulation efficiencies and identified approximately 1,600 meiotically-regulated genes in each strain with a 60% overlap between the two strains [7]. While these two examples are yeast specific, other model organisms have also been used to study meiosis with microarray technology, including fruit flies (*Drosophila melanogaster*), mice (*Mus musculus*), nematodes (*Caenorhabiditis elegans*) and rats (*Rattus rattus*) [8-11].

The current study provides information that links to the transcript profiling work conducted in yeast and animal systems and to the extensive cytological and genetic data for wheat to provide a view of meiosis in a complex polyploid and one of the world's most important agricultural crops. Using the Affymetrix GeneChip® Wheat Genome Array, which contains 61,127 probe sets (55,052 transcripts) (Affymetrix), 1,350 transcripts were found to be expressed across a sub-staged meiotic time series of whole wheat anthers. Four hundred and sixty seven have no detectable similarities to entries in sequence databases. While there have been extensive studies on the duration and timing of meiosis in bread wheat [12-15] and also on chromatin condensation and chromosome pairing [16-18], the transcript *in silico* research presented here advances our limited understanding of meiosis at the molecular level and complements the previous *in planta* studies cited.

Results and Discussion

The basic aim of the work outlined here was to develop a view of gene expression over the various stages of meiosis in wheat. The resulting data set helps define the wheat meiome (meiotic transcriptome) and will provide a key resource for work aimed at explaining the control of meiosis and chromosome pairing in a complex polyploid relative to diploid plant, animal and yeast systems.

Comparison of tissue expression profiles

There are two key components of the experimental system. First, whole anthers were used for preparing the RNAs. The meiocytes themselves form a major proportion

of the tissues in the anthers but RNA from other cell types, notably epidermal cells and tapetum, will be included in the extracts and will contribute to the results. Therefore, the data represents gene expression from a number of different cell types with meiocytes as the major constituent.

The second component is the Affymetrix wheat Gene-Chip®. This is a 'discovery' chip and is not representative of the complete wheat genome nor does it allow differentiation between genes expressed from the three wheat genomes. Further, many of the sequences used to design the chip were not of high quality. Therefore, data generated from this chip must be carefully checked and key results confirmed using alternative expression analysis methods. In addition, it is important to note that at the time the wheat GeneChip® was designed, wheat meiotic floret cDNA and cDNA from anthers undergoing meiosis represented approximately 6% of the total representations available in the wheat EST database. Therefore, the wheat GeneChip® is assumed to provide a good representation of meiotic expressed genes.

Scatter plots illustrated the similarity of replicates, and the broad relationship of the expression profiles from pre-meiosis through to the tetrad stage (Figure 1). However, marked differences were apparent in the expression profiles of both immature pollen and mature anthers when compared to each other and the meiotic-specific sub-stages; pre-meiosis through to tetrads. Given that both of these tissues and the regulation of gene expression during pollen development is complex, this level of variance is not surprising. It has been shown in several plants including tomato (*Lycopersicon esculentum*) and maize (*Zea mays*) that up to 70% of plant genes are expressed post-meiotically [19,20]. A study of the barley transcriptome also found that anthers were the most complex of tissues [21]. The results presented here reflect these findings with 67% of transcripts expressed in tetrads, immature pollen and/ or mature anthers (RMA average signal intensity > 5).

Gene filtration, identification and analysis of meiotically-regulated transcripts

The Affymetrix wheat GeneChip® contained 61,127 probe sets, which was reduced to 55,000 upon the removal of control, reporter, duplicate and 'rogue' probe sets (see Methods – Microarray analysis). The majority of the available annotations for the probe sets are based on homologies to genes from organisms other than wheat. This was due to the lack of sequence information, characterised genes and their protein products for wheat.

T-tests between expression levels at different stages of meiosis were used to identify genes showing regulation of expression during meiosis. The comparisons made were as follows: pre-meiosis (PM) with leptotene-pachytene

(LP); PM with diplotene-anaphase I (DA); PM with telophase I-telophase II (TT); LP with DA; LP with TT and DA with TT (p values = 0.05) (Figure 1). This resulted in the classification of transcripts from 1,350 non-redundant genes as being meiotically-regulated of which 467 had no annotation (Figure 2). A similar strategy was used by Schlecht and colleagues [10] with a rat data set to examine both meiosis and gametogenesis. The rat analysis resulted in the identification of 1,268 diverse meiotic transcripts from a total of 11,955.

When compared to the 55,000 relevant probe sets on the current wheat GeneChip®, the 1,350 meiotically-regulated transcripts represent only 2.45%. Thirty prominent profiles within the 1,350 meiotically-regulated transcripts showed at least an eight-fold expression change between combinations of PM, LP, DA and TT. Of these 30 transcripts, no similarities to any database entries currently on record (August 2006) could be found for 16. Consequently, these represent a source of new and potentially wheat meiosis-specific transcripts. Seven of the 30 transcripts significantly change in level of expression during the first three meiotic time points investigated in this study (Figure 3). It is during these stages where events including chromosome pairing, synapsis and homologous recombination occur. The temporal expression of the genes encoding these transcripts at the time points where homologous recombination occurs make them particularly interesting targets for further work aimed at investigating homologous pairing and recombination.

The mature anthers (MAN) accounted for the majority of variability detected (73%) between transcript profiles across the developmental stages. This is consistent with work on pollen development in *Tradescantia* and maize. Pollen germination and pollen tube growth are two processes that carry a significant metabolic cost, since it involves storage of mRNA and other organic molecules [22]. Previous studies of pollen development have typically used inhibitors of transcription and translation to show that mRNAs are produced during pollen maturation and stored for use during pollen germination [for reviews see [23,24]]. Further, many of the protein products of these genes are already present in mature pollen prior to germination [25-27].

Transcript expression during pollen maturation is generally defined as either early or late, with early transcripts present in microspores subsequently down regulated before pollen maturation, while late transcripts are produced and accumulated after pollen mitosis I [reviewed in [28]]. *In situ* studies from tomato and maize suggest that many of the late genes are the product of the vegetative cell [29,30]. Studies in both *Tradescantia* and maize have
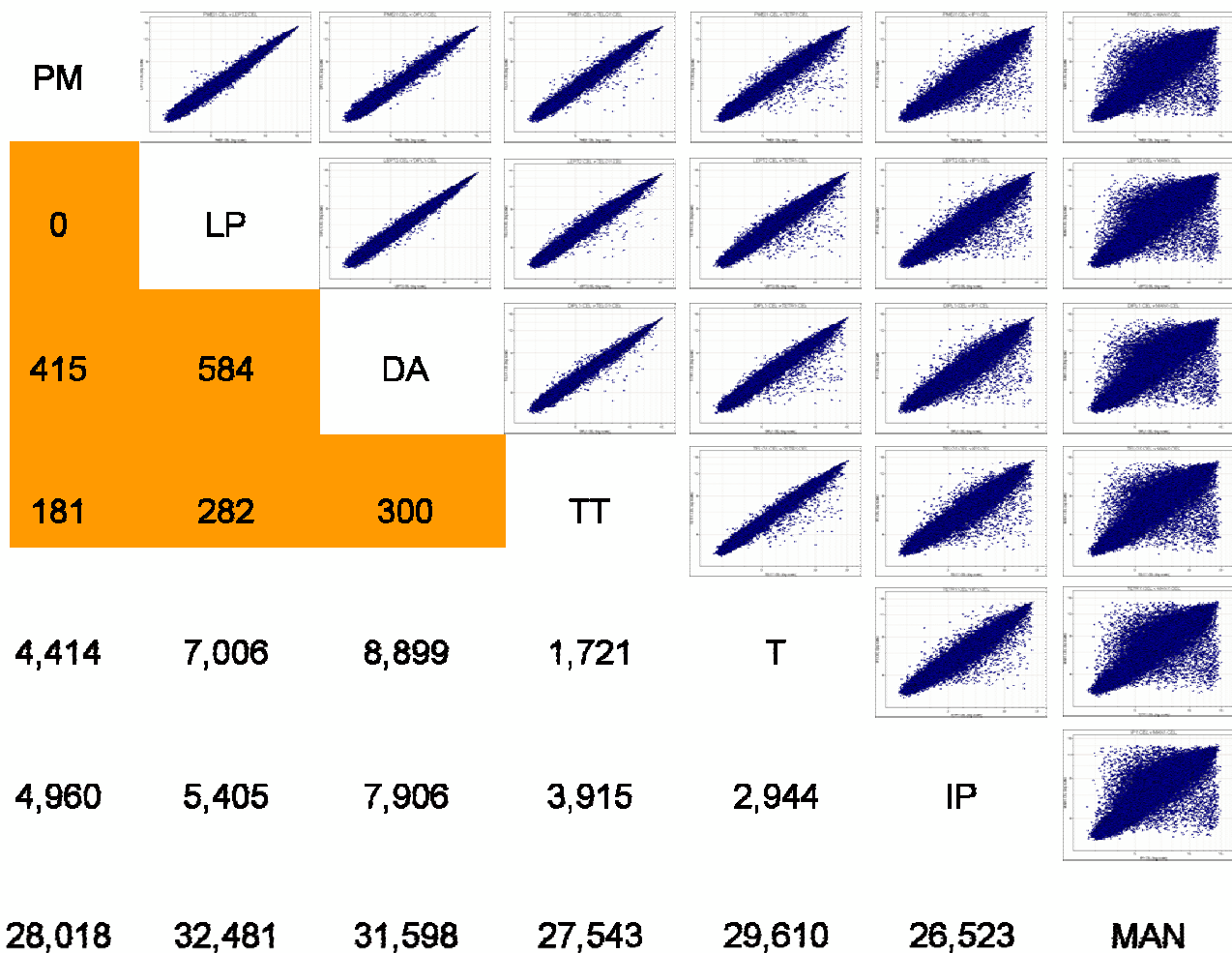
Figure 1
Scatter plot and statistical analysis comparing all seven stages investigated with the wheat Affymetrix Gene-Chip® to one another. PM = pre-meiosis; LP = leptotene to pachytene; DA = diplotene to anaphase I; TT = telophase I to telophase II; T = tetrads; IP = immature pollen; MAN = mature anthers. All values in the figure represent the number of transcripts with corrected p-values ≤ 0.05 from t-tests performed between the two tissues of interest. The orange shading represents the pooled stages from where the 1,350 non-redundant meiotically-regulated transcripts were identified.

revealed that about 10% of mRNAs stored in mature pollen grains are pollen-specific [31,32].

Over the seven stages investigated in this study, 38,242 transcripts were differentially expressed in mature anthers when compared to the first four stages of the meiotic time course (p ≤ 0.05 between PM v MAN, LP v MAN, DA v MAN and TT v MAN). Similarly, when immature pollen (IP) was compared to the four meiotic stages, considerable variation was still detected with 9,385 transcripts showing differential expression.

Expression analysis in the developing wheat anther
The complexity of the anther tissues used in this study meant that interpretation of the data required a consideration of developmental changes that were occurring in anther cells other than just the meiocytes. To obtain a view of gene expression changes that may be indicative of the meiotic process and also general developmental shifts, ten biological categories of potential significance were used to group members of the 1,350 diverse transcripts found to show variable expression (see Methods – Microarray analysis). These groups covered genes likely to be involved in tissue growth and differentiation such as
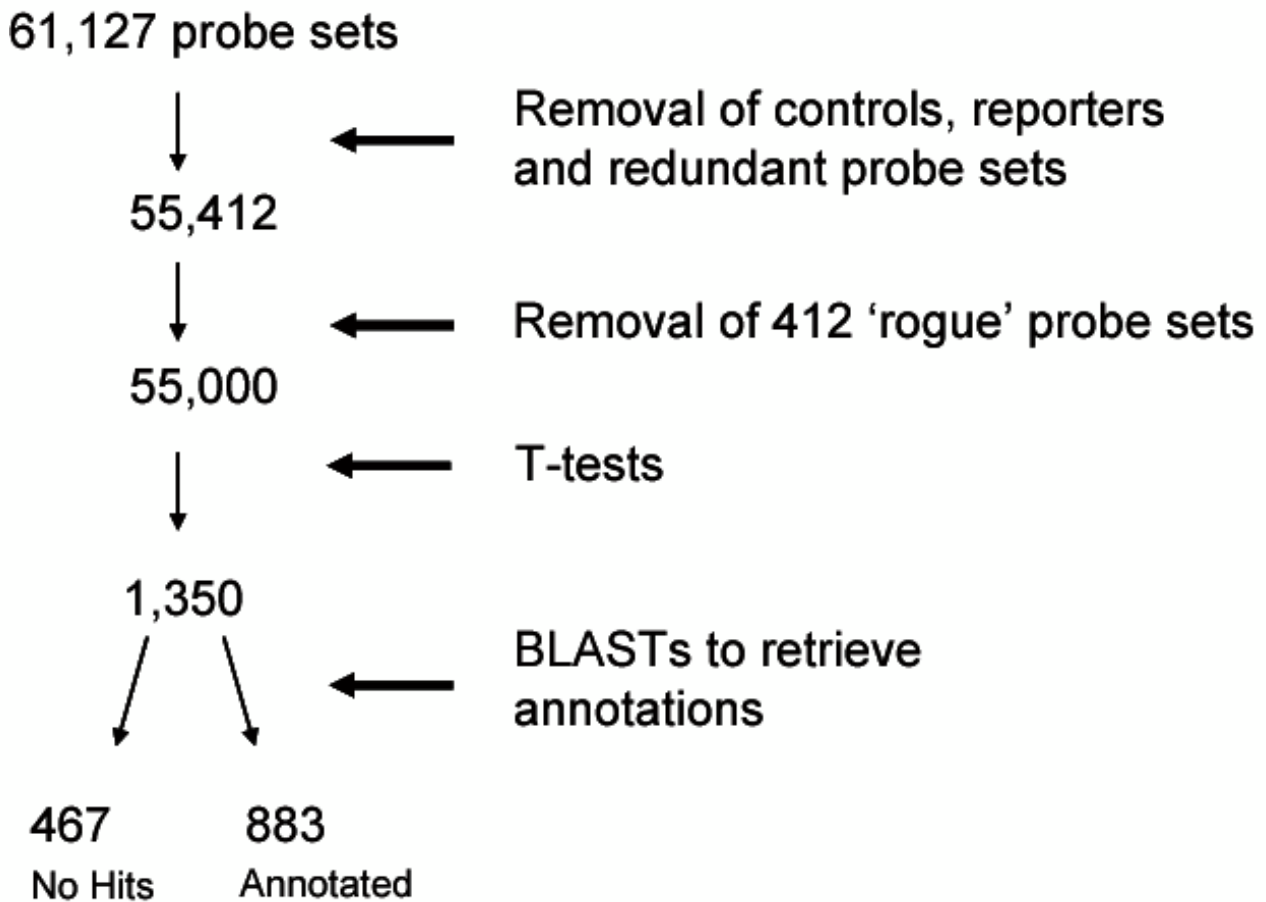
Figure 2
Filtration process used for Affymetrix wheat GeneChip® data. The controls and 'rogue' probe sets were removed from the data prior to filtration. Meiotically-regulated transcripts were then identified using t-tests, with NCBI database annotations retrieved for the remaining transcripts where available (*E*-value < e^{-10}).

those related to hormone regulation, signal transduction and development, as well genes involved in metabolic process. 146 probe sets fell into one of ten categories (Figure 4).

During the first five meiotic stages used in this study, the majority of the categories showed no significant increase or decrease in the level of expression, indicating a degree of transcriptional stability in the anthers over these stages of development. However, there were more pronounced effects when comparing the mature anther stage across all 10 functional categories. In general, all 10 categories showed decreased levels of expression during this stage of development when compared to the other tissues investigated. This trend is particularly evident in the meiosis/cell

division and ribosomal categories, inferring that the mRNA of these candidates is down-regulated in mature anthers. While not as significant, the transcription factors, organelle activity, signal transduction, lipid metabolism, development and protein metabolism categories also displayed this downward trend as the anther matured. This decline is occurring as the pollen matures and reflects the shutting down of cell division, expansion and differentiation.

Meiotic clusters
Hierarchical clustering
Hierarchical clustering of the 1,350 meiotically-regulated transcripts was performed to identify common gene expression patterns (Figure 5). This revealed two clusters
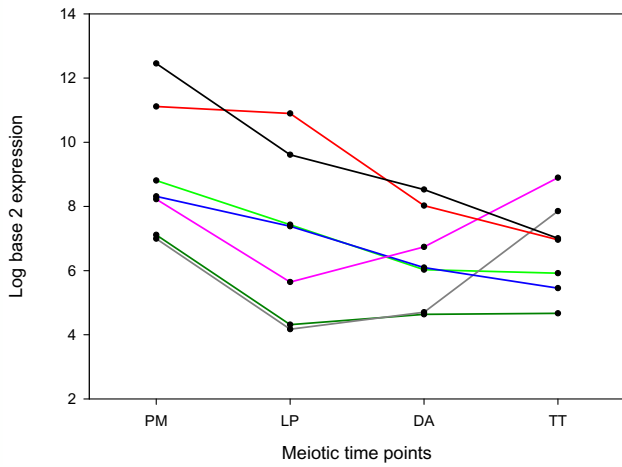
Figure 3
Transcripts with at least an eight-fold change in expression level between and including pre-meiosis to telophase II. Black = TaAffx.9800.1.S1_at; red = TaAffx.60258.2.S1_s_at; light green = Ta.10020.1.S1_at; blue = Ta.6922.1.S1_at; pink = TaAffx.38162.1.S1_at; dark green = Ta.16669.1.S1_x_at; and grey = Ta.6831.1.S1_at. PM, LP, DA and TT are as described in Figure 1.

with 88 and 50 transcripts (indicated by I and II on Figure 5) that were expressed at low levels throughout pre-meiosis to immature pollen, only to then rise sharply at the onset of mature anther development (fold changes of 12.91 and 3.12, respectively). Within these two clusters, there were a number of transcripts present with known annotations to genes that have roles in flower development. One such candidate is the GRAB2 protein [33], which contains a NAM (no apical meristem) domain. NAM domains are part of the NAC domain family [34], which have been shown to have roles in cell division and cell expansion in floral organs, as well as determining the positions of meristems and primordia [35]. Another identified transcript, *NEC1*, has been reported to have a role in the opening of anthers in petunia (*Petunia hybrida*) [36].

In addition to these flowering candidates, two *PIP1* aquaporin transcripts that have previously been isolated from wheat were identified. One could speculate that the up-regulation of aquaporins during pollen maturation helps prevent damage to reproductive structures. Previous work suggests that the products of this gene family help prevent chilling injury [37]. Although other annotated candidates were identified from these two clusters, approximately 53% of the transcripts showed no similarity to any known genes or proteins in the public databases (August 2006). An investigation of the roles of these unknown transcripts is likely to be useful in clarifying the developmental process involved in pollen maturation in
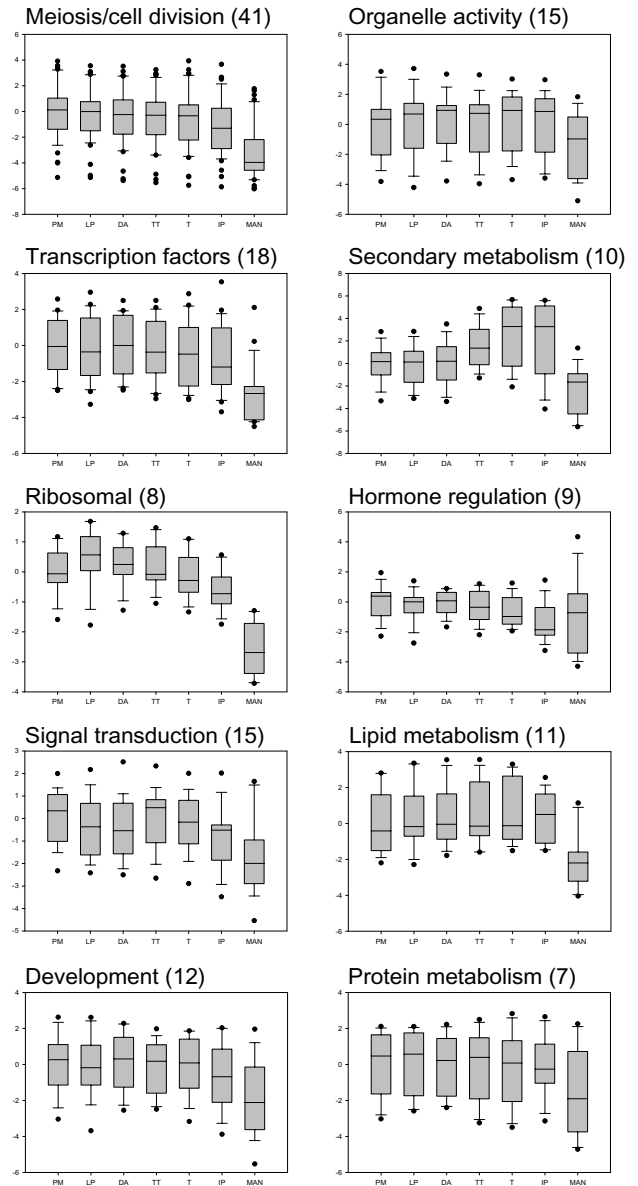
Figure 4
Functional classifications and expression analysis from the developing wheat anther. Transcripts were pooled into categories based upon their annotations and having satisfied the following criteria: an *E*-value < e^{-30}, a sequence length > 250 bp and their cross-hybridizing status (based on the Affymetrix designation). The data for each functional category is represented as log base 2, RMA normalized values that were centered on the average of the pre-meiosis (PM) value. Representations (n) assigned to each functional category are indicated in brackets.
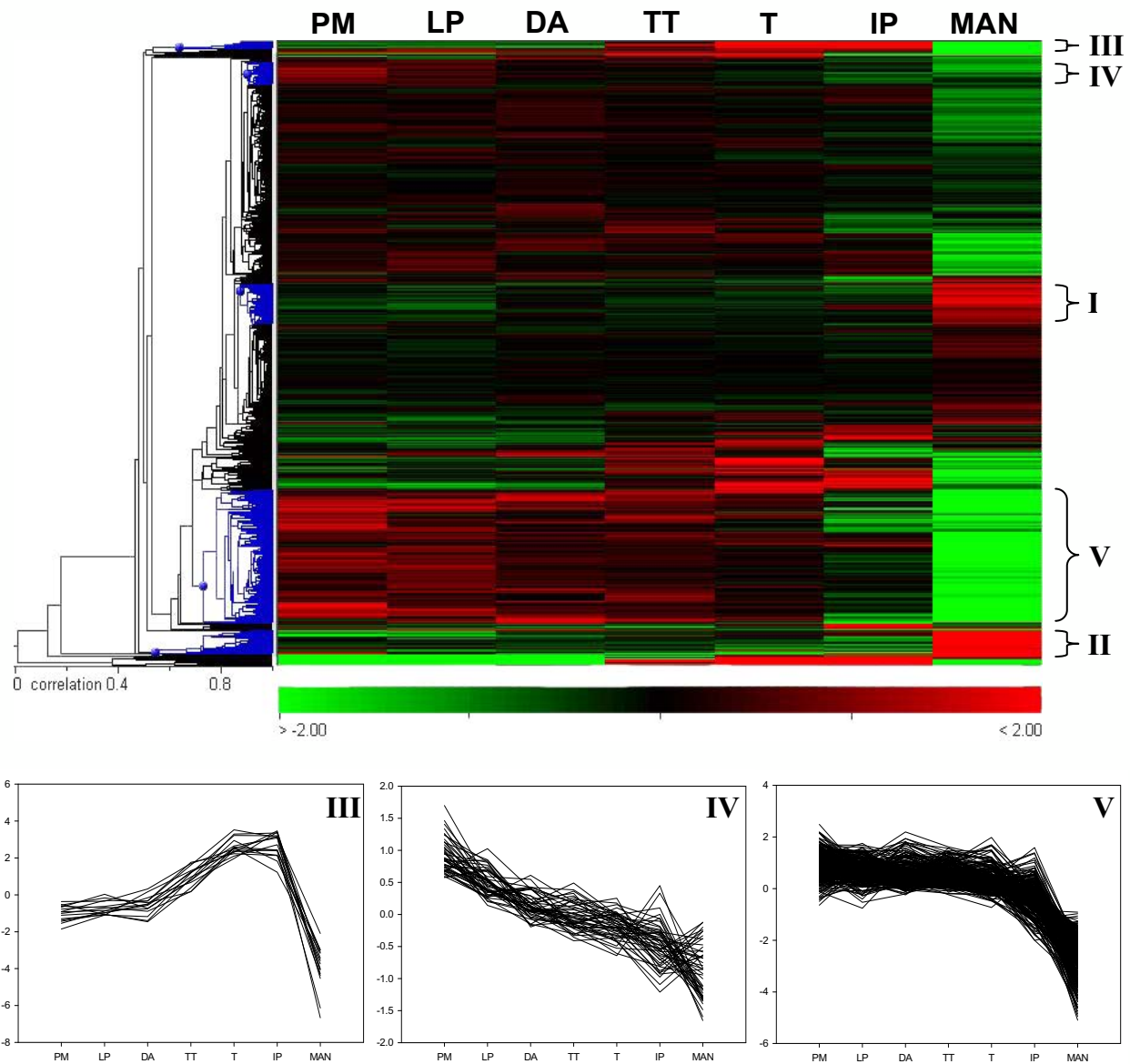
Figure 5
Hierarchical clustering of 1,350 meiotically-regulated transcripts. The expression profiles of 1,350 transcripts (rows) were grouped across seven staged anthers (columns); pre-meiosis (PM), leptotene to pachytene (LP), diplotene to anaphase I (DA), telophase I to telophase II (TT), tetrads (T), immature pollen (IP) and mature anthers (MAN) (averages shown). Clusters of interest (described in text) are highlighted in blue and labelled I and II (pollen clusters); III, IV and V (meiotic clusters). The Y-axis for cluster groups III, IV and V is centered, log base 2, RMA normalized values.

wheat and other cereals. In particular, these genes are expressed shortly before full pollen maturity and dehiscence. As the anthers used to prepare this RNA were still green, at this stage there will be genes likely to be involved in preparing the pollen for release. This is consistent with the putative role for the *PIP* genes in desiccation protec-

tion. Investigation of other genes in this group may provide valuable targets for general stress or desiccation tolerance.

Although the meiotic stages examined in this study could have been more tightly defined (for example, leptotene

could have been separated from pachytene), the timing and collection of such specific events during wheat meiosis would not have guaranteed producing improved resolution. While Chu and colleagues [6] and Primig *et al.* [7] divided their meiotic profiles into seven different categories, these experiments used yeast, where synchronization and identification of specific individual meiotic stages is simple. The meiotic time series used here is significantly more detailed than those examined in other plant systems. Meiosis I and II in bread wheat anthers is completed within 24 hours, with prophase I (which includes leptotene, zygotene, pachytene, diplotene and diakinesis) taking 17 hours [14]. In contrast to other grasses, this is one of the most rapid to complete meiosis with rye (*Secale cereale*) taking 51 hours and barley (*Hordeum vulgare*) taking 39 hours [15]. This is partially explained by Bennett and Smith [14] who showed that in wheat, rye and *Triticale* the duration of meiosis decreases as the ploidy level increases.

Besides cluster groups I and II previously described, at least three clusters (indicated by III, IV and V on Figure 5) appeared to be meiotically-regulated, suggesting that meiotic genes undergo subtle changes in expression, rather than sharp increased or decreased bursts of expression. Possible reasons accounting for these observations include; 1) there may not be a large number of genes exclusively involved in meiosis, irrespective of the number of genes within the organism's genome; 2) meiosis classifications are largely based on cytological observations and may not reflect what is occurring at the transcript level, and 3) the 'dilution effect' of other tissues present in wheat anthers. It should be noted that during meiosis, chromatin is heavily condensed and this may pose limitations for the transcriptional machinery of the cell. Consequently, the expectation would be for gene expression to be restricted to genes essential to the meiotic process. Transcripts required for other functions, such as general cell metabolism, would most effectively be provided prior to the onset of meiotic condensation.

Of the meiotically-regulated clusters identified, one cluster contained only 15 transcripts, while the other two contained 48 and 287 transcripts (indicated on Figure 5 by III, IV and V respectively). The cluster of 15 transcripts (III) showed enhanced expression during the latter stages of meiosis I. Consequently, these genes may be involved in the latter stages of meiosis or the early stages of pollen maturation. While 33% of these transcripts showed no similarity to any known sequences in the public databases (August 2006), one transcript was similar to a gene encoding a male fertility protein from both maize (Accession Number: NP_912416) and wheat (Accession Number: AAV70496) suggesting that this transcript has a role in pollen maturation as opposed to meiosis. When examin-

ing the other two cluster groups (indicated by IV and V on Figure 5), many transcripts were identified that have already been reported to have roles in processes that occur during early meiosis. Not only were transcripts that had significant similarities to cell cycle proteins, kinesin-related proteins and chromomethylases identified but candidates implicated in chromosome pairing, synapsis and recombination were also represented.

To gain insight into the functional roles of genes identified in these three clusters a similar strategy to that of Iguchi and colleagues [38] was used, whereby transcripts were assigned to a biological category based on annotated functions. In cluster groups III, IV and V, approximately 40% of the 350 transcripts (pooled value from the three clusters) were either functionally not annotated or novel (with no database matches returned) (Table 1). While the classifications of the 350 transcripts ranged from functional categories as diverse as abiotic stress-related and secondary metabolism, a reasonable proportion (17%) represented unambiguous meiotic and/or cell division candidates (Table 1). These transcripts were assigned to a specific meiotic and/or cell division category based on their annotation (Figure 6). Transcripts showing significant database matches to histones, cell cycle and cytoskeletal candidates isolated from other organisms, as well as chromosome-associated, recombination and mismatch repair genes were all identified.

Table 1: Functional classifications for 350 meiotically-regulated transcripts.

Category	Representations (%)
Meiosis/cell division	60 (17.1)
Cellular metabolism	24 (6.86)
Transcription factors and DNA binding	18 (5.14)
Ribosomal	15 (4.29)
Biotic stress-related	12 (3.43)
Membrane transport	12 (3.43)
Signal transduction	10 (2.86)
RNA processing	10 (2.86)
Development	8 (2.29)
Organelle activity	8 (2.29)
Secondary metabolism	7 (2.00)
Hormone regulation	5 (1.43)
Abiotic stress-related	5 (1.43)
Lipid metabolism	4 (1.14)
Protein metabolism	4 (1.14)
Protein transport	4 (1.14)
Protein folding	2 (0.57)
Function not annotated	52 (14.86)
No hits found	90 (25.71)

These transcripts were pooled from clusters III, IV and V (Figure 5), with each individual transcript then allocated a functional category based on annotation and literature searches
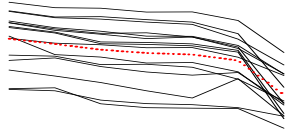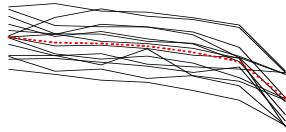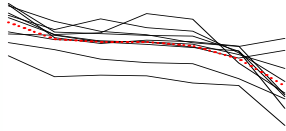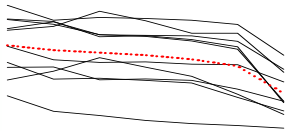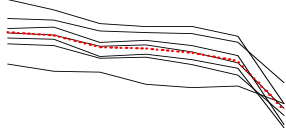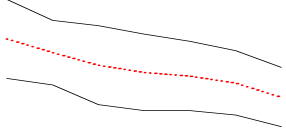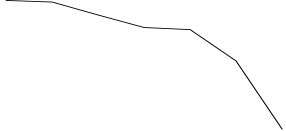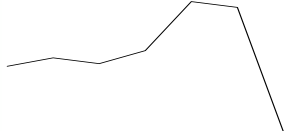
Category	Representations (%)	Histogram	Expression Profile
Histone-related	15 (25.00)		
Cell cycle regulation	14 (23.33)		
Cytoskeletal-associated	10 (16.67)		
Chromosome-associated	10 (16.67)		
Recombination	7 (11.67)		
Mismatch repair	2 (3.33)		
Synaptonemal complex	1 (1.67)		
Fertility-related	1 (1.67)		

Figure 6
Functional classifications for the 60 meiosis and/or cell division transcripts identified from Table 1. These transcripts were classified into functional categories based on the annotation obtained. The histogram represents the absolute values for each category, while the expression profiles for each of the candidates within each of the categories has also been shown. The red dotted line in the expression profile graphs represents the overall trend line for that category.

Transcripts involved in early meiosis

The key aim of the experiments described here was to identify genes that may be involved in controlling the early stages of meiosis. Therefore we were particularly interested in transcripts that showed expression only in the early meiotic stages. These were identified based on transcripts with an RMA normalized value > 6 for either PM or LP and < 5 for all stages thereafter. Interestingly only four transcripts were identified, of which three (TaAffx.11970.3.S1_s_at, TaAffx.29005.1.S1_at and TaAffx.86700.1.S1_at) showed no significant similarity to sequences in the NCBI and TIGR databases. The remaining transcript (Ta.400.2.A1_at) returned a significant hit of $6e^{-59}$ to a putative condensin complex subunit from rice (BLASTx). The condensin complex has been reported to have varying roles during both mitosis and meiosis, including chromosome segregation and spindle assembly. These genes are clearly prime candidates for further study since they might have a role in coordinating the early meiotic event of recombination.

From the 1,350 putative meiotic transcripts identified through gene filtration, many appear to be orthologous to genes from other organisms that are known to be involved in meiosis. Specifically, there are representatives of genes involved in processes such as synapsis, *TaASY1* (an orthologue of *AtASY1*, *Arabidopsis* asynapsis 1) (Boden *et al.*, unpublished data). Furthermore, there are several mismatch repair genes including wheat MutS homologue 2 (*TaMSH2*), wheat MutS homologue 6 (*TaMSH6*), and the previously characterised wheat MutS homologue 7 (*TaMSH7*) [39]. Other putative meiotic transcripts identified within the microarray data include candidates for recombination, such as radiation sensitive *RAD51B* and *RAD51C*, disrupted meiotic cDNA (*DMC1*) and the rice replication protein A1 (*RPA*). Osakabe and colleagues [40] and Bleuyard and colleagues [41] have previously characterised *Arabidopsis* RAD51B (*AtRAD51B*) and found that it is important for double stranded DNA break repair in somatic cells. RAD51C on the other hand, is necessary for homologous recombination in meiosis and mitosis [41-43]. From previously published research, it is evident that RPA is essential for various aspects of DNA metabolism in eukaryotes [for review see [44]]. In rice and *Arabidopsis* there are two different types of RPA [45] with inactivation of the *AtRPA70a* resulting in lethality, thus suggesting a role in DNA replication. However, even though the phenotype appeared normal under standard growth conditions, disruption of *AtRPA70b* resulted in hypersensitivity to mutagens such as UV-B and methyl methanesulfonate. This implied a role in DNA repair processes [45].

Many of the transcripts with significant similarities to previously characterised meiotic genes (some of which have

been described above) displayed analogous patterns within our data set. Therefore it appears that the wheat genes identified here are indeed orthologues of the meiotic genes identified in other organisms. Information on transcript abundance can help identify previously uncharacterized genes that may have roles in homologous recombination. Such transcripts would show co-regulation with known meiotic genes from within this meiotic data set. This assumption is supported by the close similarities in expression profiles between two related mismatch repair genes, *TaMSH7* [39] and *AtMLH1* [46] (correlation coefficient of 0.997).

In addition to the 'known' meiotic genes described above, the wheat data set contains many meiotic transcripts that do not show significant similarity to sequences in the NCBI and TIGR databases (*E*-value < e^{-10}). Three of these transcripts display radically different levels of expression across the meiotic time course investigated (Figure 7). In particular, the transcript corresponding to the Affymetrix probe set TaAffx.38162.1.S1_at displays an extreme expression pattern in the microarray data. This expression profile was confirmed in the Q-PCR analysis. With more than a four-fold drop from PM to LP, and then a rapid 64-fold increase in expression between LP to T, this gene might encode a repressor of an event occurring within the leptotene to pachytene stages such as chromosome pairing, synapsis or recombination. Significantly, there does not appear to be a transcript within the entire data set that
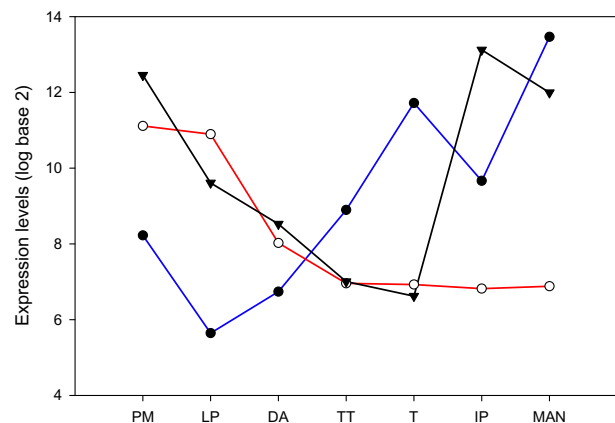
Figure 7
Three novel candidates with significant expression variability across the seven stages investigated. TaAffx.38162.1.S1_at (blue), TaAffx.9800.1.S1_at (black) and TaAffx.60258.2.S1_s_at (red) are highlighted. TaAffx.38162.1.S1_at shows more than a 64-fold increase in expression from LP to T, while TaAffx.9800.1.S1_at drops approximately 64-fold from PM to T. TaAffx.60258.2.S1_s_at is also down-regulated from PM to T approximately 16-fold. PM, LP, DA, TT, T, IP and MAN are as described in Figure 1.

shares a similar expression profile to probe set TaAffx.38162.1.S1_at. Consequently TaAffx.38162.1.S1_at is a worthy candidate for further work to elucidate its role during bread wheat meiosis.

Q-PCR confirmation of microarray data

Q-PCR was conducted in order to validate representative microarray results and examine the correlation between the two expression profiling platforms. A total of 15 primer sets were designed to amplify fragments representing probe sets on the Affymetrix GeneChip® (Table 2). Transcripts were selected based on their meiotic expression profiles and similarity to known meiotic genes (where there was an expression profile to support conservation of function).

The microarray and Q-PCR profiles were closely related. Correlation coefficients ranged from R = 0.73 to R = 0.98, with the exception of one outlier (R = 0.50) (Figure 8). The median correlation coefficient for the microarray/Q-PCR data set was R = 0.95. Overall expression patterns were similar, confirming a high degree of reproducibility between the two platforms. These results parallel those of Honys and Twell [47] and Shary and colleagues [48] who showed similar levels of correlation with reverse transcription PCR and northern blots, respectively.

A pairwise comparison between the Q-PCR results highlighted co-expression between many of the transcripts (Table 3) with a significant number of these transcripts having a correlation of over 0.9. These findings suggest that there are a discrete number of transcription factors that control meiotic genes and hence the regulation of meiotic progression in bread wheat, as has been suggested for yeast [49,50]. In order to further our understanding of meiotic regulation and determine whether any of these candidates are co-regulated, a yeast one-hybrid approach could be employed using the promoter regions of the candidates.

Conclusion

The transcript profiling information generated in this study was designed to help decipher the bread wheat meiome as an important step to manipulate pairing and recombination in plant breeding programs. Over 1,300 transcripts showed meiotic regulation over the tissue series used in this study, with 467 novel transcripts identified. Through hierarchical clustering 60 meiosis and/or cell division candidates were identified as meiotically-regulated. Histone-related, chromosome-associated, recombination and fertility candidates were among those identified in this group. Through comparison with similar research in simpler eukaryotes, it has been possible to draw parallels with the more complex genome of hexaploid bread wheat. A select number of novel candidates in addition to known meiotic genes will now form the basis for further research. The key objective of the study outlined here, has been to provide a resource for meiosis research that can link the strong cytogenetic, genetic and practical research base of wheat to the detailed biochemical and molecular information now emerging from model organisms such as yeast.

Methods

Tissue isolation and RNA extraction

Wild-type wheat (*Triticum aestivum* L. cv. Chinese Spring) was grown in a temperature-controlled glass house at 23°C (day) and 15°C (night) with a 14 hour photoperiod. Anthers were collected and dissected using a Leica MZ6 dissecting microscope. Anther squashes were prepared in order to determine the stage of meiosis. Squashed anther preparations were viewed using a Leica DM1000 compound microscope.

The seven stages collected were pre-meiosis (PM), leptotene to pachytene (LP), diplotene to anaphase I (DA), telophase I to telophase II (TT), tetrads (T), immature pollen (IP) and mature anthers (MAN). Immediately after determining the stage, the remaining two anthers from the floret were placed into liquid nitrogen. After collecting at least 25 staged anthers for each time point from several biological samples, anthers from the respective stages were pooled. Leaf material used in this study was collected from glasshouse-grown plants (six weeks) and total RNA isolated using Trizol® (Gibco BRL, Australia) according to the manufacturer's protocol.

Microarray processing

aRNA from the seven stages were amplified and labelled from one microgram of total RNA with two rounds of amplification. The GeneChip® Two-Cycle cDNA Synthesis Kit (Affymetrix, CA, USA) was used to produce reverse transcribed double-stranded cDNA containing a T7 promoter, which was *in vitro* transcribed using the Ambion Megascript T7 amplification kit (Ambion, TX, USA). This unlabelled aRNA was subsequently reverse transcribed to double stranded cDNA using the GeneChip® Two-Cycle cDNA Synthesis Kit and biotin labelled aRNA was then produced using the GeneChip® IVT Labelling Kit (Affymetrix, CA, USA). Twenty micrograms of aRNA from each of the seven samples were fragmented for hybridization to each microarray. In total three technical replicates were conducted for each of the seven stages examined. Affymetrix GeneChip® Wheat Genome Arrays were used for all samples. The arrays were hybridized and processed according to the manufacturer's specifications.

Microarray analysis

Normalization of the microarray data was conducted using RMA. The software package Acuity 4 (Molecular

Table 2: Primer sets used in Q-PCR analysis.

Candidate	Affymetrix probe set	Acquisition temperature	Sense	Antisense	Product size (bp)
			Sequence	Sequence	
ASY1	Ta.9186.1.S1_at	83	AGGACTCCCACAAGCAATCG	ACCTGCTGGAGGATCGGCTC	159
DMC1	Ta.30833.1.S1_at	80	GCTGAGGAAAGGCAAAGGCG	CGGTGCAGTAGCCTTTGTCGATTT	195
MSH4	Ta.25861.1.A1_at	83	CTGAAGGATGGTGTCCGACG	AGGTCCTGCAATGCTTCACG	252
MSH6	Ta.24096.1.S1_at	80	CATAATATTGGCACAGATTGGAG	CTGACGAAAGCACGGAAGC	161
PHS1	TaAffx.47591.1.S1_at	80	TGATGCTGCTGGTGGAAATTCG	CGGACACTAGGCATGATAGGCG	270
RAD51B	Ta.7197.1.A1_at	81	CTGCCTGGCTGAAGCTGAAG	GATAGAACAAGCAAACTATGGGAG	267
RAD51C	Ta.10540.1.S1_at	79	TATTGATACAGAGGGCAGTTTC	AGCTGCATATTCGGAAGTAG	173
RAD54	Ta.7706.1.S1_at	82	GCTGTCGCAAACCCTTTCG	GTCGTAGGCACCAATCATCCATC	344
RPA	Ta.6986.1.S1_at	83	GAATGTCTTCCGTGAACCG	CATCTAAGGACGGGTGCTAG	274
WM5	Ta.25342.1.S1_at	81	CATCGAGTGGGCTTTAGCTATAG	CAACACGTAGTACGATAGATCCAAG	178
WMC3*	Ta.28776.1.A1_at	79	CGACCGACGGAATTGATATG	CTGTGAGAAGTTTCAGCATTATC	171
WMC4	Ta.30383.1.A1_at	80	GATTCCCAAATGTTCGAC	CAAATTGTCCTCCTTACG	266
WMC5	Ta.3224.2.S1_at	81	CTTGCTGCTCCCAATGATAATTC	CAGTTAGCTGCCAGGTCATCTTTC	245
WMC6	Ta.3385.1.A1_at	80	CGGACAGTCCAGATGTGC	CTATGCTTGCTGCCTGATG	271
WMC10*	TaAffx.38162.1.S1_at	79	AGGAGTTGACATGACAAGATTAGGGAGG	GCCACTTCACATGCACCCATCTAATC	166
Controls					
Cyclophilin		82	CAAGCCGCTGCACTACAAGG	AGGGGACGGTGCAGATGAA	227
EFA1		82	CAGATTGGCAACGGCTACG	CGGACAGCAAAACGACCAAG	227
GAPdH		*78*	TTCAACATCATTCCAAGCAGCA	CGTAACCCAAAATGCCCTTG	220
Actin		77	GACAATGGAACCGGAATGGTC	GTGTGATGCCAGATTTTCTCCAT	236
Flat gene 1	*Ta.9657.1.S1_at*	*83*	CCCTCAGACCGCTGGCAA	GAGGCGGACAGACATGGAAGAA	300
Flat gene 2	*Ta.28350.1.S1_a_at*	*80*	ACGCAGCTACCTGTATCATTCGGATC	GAAGCGACGATGTCCACATGACC	160

Primer sets used and the product sizes obtained in addition to the acquisition temperatures used. Control genes in italics were those selected by geNorm for normalisation.
* indicates those transcripts that have an unclear orientation (not known whether sense or antisense).
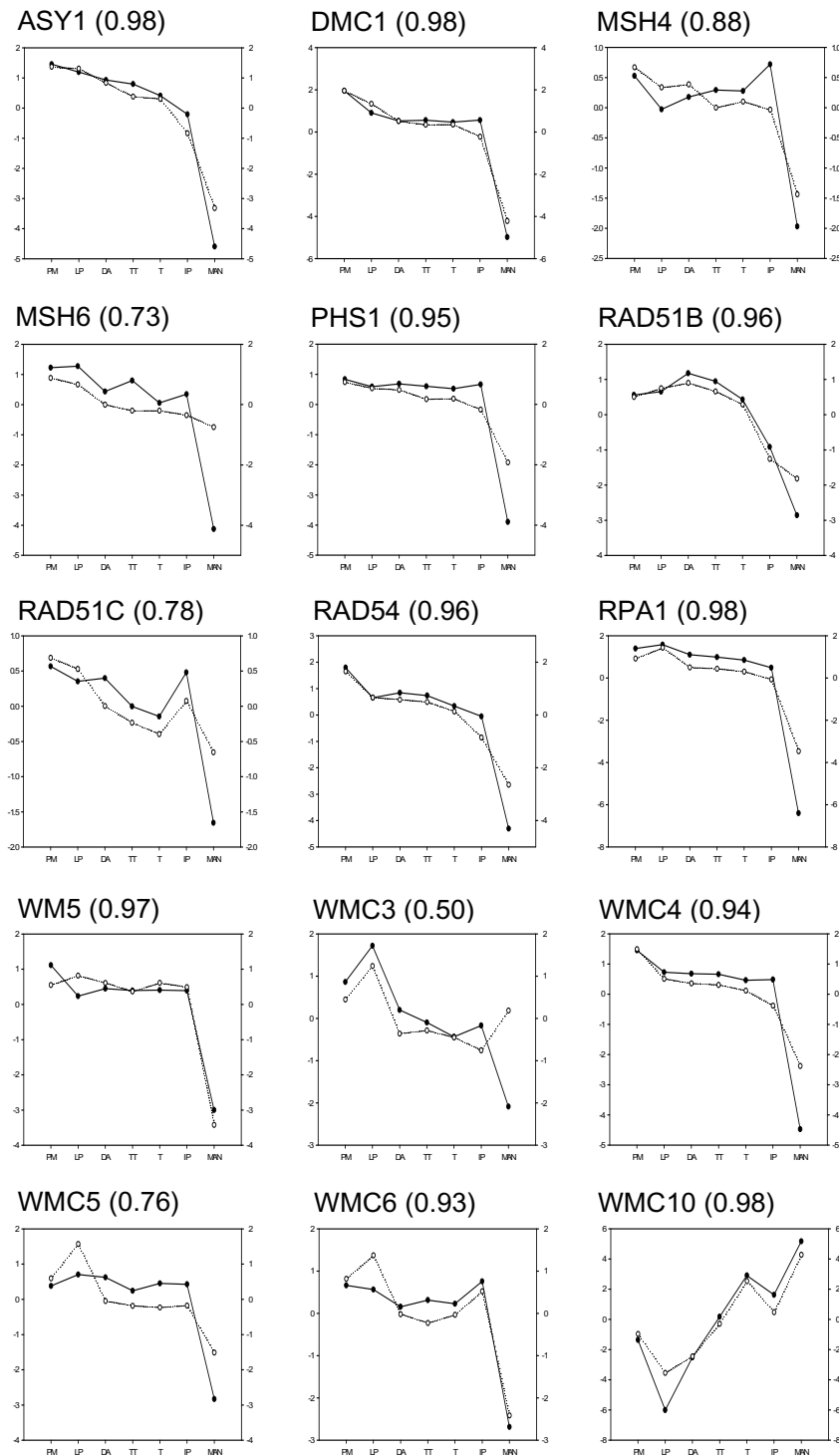
Figure 8
Correlation of the microarray profile with the Q-PCR data from the corresponding transcript. Lines with the open circles represent microarray data, while lines with solid circles represent the Q-PCR data. The data for each transcript from the microarray is log base 2, RMA normalized and centered about its average across the seven stages, while the data for the Q-PCR is log base 2, normalized mRNA copies/μL and centered. Correlation values for each of the transcripts investigated using both technology platforms are indicated.

Table 3: Q-PCR correlation of 15 candidates with one another.

	TaASY1	TaDMC1	TaMSH4	TaMSH6	TaPHS1	TaRAD51B	TaRAD51CS	TaRAD54	TaRPA	TaWM5	TaWMC#3	TaWMC#4	TaWMC#5	TaWMC#6	TaWMC#10
TaASY1	1.00														
TaDMC1	**0.98**	1.00													
TaMSH4	*0.90*	**0.95**	1.00												
TaMSH6	**0.99**	**0.98**	*0.92*	1.00											
TaPHS1	**0.97**	**0.98**	**0.97**	**0.98**	1.00										
TaRAD51B	*0.94*	0.87	0.76	0.89	0.88	1.00									
TaRAD51CS	*0.93*	**0.96**	*0.94*	**0.95**	**0.96**	0.79	1.00								
TaRAD54	**0.99**	**0.99**	*0.92*	**0.98**	**0.97**	*0.92*	*0.94*	1.00							
TaRPA	**0.99**	**0.98**	*0.93*	**0.99**	**0.99**	*0.91*	**0.95**	**0.98**	1.00						
TaWM5	**0.97**	**0.99**	**0.97**	**0.97**	**0.99**	0.87	**0.95**	**0.99**	**0.98**	1.00					
TaWMC#3	0.87	0.84	0.67	0.89	0.79	0.76	0.84	0.83	0.84	0.78	1.00				
TaWMC#4	**0.99**	**1.00**	**0.96**	**0.99**	**0.99**	0.89	**0.96**	**0.99**	**0.99**	**1.00**	0.82	1.00			
TaWMC#5	**0.97**	**0.96**	*0.94*	**0.97**	**0.99**	0.89	**0.95**	**0.95**	**0.99**	**0.96**	0.82	**0.98**	1.00		
TaWMC#6	*0.94*	**0.98**	**0.97**	**0.97**	**0.99**	0.80	**0.97**	*0.94*	**0.97**	**0.97**	0.81	**0.98**	**0.97**	1.00	
TaWMC#10	-0.74	-0.65	-0.46	-0.74	-0.62	-0.71	-0.70	-0.68	-0.69	-0.59	-0.93	-0.65	-0.68	-0.62	1

Q-PCR products with a transcript correlation greater than or equal to 0.95 and less than 1 are in bold, while correlations smaller than 0.95 but greater than or equal to 0.9 are italicized.

Devices, CA, USA) was then used to analyze the microarray data. Microarray expression ratios were presented as log-transformed base 2. Gene annotations were obtained through batch BLASTs (BLASTx; E-value < e^{-10}) using the Affymetrix probe set sequences in tandem with sourcing annotations directly from the Affymetrix website. In total, 412 'rogue' probe sets were discarded from the analysis due to technical problems during the microarray processing.

All p-values referred to in the text are corrected p-values that were obtained using student's t-tests assuming equal variances and using the Benjamini-Hochberg method [51]. These p-values were used to determine whether transcripts were temporally-regulated during meiosis.

Suitable probe sets from the 1,350 transcripts used for expression analysis in the developing wheat anther were selected based on several criteria. Probe sets designated by Affymetrix not to cross-hybridize outside of their gene family were selected if they had a consensus sequence > 250 bp and had a BLASTx match with an E-value < e^{-30}. The 633 transcripts that remained were then assigned to functional categories of interest based on literature searches of the BLASTx matches. The average of the pre-meiosis (PM) values for each respective functional category was then subtracted from every data point. The line graphs and box and whisker plots presented here were produced using Sigma Plot (Version 9) (Systat Software, IL, USA).

Hierarchical clustering analysis focussed on transcript expression patterns rather than absolute values and the triplicate data over the seven stages was averaged. The average of every row (that is, every transcript) was then subtracted from every signal intensity in the gene expression matrix. The rows were then clustered using a Euclidean squared similarity metric and the average linkage method. Acuity 4.0 (Molecular Devices, CA, USA) was also used to apply principal component analysis to the data set.

Microarray data set
The microarray data set has been deposited in the Gene Expression Omnibus (GEO) database (Accession: GSE6027).

cDNA synthesis and Quantitative Real-Time PCR
Seven independent cDNA synthesis reactions were made for the staged anthers (PM, LP, DA, TT, T, IP and MAN) using the same RNA that was hybridized to the wheat GeneChip®. RNA (1 µg) was used as template for the cDNA synthesis reaction with Superscript III RNAse H-

Reverse Transcriptase (Invitrogen, Australia) according to the manufacturer's instruction.

For each gene investigated using Q-PCR, a dilution series covering seven orders of magnitude was prepared from 10^9 copies/µL stock solution as detailed in Burton and colleagues [52]. Three replicates of each of the seven standard concentrations were included with every Q-PCR experiment together with a minimum of three no template controls. Q-PCR experiments were assembled by a liquid handling robot, a CAS-1200 robot (Corbett Robotics, Australia). Three replicate PCRs for each of the cDNAs were included in every run.

Two µL of the cDNA solution or the diluted standard or water was used in a reaction containing 5 µL of IQ SYBR Green PCR reagent (Bio-Rad Laboratories, California, USA), 1.2 µL each of the forward and reverse primers at 4 µM, 0.3 µL of 10X SYBR Green in water and 0.3 µL of water. The total volume of this PCR was 10 µL.

Reactions were performed in a RG 3000 Rotor-Gene Real Time Thermal Cycler (Corbett Research, Australia) as follows; 3 minutes at 95°C followed by 45 cycles of 1 second at 95°C, 1 second at 55°C, 30 seconds at 72°C and 15 seconds at the optimal acquisition temperature described in Table 2. A melt curve was obtained from the product at the end of the amplification by heating from 70°C to 99°C. Using the Rotor-Gene V6 software (Corbett Research, Australia) the optimal cycle threshold (CT) was determined from the dilution series, with the raw expression data derived. The mean expression level and standard deviation for each set of three replicates for each cDNA was calculated.

Quantitative Real-Time PCR normalisation
The normalisation strategy by Burton and colleagues [52] was used in this time course experiment. Four control genes were assessed (*actin*, *GAPdH*, *EFA* and *cyclophilin*). The three best control genes from this set were selected, with normalisation factors calculated using the geNorm program [53].

While these genes have been used in other studies the consistency of expression of the best three control genes in this case was found to be poor. A measure of consistency was obtained by examining the M value [53], where a high M value indicates that a control gene has a very disparate expression with respect to other control genes. The highest M value from the best three genes in these experiments was approximately 1.7. Based on other time course experiments conducted, we anticipated M values of approximately 1.0. To address this concern, further control genes were tested until an acceptable M value was obtained. Two

additional genes were selected from the microarray data (Ta.9657.1.S1_at and Ta.28350.1.S1_a_at) in addition to the four 'standard' Q-PCR control genes mentioned above.

Selection criteria imposed for identifying the additional control transcripts were based on a similar strategy to Czechowski and colleagues [54]. Additionally, the signal intensities were greater than five (log base 2) in all 21 arrays with the triplicate data for the transcripts having a standard deviation of less than 0.1. Probes sets that Affymetrix denoted as being likely to cross hybridize were not selected. After re-calculating the normalization factors using geNorm, the highest M value from the three best control genes was reduced to 0.68 and the raw expression values for the genes of interest in each cDNA were divided by the normalization factor for that cDNA to produce the normalized expression data.

Authors' contributions
WC conducted the research, analyzed the data and drafted the manuscript. UB and TS designed the research, analyzed the data and drafted the manuscript. NS, TW and GS contributed analytical tools and analyzed the data. PL designed the research and drafted the manuscript. JAA designed and conducted the research, analyzed the data and drafted the manuscript. All authors read and approved the final manuscript.

Acknowledgements

References
1. Chao S, Sharp PJ, Worland AJ, Warham EJ, Koebner RMD, Gale MD: **RFLP-based genetic maps of wheat homoeologous group 7 chromosomes.** *Theor Appl Genet* 1989, **78**:495-504.
2. Hulbert SH, Richter TE, Axtell JD, Bennetzen JL: **Genetic mapping and characterization of sorghum and related crops by means of maize DNA probes.** *Proc Natl Acad Sci USA* 1990, **87**:4251-4255.
3. Devos KM: **Updating the 'crop circle'.** *Curr Opin Plant Biol* 2005, **8**:155-162.
4. Paterson AH, Bowers JE, Burow MD, Draye X, Elsik CG, Jiang CX, Katsar CS, Lan TH, Lin YR, Ming RG, Wright RJ: **Comparative genomics of plant chromosomes.** *Plant Cell* 2000, **12**:1523-1540.
5. Francki M, Carter M, Ryan K, Hunter A, Bellgard M, Appels R: **Comparative organization of wheat homoeologous group 3S and 7L using wheat-rice synteny and identification of potential markers for genes controlling xanthophyll content in wheat.** *Funct Integr Genom* 2004, **4**:118-130.
6. Chu S, DeRisi J, Eisen M, Mulholland J, Botstein D, Brown PO, Herskowitz I: **The transcriptional program of sporulation in budding yeast.** *Science* 1998, **282**:699-705.
7. Primig M, Williams RM, Winzeler EA, Tevzadze GG, Conway AR, Hwang SY, Davis RW, Esposito RE: **The core meiotic transcriptome in budding yeasts.** *Nat Genet* 2000, **26**:415-423.
8. Andrews J, Bouffard GG, Cheadle C, Lu JN, Becker KG, Oliver B: **Gene discovery using computational and microarray analysis of transcription in the *Drosophila melanogaster* testis.** *Genome Res* 2000, **10**:2030-2043.
9. Reinke V, Smith HE, Nance J, Wang J, Van Doren C, Begley R, Jones SJM, Davis EB, Scherer S, Ward S, Kim SK: **A global profile of germline gene expression in *C. elegans* .** *Mol Cell* 2000, **6**:605-616.
10. Schlecht U, Demougin P, Koch R, Hermida L, Wiederkehr C, Descombes P, Pineau C, Jegou B, Primig M: **Expression profiling of mammalian male meiosis and gametogenesis identifies novel candidate genes for roles in the regulation of fertility.** *Mol Biol Cell* 2004, **15**:1031-1043.
11. Pang AL, Johnson W, Ravindranath N, Dym M, Rennert OM, Chan WY: **Expression profiling of purified male germ cells: stage-specific expression patterns related to meiosis and postmeiotic development.** *Physiol Genomics* 2006, **24**:75-85.
12. Bennett MD: **The duration of meiosis.** *Proc R Soc London Ser B* 1971, **178**:277-299.
13. Bennett MD, Chapman V, Riley R: **The duration of meiosis in pollen mother cells of wheat, rye and *Triticale* .** *Proc R Soc London Ser B* 1971, **178**:259-275.
14. Bennett MD, Smith JB: **The effects of polyploidy on meiotic duration and pollen development in cereal anthers.** *Proc R Soc London Ser B* 1972, **181**:81-107.
15. Bennett MD, Finch RA, Smith JB, Rao MK: **The time and duration of female meiosis in wheat, rye and barley.** *Proc R Soc London Ser B* 1973, **183**:301-319.
16. Roberts MA, Reader SM, Dalgliesh C, Miller TE, Foote TN, Fish LJ, Snape JW, Moore G: **Induction and characterization of *Ph1* wheat mutants.** *Genetics* 1999, **153**:1909-1918.
17. Martinez-Perez E, Shaw P, Moore G: **The *Ph1* locus is needed to ensure specific somatic and meiotic centromere association.** *Nature* 2001, **411**:204-207.
18. Prieto P, Shaw P, Moore G: **Homologue recognition during meiosis is associated with a change in chromatin conformation.** *Nat Cell Biol* 2004, **6**:906-908.
19. Tanksley SD, Zamir D, Rick CM: **Evidence for extensive overlap of sporophytic and gametophytic gene expression in tomato.** *Science* 1981, **213**:453-455.
20. Gorla MS, Frova C, Binelli G, Ottaviano E: **The extent of gametophytic-sporophytic gene expression in maize.** *Theor Appl Genet* 1986, **72**:42-47.
21. Druka A, Muehlbauer G, Druka I, Caldo R, Baumann U, Rostoks N, Schreiber A, Wise R, Close T, Kleinhofs A, Graner A, Schulman A, Langridge P, Sato K, Hayes P, McNicol J, Marshall D, Waugh R: **An atlas of gene expression from seed to seed through barley development.** *Funct Integr Genomics* 2006, **6**:202-211.
22. Taylor LP, Hepler PK: **Pollen germination and tube growth.** *Annu Rev Plant Physiol Plant Mol Biol* 1997, **48**:461-491.
23. Mascarenhas JP: **Molecular mechanisms of pollen tube growth and differentiation.** *Plant Cell* 1993, **5**:1303-1314.
24. McCormick S: **Control of male gametophyte development.** *Plant Cell* 2004:142-153.
25. Muschietti J, Dircks L, Vancanneyt G, McCormick S: **LAT52 protein is essential for tomato pollen development: pollen expressing antisense LAT52 RNA hydrates and germinates abnormally and cannot achieve fertilization.** *Plant J* 1994, **6**:321-338.
26. Muschietti J, Eyal Y, McCormick S: **Pollen tube localization implies a role in pollen-pistil interactions for the tomato receptor-like protein kinases LePRK1 and LePRK2.** *Plant Cell* 1998, **10**:319-330.
27. Kim HU, Cotter R, Johnson S, Senda M, Dodds P, Kulikauskas R, Tang WH, Ezcurra I, Herzmark P, McCormick S: **New pollen-specific receptor kinases identified in tomato, maize and Arabidopsis: the tomato kinases show overlapping but distinct localization patterns on pollen tubes.** *Plant Mol Biol* 2002, **50**:1-16.
28. Mascarenhas JP: **Gene activity during pollen development.** *Annu Rev Plant Physiol Plant Mol Biol* 1990, **41**:317-338.
29. Hanson DD, Hamilton DA, Travis JL, Bashe DM, Mascarenhas JP: **Characterization of a pollen-specific cDNA clone from *Zea mays* and its expression.** *Plant Cell* 1989, **1**:173-179.
30. Ursin VM, Yamaguchi J, McCormick S: **Gametophytic and sporophytic expression of anther-specific genes in developing tomato anthers.** *Plant Cell* 1989, **1**:727-736.
31. Willing RP, Mascarenhas JP: **Analysis of the complexity and diversity of mRNAs from pollen and shoots of *Tradescantia* .** *Plant Physiol* 1984, **75**:865-868.

32. Willing RP, Bashe D, Mascarenhas JP: **An analysis of the quantity and diversity of messenger RNAs from pollen and shoots of *Zea mays*.** *Theor Appl Genet* 1988, **75**:751-753.
33. Xie Q, Sanz-Burgos AP, Guo HS, Garcia JA, Gutierrez C: **GRAB proteins, novel members of the NAC domain family, isolated by their interaction with a geminivirus protein.** *Plant Mol Biol* 1999, **39**:647-656.
34. Aida M, Ishida T, Fukaki H, Fujisawa H, Tasaka M: **Genes involved in organ separation in Arabidopsis: an analysis of the cup-shaped cotyledon mutant.** *Plant Cell* 1997, **9**:841-857.
35. Souer E, van Houwelingen A, Kloos D, Mol J, Koes R: **The no apical meristem gene of *Petunia* is required for pattern formation in embryos and flowers and is expressed at meristem and primordia boundaries.** *Cell* 1996, **85**:159-170.
36. Ge YX, Angenent GC, Dahlhaus E, Franken J, Peters J, Wullems GJ, Creemers-Molenaar J: **Partial silencing of the NEC1 gene results in early opening of anthers in *Petunia hybrida*.** *Mol Genet Genomics* 2001, **265**:414-423.
37. Aroca R, Amodeo G, Fernandez-Illescas S, Herman EM, Chaumont F, Chrispeels MJ: **The role of aquaporins and membrane damage in chilling and hydrogen peroxide induced changes in the hydraulic conductance of maize roots.** *Plant Physiol* 2005, **137**:341-353.
38. Iguchi N, Tobias J, Hecht N: **Expression profiling reveals meiotic male germ cell mRNAs that are translationally up- and down-regulated.** *Proc Natl Acad Sci USA* 2006, **103**:7712-7717.
39. Dong CM, Whitford R, Langridge P: **A DNA mismatch repair gene links to the *Ph2* locus in wheat.** *Genome* 2002, **45**:116-124.
40. Osakabe K, Abe K, Yamanouchi H, Takyuu T, Yoshioka T, Ito Y, Kato T, Tabata S, Kurei S, Yoshioka Y, Machida Y, Seki M, Kobayashi M, Shinozaki K, Ichikawa H, Toki S: **Arabidopsis Rad51B is important for double-strand DNA breaks repair in somatic cells.** *Plant Mol Biol* 2005, **57**:819-833.
41. Bleuyard J, Gallego ME, Savigny F, White CI: **Differing requirements for the Arabidopsis Rad51 paralogs in meiosis and DNA repair.** *Plant J* 2005, **41**:533-545.
42. Abe K, Osakabe K, Nakayama S, Endo M, Tagiri A, Todoriki S, Ichikawa H, Toki S: **Arabidopsis *RAD51C* gene is important for homologous recombination in meiosis and mitosis.** *Plant Physiol* 2005, **139**:896-908.
43. Li W, Yang X, Lin Z, Timofejeva L, Xiao R, Makaroff CA, Ma H: **The *AtRAD51C* gene is required for normal meiotic chromosome synapsis and double-stranded break repair in Arabidopsis.** *Plant Physiol* 2005, **138**:965-976.
44. Wold MS: **Replication Protein A: A heterotrimeric, single-stranded DNA-binding protein required for eukaryotic DNA metabolism.** *Annu Rev Biochem* 1997, **66**:61-92.
45. Ishibashi T, Koga A, Yamamoto T, Uchiyama Y, Mori Y, Hashimoto J, Kimura S, Sakaguchi K: **Two types of replication protein A in seed plants.** *FEBS J* 2005, **272**:3270-3281.
46. Jean M, Pelletier J, Hilpert M, Belzile F, Kunze R: **Isolation and characterization of *AtMLH1*, a MutL homologue from *Arabidopsis thaliana*.** *Mol Gen Genet* 1999, **262**:633-642.
47. Honys D, Twell D: **Comparative analysis of the Arabidopsis pollen transcriptome.** *Plant Physiol* 2003, **132**:640-652.
48. Shary S, Kumar R, Guha-Mukherjee S: **Isolation of pollen early genes and analysis of expression pattern during the development of male gametophyte.** *Plant Sci* 2006, **170**:417-425.
49. Kon N, Krawchuk MD, Warren BG, Smith GR, Wahls WP: **Transcription factor Mts1/Mts2 (Atf1/Pcr1, Gad7/Pcr1) activates the *M26* meiotic recombination hotspot in *Schizosaccharomyces pombe*.** *Proc Natl Acad Sci USA* 1997, **94**:13765-13770.
50. Cunliffe L, White S, McInerny CJ: **DSC1-MCB regulation of meiotic transcription in *Schizosaccharomyces pombe*.** *Mol Gen Genomics* 2004, **271**:60-71.
51. Benjamini Y, Hochberg Y: **Controlling the false discovery rate: a practical and powerful approach to multiple testing.** *J Roy Stat Soc B Met* 1995, **57**:289-300.
52. Burton RA, Shirley NJ, King BJ, Harvey AJ, Fincher GB: **The CesA gene family of barley. Quantitative analysis of transcripts reveals two groups of co-expressed genes.** *Plant Physiol* 2004, **134**:224-236.
53. Vandesompele J, De Preter K, Pattyn F, Poppe B, Van Roy N, De Paepea A, Speleman F: **Accurate normalization of real-time quantitative RT-PCR data by geometric averaging of multiple internal control genes.** *Genome Biol* 2002, **3(7)**:RESEARCH0034.
54. Czechowski T, Stitt M, Altmann T, Udvardi MK, Scheible WR: **Genome-wide identification and testing of superior reference genes for transcript normalization in Arabidopsis.** *Plant Physiol* 2005, **139**:5-17.

Chapter 3 Addendum – Chromosome location of meiotically-regulated transcripts

Research conducted but not presented in Crismani *et al*. (2006).

3.1 – Introduction

While the bread wheat genome is currently being sequenced, the project is far from complete. Although a significant number of expressed sequence tags (ESTs) exist, only a single chromosome has been assembled to date (Paux *et al.*, 2008). It is reasonable to assume that unless a significant breakthrough in sequencing technology becomes available (and affordable), a publicly-available database for bread wheat containing the complete genomic sequence and a genetic map indicating where particular genes reside is some way off. Until such a time, "manual" mapping will frequently be employed to identify the location and copy number of transcripts within this important cereal crop.

Historically, there have been multiple bread wheat loci shown to have a role(s) in chromosome pairing control. These loci, termed *p*airing *h*omoeologous (*Ph*) (Wall *et al.*, 1971b), either suppress homoeologous chromosome associations or promote homologous chromosome interactions (Driscoll, 1972; Riley & Chapman, 1958; Sears, 1976; Sears & Okamoto, 1958). These loci are very large, ranging from 70 to 80 Mbp X-ray induced deletions, to chromosome arms and sometimes, even entire chromosomes. The one exception is *Ph1* which has recently been delineated to a region no larger than 2.5 Mbp (see – Discussion).

Multiple approaches could be taken to further refine these loci. This includes map-based cloning, which can be successful when a single gene or small region is responsible

for the phenotype of interest. Alternatively, comparative genetics can identify candidate genes that fall in large genomic regions which can then be further analysed, such as the study by Sutton *et al.* (2003) which used comparative genetics between the sequenced rice genome and wheat to analyse the *Ph2* locus and identify putative genes in that region which could provide potential targets for further research. More recently, transcriptomics has become increasingly popular with several studies (including that which was reported by Crismani *et al.*, 2006) showing that this technique can be invaluable for identifying key targets that may be associated with trait or developmental process under investigation (see also Kawaura *et al.*, 2008 and Wan *et al.*, 2008).

The following addendum extends the research presented by Crismani and colleagues (2006), by mapping the chromosome location of selected candidate genes from bread wheat which were deemed to be meiotically regulated based on their expression profile. While building our knowledge on these candidate genes, this addendum also interrogates the theory as to whether these meiotically-regulated transcripts preferentially map to known loci involved in meiotic processes, specifically chromosome pairing.

3.2 – Materials and methods

3.2.1 – The candidates

13 of the meiotically-regulated transcripts identified in Crismani *et al.* (2006) were mapped in this study. The eight transcripts with homology to known meiotic genes in other organisms were selected because of their reported roles in chromosome pairing, recombination and synapsis (Bleuyard *et al.*, 2005; Couteau *et al.*, 1999; Grelon *et al.*, 2001; Pawlowski *et al.*, 2004) and their relatively high expression levels (Crismani *et al.*,

2006). The five previously unidentified candidates, termed *Wheat Meiosis Clone 3*, *4*, *5*, *6* and *9* respectively (*TaWMC3*, *TaWMC4*, *TaWMC5*, *TaWMC6*, *TaWMC9*) were selected as they displayed expression profiles similar to the known genes.

Table 3.1 – Meiotically-regulated transcripts mapped using Southern blot analysis. The list includes genes known to be involved in processes including chromosome pairing, recombination and/or synapsis. The Affymetrix accession numbers relate to the accession numbers of the given transcripts on the Affymetrix wheat GeneChip®.

Affymetrix accession	Assigned known homologue if identified	Abbreviation
Ta.30833.1.S1_at	*Disrupted Meiotic cDNA 1*	*DMC1*
Ta.24096.1.S1_at	*MutS Homologue 6*	*MSH6*
TaAffx.47591.1.S1_at	*Poor Homologous Synapsis 1*	*PHS1*
Ta.7197.1.A1_at	*RADiation-sensitive 51 A-2*	*RAD51A-2*
Ta.10540.1.S1_at	*RADiation-sensitive 51 C*	*RAD51C*
Ta.7706.1.S1_at	*RADiation-sensitive 54*	*RAD54*
Ta.6986.1.S1_at	*Replication Protein A*	*RPA*
Ta.14188.1.S1_at	*SPOrulation deficient 11*	*SPO11-1*
Ta.28776.1.A1_at	*Wheat Meiosis Clone 3*	*WMC3*
Ta.30383.1.A1_at	*Wheat Meiosis Clone 4*	*WMC4*
Ta.3224.2.S1_at	*Wheat Meiosis Clone 5*	*WMC5*
Ta.3385.1.A1_at	*Wheat Meiosis Clone 6*	*WMC6*
TaAffx.120000.2.S1_s_at	*Wheat Meiosis Clone 9*	*WMC9*

3.2.2 – Probe design and amplification

Oligonucleotides used to produce Southern probes correspond to those in Table 2 from Crismani *et al.* (2006). Target products were amplified using PCR, with either genomic or complementary wheat DNA (gDNA and cDNA respectively) (cultivar *Chinese Spring*). Each PCR tube (25 µL) contained the following: a 5′ gene-specific oligonucleotide (1 µL, 10 µM), a 3′ gene-specific oligonucleotide (1 µL, 10 µM), 10X PCR buffer (2.5 µL, Invitrogen, U.S.A.), MgCl$_2$ (0.75 µL, 50 mM, Invitrogen), dNTPs (4 µL, 1.25 mM), *Taq* DNA polymerase (0.25 µL, 5 U µL^{-1}, Invitrogen), a cDNA or gDNA library aliquot (1 µL), and milli-Q (MQ) H$_2$O (to 25 µL). Cycling parameters were; denaturation at 95°C for 5 minutes, followed by 35 cycles of denaturation (96°C for 30 seconds), primer annealing

(55°C for 30 seconds) and elongation (68°C for 30 seconds), with a final additional elongation cycle of 72°C for 10 minutes. PCR products were separated on an agarose gel (1.5% w/v), and visualised with ethidium bromide. Product bands were excised and purified using the PureLink Quick Gel Extraction Kit (Invitrogen) according to the manufacturer's instructions.

3.2.3 – Radioactive labelling and binding of probes

Purified PCR products were radioactively labelled as follows: purified DNA (4 µL, probe template) was added to random 9 mers (3 µL) and sterile de-ionised water (0.5 µL). This solution was then incubated in boiling water (100°C for 10 minutes), and then immediately snap frozen on ice for 5 minutes. Oligo buffer (12.5 µL) was then added, followed by Klenow (1 µL, 2 U µL^{-1}, GIBCO BRL, Australia) and ^{32}P (4 µL, α-dCTP, 10 mCi/mL, Amersham, Australia). The tubes were then incubated at 37°C for 2 hours. The labelled products were then purified using the QIAquick® PCR Purification Kit (QIAGEN, Australia). Purified products were then added to individual hybridisation bottles containing membranes with immobilised genomic DNA from a series of 21 nullisomic-tetrasomic plants in a Chinese Spring background representing each chromosome from bread wheat (kindly supplied by Margaret Pallotta; ACPFG, Adelaide, Australia) for 24 hours at 65°C. Typically, all membranes used had already been incubating in a hybridisation oven for 24 hours at 65°C with 10 mL pre-hybridisation buffer (1.5 X HSB [0.9 M NaCl, 30 mM PIPES, 7.5 mM Na$_2$EDTA, pH 6.8], 30% Denhardt's III [0.6% BSA, 0.6% Ficoll 400 (Sigma-Aldrich, Australia), 0.6% PVP, 3% sodium dodecyl sulphate (SDS)], 7.5% dextran sulphate, 400 µg mL^{-1} salmon sperm DNA).

3.2.4 – Membrane washing and autoradiography

Post-hybridisation, unbound probe was removed through multiple washes (20 minutes each), using wash buffers of increasing stringency (2 X standard saline citrate (SSC) [0.3 M NaCl, 0.03 M sodium citrate, pH 7.0], 0.1% SDS (w/v) and proceeded through to 1 X SSC, 0.1% SDS (w/v), 0.5 X SSC, 0.1% SDS (w/v) and 0.2 X SSC, 0.1% SDS (w/v)) until the membranes registered background counts (0.5<cps<2) using a Geiger counter. The initial wash (40 mL) was conducted in the hybridisation bottles within the hybridisation oven (65°C), while subsequent washes (200 mL) were shaken in a container within a water bath (65°C). Membranes were sealed in a plastic sleeve and X-ray film was then exposed to the radioactively-labelled membranes (Kodak Biomax, Kodak, U.S.A.) using an MS Intensifying Screen (Kodak) within a Kodak cassette. The cassette, after pre-cooling at -20°C, was transferred to -80°C for approximately 5 days. The films were developed using an AGFA CP1000 Developer (Victoria, Australia).

3.3 – Results

Using Southern blot analysis, 13 transcripts were successfully mapped to their respective chromosome group (Table 3.2). All of the transcripts investigated in this study have a copy on each of the three genomes' chromosomes (e.g. a gene located on chromosome group 5 will have a copy on 5A, 5B and 5D) (Figure 3.1). Two transcripts map to group 2, two map to group 3, three to group 5 and one to group 6. The five other transcripts mapped to chromosome group 7, which included the putative homologues of *ZmPHS1* (*Zea mays*, maize, *Poor Homologous Synapsis 1*), *AtRAD51A* (*Arabidopsis thaliana*, *Radiation-Sensitive 51A*), *AtRAD54* (*Arabidopsis thaliana RADiation-sensitive 54*) and *AtSPO11-1* (*Arabidopsis thaliana SPOrulation deficient 11*) in addition to a novel transcript, *TaWMC3*

(*Triticum aestivum*, *Wheat Meiosis Clone 3*). None of the 13 transcripts from this study mapped to chromosome groups 1 or 4.

Previously reported literature has shown that many loci whose deletion results in the known meiotic mutations in bread wheat map to either chromosome groups 3 and/or 5. To determine whether there was any significant weighting towards these chromosome groups with the candidates mapped through Southern analysis and those previously reported (an additional 14 transcripts/loci were identified; see Table 3.2 for the complete listing of all 27 combined transcripts/loci); a frequency pie chart was constructed (Figure 3.2). Chromosome group 5 contains the most meiotically-implicated loci with 10 representations, while group 3 has seven represented. Group 7 is the next highest with five, all of which were identified in this study (that is, they are not linked to any of the historical loci previously reported).

Table 3.2 – Compilation of mapping results from this study and the literature. The transcripts/loci map to all chromosome groups except for chromosome group 1. In the 'chromosome location' column, L and S infer that the transcript/loci of interest reside on the long or short arm of the respective chromosomes. A total of 27 transcripts/loci are shown.

Gene/transcript/locus	Chromosome location	Publication
ASY1 (*ASY*napsis *1*)	5A, 5B, 5D, (5BL)	Boden *et al.* (2007)
DMC1	5	This study
MSH6	5	This study
MSH7 (*M*ut*S H*omologue *7*)	3DS (Ph2 locus)	Dong *et al.* (2002)
Ph1 (*P*airing *h*omoeologous *1*)	5BL	Okamoto (1957)
Ph2 (*P*airing *h*omoeologous *2*)	3DS	Mello-Sampayo and Canas (1973)
PHS1	7	This study
RAD51A-2	7	This study
RAD51C	2	This study
RAD54	7	This study
RPA	6	This study
SPO11-1	7	This study
WM5 (*W*heat *M*eiosis *5*)	3DS (Ph2 locus)	Dong *et al.* (2005)
WMC3	7	This study
WMC4	2	This study
WMC5	3	This study
WMC6	3	This study
WMC9	5	This study
3AS homoeologous pairing suppressor	3AS	Mello-Sampayo and Canas (1973)
4D homoeologous pairing suppressor	4	Driscoll (1973)
5DL homologous pairing promoter	5	Sears (1977) and references therein
5AL homologous pairing promoter	5	Sears (1977) and references therein
5BS homologous pairing promoter	5	Sears (1977) and references therein
5DS homologous pairing promoter	5	Feldman (1968)
5AS homologous pairing promoter	5	Dvorak (1976)
2AS asynaptic mutant	2	Sears (1954)
3BL asynaptic mutant	3	Sears (1954)
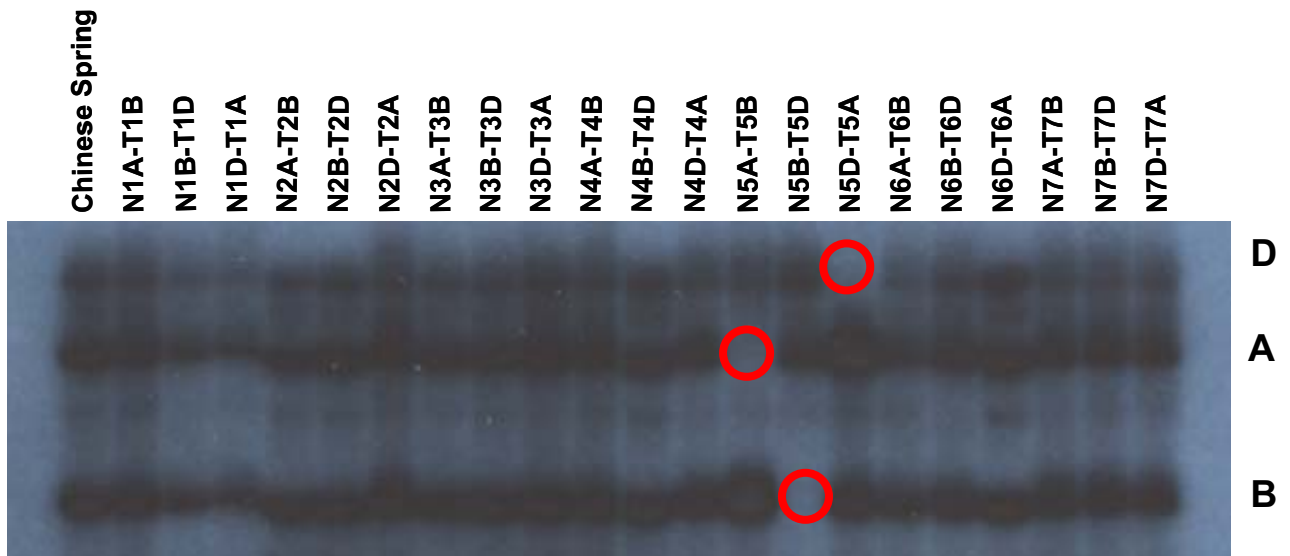
Figure 3.1 – Chromosome location of *TaDMC1* using Southern blot analysis. The missing bands in the autoradiograph that are present in all of the lanes except for those that contain immobilised genomic DNA digested with *Bam*HI that is nullisomic (N) for chromosomes 5A, 5B and 5D, and tetrasomic (T) for chromosome 5B, 5D and 5A respectively, indicate that a copy of the *TaDMC1* transcript is present on chromosomes 5A, 5B and 5D. For examples of other autoradiographs that identify transcript location, see Appendix B. "A", "B" and "D" indicates the band produced by the A, B and D genome copies of the *TaDMC1* transcript respectively.
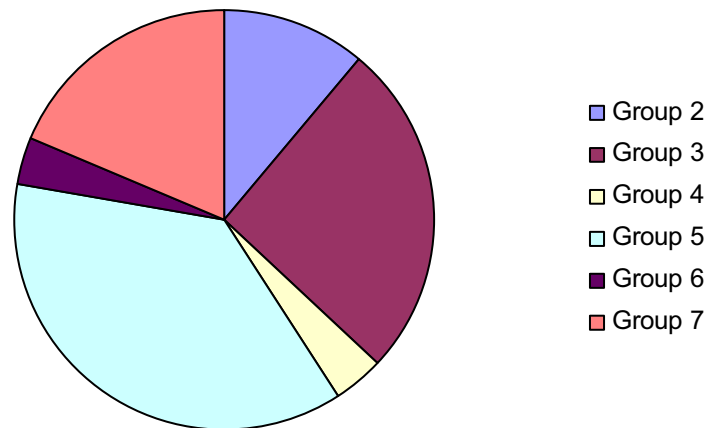
Figure 3.2 – The chromosome location of known meiotically-associated transcripts/loci in bread wheat reported in this addendum. The 27 transcripts/loci map to all chromosome groups except chromosome group 1. Group 2 has three representations, group 3 has seven, group 4 has one, group 5 has 10, group 6 has one, while group 7 has five.

3.4 – Discussion

It is the general rule rather than the exception that genes in bread wheat are located in a specific chromosome group, in each of the three genomes. This is because bread wheat was formed from a hybridisation event approximately 10,000 years ago between three very closely related genomes (Feldman & Levy, 2005). Therefore, the genomic structures of these three species were very similar. All of the transcripts mapped in this study followed this pattern.

This study has provided genetic information for 27 transcripts/loci reported to have a role during meiosis in the bread wheat genome. Given the identification of several candidates having been mapped to previously identified loci, there is a possibility that some redundancy exists. For example, *TaMSH7*, which maps to the *Ph2* locus, may turn out to be responsible for the *ph2* mutant phenotype, or *TaWMC4*, which maps to group 2 may be the

locus on 2AS responsible for the asynaptic phenotype reported previously (Sears, 1954), and so on.

Previous studies have mapped various meiotic genes throughout the bread wheat genome (Boden *et al.*, 2007; Dong *et al.*, 2005; Dong *et al.*, 2002; Mello-Sampayo & Canas, 1973), most notably however, is the research that has been conducted on the *Ph1* locus (Al-Kaff *et al.*, 2007; Griffiths *et al.*, 2006). Interestingly, the majority of the 27 loci in this study (17) were found to be located on either chromosome groups 3 or 5. The chance of a gene being located on a specific chromosome group in wheat is 1/7, if we assume that each chromosome group has roughly the same number of genes (which is not necessarily true). Therefore the chance of a gene mapping to either group 3 or 5 is 2/7. From a total of 27 genes, the number that should theoretically map to groups 3 and 5 (if they were randomly distributed) is: (27 x 2)/7 = 7.7. Given that the results presented here indicate that there are approximately 2.2-fold more than expected, is this chance or is there an evolutionary reason why the *Ph1* and *Ph2* loci, amongst other meiotic candidates are located on these two chromosome groups?

Fine mapping of the *Ph1* locus suggests that *Ph1* is composed of four *CDC2*-related genes (Griffiths *et al.*, 2006) on 5BL which control the speed of chromosome condensation at the initiation of meiosis and prevent homoeologous recombination events (Colas *et al.*, 2008). More extensive sequencing of the region by (Al-Kaff *et al.*, 2007) suggests that there are actually seven *CDK*-like genes within the *Ph1* region on 5BL. Given the size of the original X-ray induced deletion within the *Ph1* locus, it was expected that more than one gene would be responsible for the *ph1b* mutant pairing phenotype, due to a failure to reproduce the phenotype with EMS-induced mutagenesis (Wall *et al.*, 1971b). However the *ph2* mutant phenotype was reproduced with EMS-induced mutagenesis (*ph2b*), suggesting

that the mutation of a single gene is responsible for that phenotype. Single gene disruptions frequently produce dramatic phenotypes which are the result of meiotic errors as evidenced by various mutations in Arabidopsis (for a comprehensive list see Mercier & Grelon, 2008), maize, rice and wheat (Boden *et al.*, 2008; Nonomura *et al.*, 2004; Pawlowski *et al.*, 2004).

In closing, this addendum supplements the work published by Crismani and colleagues (2006) by identifying the chromosome locations for several meiotic candidates in bread wheat. In addition and based on previously known candidates associated with the meiotic process, it suggests that chromosome groups 3 and 5 contain a larger number of investigated candidates than what is statistically expected. Future work will include fine mapping the transcripts from Crismani and colleagues (2006), to discover if they reside within any of the previously identified loci that are responsible for meiotic chromosome pairing phenotypes.

Chapter 4 – Functional analysis of *TaMSH7*

4.1 – Introduction

The *MutS*-based mismatch repair system has been conserved from prokaryotes to eukaryotes and maintains genomic integrity post DNA replication, in addition to reports of suppression of homoeologous recombination in Arabidopsis and moss (Emmanuel *et al.*, 2006; Li *et al.*, 2006; Trouiller *et al.*, 2006). Eukaryotes contain six *MutS H*omologues (*MSH1-6*), with plants having an additional *MutS H*omologue, *MSH7*. *MSH7* is a plant-specific mismatch repair gene which is a paralogue of *MSH6* and is sometimes referred to as *MSH6-2*. In prokaryotes, MutS forms a homo-dimer, however in Arabidopsis *At*MSH2 forms three hetero-dimers with *At*MSH3, *At*MSH6 and *At*MSH7, with each hetero-dimer having a slightly different mismatch recognition spectrum (Culligan & Hays, 2000; Wu *et al.*, 2003).

In bread wheat, *TaMSH7* expression has previously been shown to be strongest in early meiotic spikes and is located in the *Ph2* locus (Dong *et al.*, 2002). As highlighted in chapter one, the *Ph2* locus is responsible for suppressing homoeologous chromosome interactions and was discovered after the generation of X-ray induced deletion mutants (Sears, 1982) and an EMS mutation in the same locus that gave the same phenotype (Wall *et al.*, 1971a). More recent research in transgenic barley using an RNAi *TaMSH7* construct has shown that a reduction in fertility was observed when *HvMSH7* expression was disrupted; implying that there may have been a loss of genomic stability in the absence of *HvMSH7* function possibly due to non-homologous recombination (Lloyd *et al.*, 2007). Given the results of these two studies in cereals, the objective of the research presented in

this chapter was to produce and subsequently analyse *Tamsh7* mutant plants generated using RNAi technology. Through such analysis it may be determined if *TaMSH7* has a role in the maintenance of genomic stability by suppressing recombination between homoeologous sequences.

4.2 – Materials and methods

4.2.1 – Generation of *Tamsh7* mutant plants

4.2.1.1 – *TaMSH7*-RNAi construct production

A plasmid termed p*TaMSH7*-RNAi was produced in collaboration with Professor German Spangenberg's laboratory (a collaborator within the Molecular Plant Breeding Co-operative Research Centre). The plasmid was designed to reduce expression of *TaMSH7* in plants transformed with the construct. The RNAi cassette within the plasmid was driven constitutively by the *Actin1D* promoter (act1D) and terminated by the *35S* terminator sequence (Figure 4.1). These elements drove three fragments, which would form a hairpin RNA structure when expressed: a 615 bp sense fragment of *TaMSH7* which corresponded to position 1349 to 1963 of the *TaMSH7* sequence (NCBI: AF354709), an intron and a 615 bp anti-sense fragment of *TaMSH7* which also corresponded to positions 1349 to 1963 (Figure 4.1). The construct also contained the *Bar* gene which is a selectable marker commonly used in cereal transformation. Expression of the selectable marker was driven by the *Ubiquitin* promoter (ubi) (Figure 4.1).
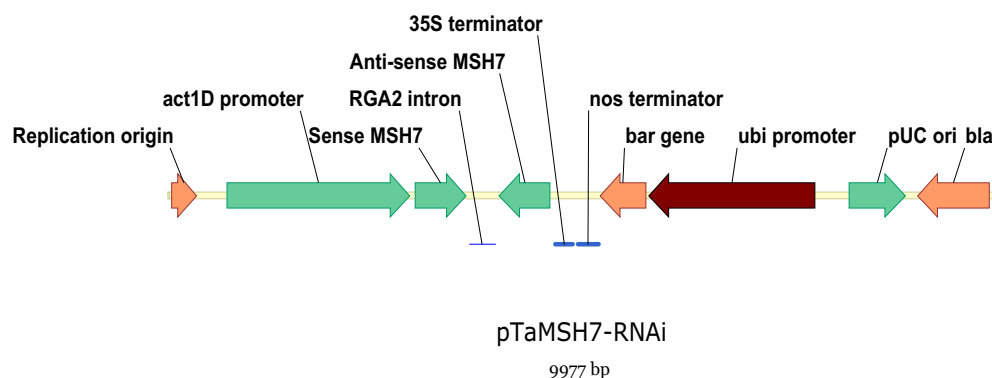
Figure 4.1 – The RNAi construct transformed into wild-type *T. aestivum.* The RNAi cassette was driven by the constitutive *Actin1D* promoter (act1D), contained a sense *TaMSH7* fragment, an intron and an anti-sense *TaMSH7* fragment, terminated by the *35S* terminator. The construct also contained the *Bar* gene providing resistance to BASTA, when applied during selection. The expression of the *Bar* gene was driven by the constitutive *Ubiquitin* promoter (ubi) and terminated by the *Nos* terminator. The plasmid is presented in a linear format.

4.2.1.2 – Transformation of bread wheat cultivar Bob White MPB26

The biolistic transformation of immature wheat embryos (cultivar MPB Bob White 26 – "grey" haplotype) approximately 15-20 days post-anthesis were performed in the laboratory of Professor German Spangenberg using methods previously described (Pellegrineschi *et al.*, 2002).

4.2.2 – Plant material and growth conditions

Wild-type *Triticum aestivum* (MPB Bob White 26 – "grey" haplotype) and mutants (*Tamsh7-1, Tamsh7-2*, *Tamsh7-3*, *Tamsh7-4* and *Tamsh7-5* and *ph2a* (Israel TA05 1996 – seed donated by Moshe Feldman)) were grown in a growth chamber with a photoperiod of 16 hours, 21°C day temperature and 17°C night temperature.

4.2.3 – Identification of positive transgenic plants using PCR

4.2.3.1 – Identification of positive T_1 and T_2 transgenic plants

All plants in the T_1 and T_2 generations were genotyped to determine if they tested positive for the presence of the RNAi cassette described in 4.2.1.1. Genomic DNA (gDNA) was used as template for PCRs with a set of oligonucleotides designed against the RNAi cassette. gDNA extractions and PCRs were performed with a REDExtract-N-Amp^{TM} Plant PCR Kit (Sigma-Aldrich, U.S.A.) according to the manufacturer's instructions. The forward primer (TGTAGATCTGCGATCCGCCGTTGTTGGG) in the PCRs was designed against the sense strand of the *Actin* promoter and the reverse primer (AGCCCCCAAAGCTGCAGACGAATCATCA) to the anti-sense strand of the sense *TaMSH7* fragment. The expected fragment size to be produced with the two primers in the presence of the RNAi construct was 526 bp. To verify the gDNA integrity, primers were also designed against endogenous wild-type wheat gDNA. *TaGWalk*_F – CATATGGAGCAAAATGAGTG and *TaGWalk*_N1 – AAGCCGATGTCTCCAATCATTCATTCTTTC or *TaSSRP1*_HJ05 – CACCGGGATCTCCTAGGTGCC and *TaSSRP1*_HJ13 – GTCGCCCGCTGGCTCTGC were used to amplify 482 bp or 921 bp endogenous fragments respectively.

4.2.4 – Staging and collection of meiotic material

Meiotic material from wild-type bread wheat (MPB Bob White 26 – "grey" haplotype), *Tamsh7* mutants and *ph2a* mutants was isolated, fixed and stored appropriately for subsequent analysis in various methods explained below.

Wheat plant stems which contained developing inflorescences at various stages of meiosis (Feeke's scale of development = 9, flag leaf ligule/collar just visible (Large, 1954)) were cleanly severed from the plant, followed by the removal of the inflorescence from the stem. The meiotic stage occurring in the three anthers of one floret was determined by removing a single anther using pin-vice and loop holders containing fine needles (Proscitech, Queensland, Australia) under a Leica MZ 6 stereo dissecting microscope (Leica Microsystems, New South Wales, Australia) and placing it on a glass microscope slide (Livingstone, New South Wales, Australia). 10 µL of acetocarmine (2% w/v) was used to stain the anther. After two minutes of staining at room temperature, the anther was cut in half latitudinally using a scalpel (# 23, Swann Morton, England), a cover slip (22 X 22 mm, HD Scientific, New South Wales, Australia) was added and the meiocytes were released from the anther halves by pressing the cover slip down with Whatman paper, thereby also removing excess acetocarmine solution. The meiotic stage was then determined using a Leica DM1000 compound microscope (Leica Microsystems). Once the stage of meiosis was determined, the two remaining anthers from the same floret were used for the methods below.

4.2.5 – Expression analysis of *Tamsh7* and *ph2a* mutant plants

Anthers staged as described in 4.2.4 were collected and placed into microcentrifuge tubes in liquid nitrogen for subsequent expression analysis *via* Q-PCR (Table 4.1). For each

cDNA for Q-PCR a minimum of six staged anthers were used. The wild-type controls (MPB Bob White 26 – "grey" haplotype) composed of three biological replicates were from four stages ranging from late G2, leptotene, zygotene and complete synapsis in pachytene. Anthers ranging from pre-meiosis to pachytene were collected from multiple *Tamsh7* mutants from five independent insertion events in addition to collecting a time course from the *ph2a* mutants consisting of pre-meiosis, leptotene – pachytene, diplotene – anaphase I and immature pollen.

Table 4.1 – Summary of the meiotic material collected for expression analysis. Numbers in parentheses indicate how many biological replicates were collected. Each biological replicate contained a minimum of six anthers at the respective stage(s). PM = pre-meiosis, L = leptotene, Z = zygotene, P = pachytene, D = diplotene, AI = anaphase I, IP = immature pollen.

Wild-type	*Tamsh7* mutants	*ph2a*
PM (late G2) (3)	*Tamsh7-1* (PM - P) (1)	PM (1)
L (3)	*Tamsh7-2* (PM - P) (1)	L-P (1)
Z (3)	*Tamsh7-3* (PM - P) (1)	D-AI (1)
P (3)	*Tamsh7-4* (PM - P) (1)	IP (1)
	Tamsh7-5 (PM - P) (1)	

4.2.5.1 – RNA extractions, cDNA synthesis and Q-PCR

RNA extractions, cDNA synthesis and Q-PCR was performed as described in chapter three: Tissue isolation and RNA extraction, cDNA synthesis and Quantitative Real-Time PCR, and Quantitative Real-Time PCR normalisation. The primers used to amplify a fragment of the *TaMSH7* transcript were *TaMSH7*-F (CGCACCTGGACGAGGACACC) and *TaMSH7*-R (GCTCATCTTCCTCCTTCAGAC). Primers were also designed against a putative *TaMLH1* (*TaMLH1-F* CAATGGCACTGAAAGATGACGAGTCAATGA and *TaMLH1-R*

CGTCCCAGGCAATATCATTTCCTAGAGTCA), in order to determine expression levels of this transcript in wild-type controls and the *ph2a* mutant.

4.2.6 – Fertility analysis of *Tamsh7* mutants

4.2.6.1 – Analysis of whole plant morphology

Whole plant morphology was observed for the *Tamsh7* mutants and wild-type controls, with germination rate, plant height, leaf development and flowering development monitored. Upon complete emergence of the wheat spikes from the sheaths, images of whole plants and spikes were captured using a Kodak EasyShare digital camera (Eastman Kodak Company, U.S.A.).

4.2.6.2 – Analysis of pollen viability and seed set in the *Tamsh7* mutant background

Pollen viability was analysed from three different plants for a given genotype using Alexander stain (95% ethanol (10 mL), 1% malachite green in 95% ethanol (5 mL), 1% acid fuchsine in milli-Q water (5 mL), 1% Orange G in milli-Q water (5 mL), glacial acetic acid (2 mL), glycerol (2 mL), phenol (5 g) and milli-Q water (to a total volume of 100 mL)). Anthers adjacent to florets that had recently dehisced were isolated by using fine forceps (Proscitech) to remove the glumes, thus enabling isolation of anthers just prior to dehiscence. Anthers were cut in half on a glass microscope slide using a scalpel and then 20 µL of sterile de-ionised water was added. The pollen grains then flowed autonomously from the anthers into the water in large numbers. The anther debris was then removed from the solution. 20 µL of Alexander stain was added to the pollen and water. A cover slip was

gently placed onto the preparation and excess stain was removed by lowering Whatman paper onto the cover slip edges without applying force so that pollen cell morphology was not perturbed. Preparations were then incubated at 50°C for three hours. The treated pollen was visualised using a Leica DM LA microscope which was operated with a Leica Microscope Control Unit (Leica Microsystems, Wetzlar, Germany). Images were obtained using a HV-C20A camera (Hitachi, Japan) and imported with Laser Microdissection System version 4.3.1.0 (Leica Microsystems). Seed set numbers per spike in the *Tamsh7* mutant generations were also used to determine if there was a significant difference between the levels of fertility between wild-type controls and the *Tamsh7* mutants. Two heads were used per plant from the primary and tertiary tillers if the material was available. Two tailed student's t-tests assuming equal variance (Microsoft® Office Excel 2003, Microsoft Corporation, U.S.A.) were conducted to compare the seed set and pollen viability in the wild-type controls and *Tamsh7* mutants.

4.2.7 – Chromosome morphology and meiotic progression in the *Tamsh7* mutant background

Chromosome morphology and behaviour during meiotic metaphase I were analysed in *Tamsh7* mutants relative to the wild-type controls. Additional preparations of very specific meiotic events ranging from late pre-meiotic interphase until diplotene were also analysed in *Tamsh7* mutants and wild-type controls.

4.2.7.1 – Feulgen staining of meiotic metaphase I chromosomes

4.2.7.1.1 – Fixation of meiotic material

Meiotic wheat anthers were collected as described in 4.2.4. The anthers at appropriate stages of meiosis were then fixed overnight at room temperature in fresh Carnoy's fixative (75% ethanol, 25% glacial acetic acid) in a 1.5 mL microcentrifuge tube. The following day the anthers were washed in 70% ethanol at room temperature five times for two minutes per wash. The anthers were stored at 4°C until required.

4.2.7.1.2 – Staining of meiotic metaphase I chromosomes

The supernatant was aspirated and HCl (100 µL, 1 M) was added to the anthers. The anthers were incubated at 60°C for 13 minutes. The supernatant was removed by aspiration and Feulgen's stain (100 µL, 0.4% Basic Fuschin, 1.8% sodium sulphate, 0.15 M hydrochloric acid) was used to stain the DNA of all cells which made up the whole anthers. The incubation occurred at room temperature in the dark for three hours. Two anthers were removed from the tubes and placed on a glass microscope slide. A drop of fresh glacial acetic acid solution (20 µL, 45% v/v) was added to the anthers. Meiocytes were released from the anthers by gently tapping with the blunt side of a hook-shaped needle. The empty anther debris was then removed from the solution containing the meiocytes. A cover slip (22 X 22 mm) was placed onto the samples. The preparations were then pressed with Whatman's paper to remove excess glacial acetic acid solution. The slides were heated gently over an alcohol burner sufficiently to make the slide slightly warmer than room temperature. The slides were then immersed in liquid nitrogen until ceasing to bubble. The cover slips were separated from the slides with a razor blade. Preparations were then dried

for 30 minutes. A drop of Crystal Mount™ Aqueous Mounting Medium (Sigma-Aldrich) was then applied before immediately placing a cover slip (22 X 50 mm) onto the slide (which was then allowed to set for 30 minutes). The results were visualised and images were captured as described in 4.2.6.2.

4.2.7.2 – Collection and fixation of meiotic material for three dimensional imaging of prophase I chromosomes in bread wheat

The following protocol in sections 4.2.7.3, 4.2.7.4 and 4.2.7.5 is based on a previously reported method (Franklin *et al.*, 1999) with modifications that were generously provided by Assistant Professor Wojtek Pawlowski (Cornell University, U.S.A.). Meiotic wheat anthers were isolated as described in 4.2.4. The staged anthers were placed into filter-sterilised (0.2 µm, Sartorius, Germany) 1 X Buffer A (2 mL). 2 X Buffer A contained; 15 mM Pipes-NaOH (pH 6.8), 80 mM KCl, 20 mM NaCl, 0.5 mM EGTA, 2 mM EDTA, 0.15 mM spermine tetra-HCl, 0.05 mM spermidine, 1 mM DTT, 0.32 M sorbitol and sterile de-ionised water to the appropriate volume. The anthers were then fixed by adding paraformaldehyde (1 mL, 16%, Electron Microscopy Services, U.S.A.) and 2 X Buffer A (1 mL) to the 2 mL of 1 X buffer A that the anthers were already immersed in. This resulted in a fixing solution that contained 1 X buffer A and 4% paraformaldehyde. The anthers were fixed for 30 minutes on a rotary shaker at room temperature and then washed in 1X buffer A on a rotary shaker at room temperature for 30 minutes. A second wash in 1 X buffer A was then conducted for 15 minutes on the rotary shaker before removing and adding fresh 1 X buffer A and storing the anthers in an air tight vessel at 4°C until required.

4.2.7.3 – Embedding wheat meiocytes in polyacrylamide pads for three dimensional microscopy

A wheat anther which had been fixed as described in 4.2.7.2 was placed adjacent to a drop of 1 X buffer A (60 µL) on a piece of parafilm wrapped around a petri dish. The anther was held with fine forceps at one end and the opposite end of the anther was cut off with a scalpel. The meiocytes were then extruded from the anther into another drop of buffer A by gently using the shaft of a fine needle (25 gauge, Becton Dickinson, New South Wales, Australia) to apply pressure to the anther. All anther debris was removed from the droplet. This was repeated so that each preparation contained meiocytes from a total of five anthers. The drop was then stirred gently before taking 10 µL, which was added to the centre of a poly-L-lysine coated cover slip (22 X 22 mm). Activated acrylamide/bisacrylamide solution (5 µL) was added to the meiocytes and swirled gently. The activated acrylamide/bisacrylamide solution was made by the addition of acrylamide/bisacrylamide (50 µL, 30% acrylamide, 0.8% bisacrylamide) to 2 X buffer A (50 µL), sodium sulfite (5 µL, 20%) and sodium persulfate (5 µL, 20%) before vortexing the solution briefly.

Immediately after the addition of the activated acrylamide/bisacrylamide solution, a cover slip (22 X 22 mm) which had not been coated in poly-L-lysine was placed on top of the preparation at a 45° angle relative to the bottom cover slip. The acrylamide pads were left for one hour to polymerise. The top cover slip was then gently removed from the poly-L-lysine-coated cover slip and the attached poly-acrylamide pad.

4.2.7.4 – Meiocyte immunisation

The cover slips were placed into a six well Microplate (Iwaki, Japan) with the meiocytes/poly-acrylamide pads facing up. The meiocytes were washed with 1 mL of 1 X PBS (NaCl (8 g), KCl (0.2 g), Na_2HPO_4 (1.44 g), KH_2PO_4 (0.24 g) de-ioinised water to 1 L, with the pH adjusted to 7.4, and then sterilised by autoclaving) for 10 minutes twice. The meiocytes were then permeabilised for one hour with a permeabilisation solution (1 mL) comprised of 1 X PBS, Triton X-100 (1% v/v) and EDTA (1 mM). Following permeabilisation the preparations were blocked for two hours with a blocking buffer (1 mL) made from 1 X PBS, BSA (3%), normal donkey serum (5%), EDTA (1 mM) and Tween 20 (0.1%). The blocking buffer was then removed by aspiration and 50 μL of anti-*Ta*ASY1 solution (anti-*Ta*ASY1 raised in rabbit (1%) (Boden *et al.*, 2007), blocking buffer (99%)) was added directly onto the meiocytes embedded in poly-acrylamide pads. The six well Microplate was placed in an airtight container on a layer of several wet paper towels which were soaked in sterile de-ionised water. The reaction was left to immunise overnight at room temperature.

4.2.7.5 – Washes

Non-specifically bound anti-*Ta*ASY1 solution was removed with a wash buffer (1 mL) composed of 1 X PBS, Tween 20 (0.1%) and EDTA (1 mM) for one hour at room temperature. The wash buffer was removed and this was repeated eight times. The final wash was left overnight at room temperature. The following day, six additional one hour washes were performed. Following the sixth wash, the wash buffer was aspirated and 50 μL of secondary antibody solution (AlexaFluor[TM] 568 conjugated donkey anti-rabbit antibody (Invitrogen, Victoria, Australia) (1%), blocking buffer (99%)) was applied directly onto the

meiocytes. The meiocytes were incubated with the secondary antibody solution overnight at room temperature as described in 4.2.7.4. The following day eight 1 hour washes were performed with the wash buffer (1 mL), leaving the last wash overnight at room temperature.

Meiocytes were subsequently washed twice with 1 X PBS (1 mL) for 10 minutes. The nuclear DNA of the meiocytes was then stained with 4′,6-diamidino-2-phenylindole (DAPI) (500 μL, 5 μg mL^{-1} diluted in 1 X PBS) for 30 minutes. Excess DAPI was removed by three 10 minute washes with 1 X PBS (1 mL). The PBS was removed and the meiocytes were washed three times for two minutes with DABCO antifade solution (2.5% w/v 1,4-diazabicyclo-[2.2.2] octane, 90% glycerol, Tris-HCl (50 mM, pH 8.0)) by immersing a 1 mL pipette tip in the solution and allowing two drops to fall onto the meiocyte pads.

The cover slips with meiocytes attached were removed from the six well Microplates and placed into the centre of a glass microscope slide with the meiocytes facing up. A cover slip was placed on top. Excess DABCO was removed and the slides were sealed with nail polish and stored at -20°C.

4.2.7.6 – Microscopy and image processing

Meiocytes were visualised using a Leica TCS SP5 spectral scanning confocal microscope with an oil immersion HCX PLAPO lamda blue 63X /1.4 lens or an N PLAN 10X/0.25 lens (Leica Microsystems, Wetzlar, Germany). A pulsed-diode 405 nm laser was used for excitation of DAPI, and emission was collected in the range of 415 nm - 480 nm. Similarly a Diode-Pumped Solid State (DPSS) 561 nm laser was used for excitation of AlexaFluor^{TM} 568 and emission was collected in the range of 571 nm - 680 nm. Scans were performed sequentially to prevent cross-talk between channels. A series of optical XY slices were

collected along the Z axis that was separated by intervals of 0.2 μm through the region of interest. Four times line averaging was used per optical section with a scan format of 1024 X 1024 pixels. Maximum intensity projections of the individual confocal images from both channels (405 nm pulsed laser (DAPI) and the DPSS 561 nm laser (anti-TaASY1)) were created and merged with Application Suite Advanced Fluorescence (LAS-AF; version 1.8.2, build 1465, Leica Microsystems, Germany).

4.3 – Results

4.3.1 – *Tamsh7* mutant analysis in the T_1 generation

Tamsh7 mutants generated from nine independent insertion events in the T_0 generation were analysed in the T_1 generation. The nine different mutant lines were analysed in order to identify lines that were positive for the presence of the transgene and those which displayed reduced *TaMSH7* transcript levels relative to wild-type.

4.3.1.1 – Genotype analysis

Plants in the T_1 generation were identified which displayed the presence or absence of the transgene using PCR (Figure 4.2). A combination of segregation patterns for the transgene was seen in the T_1 generation of *Tamsh7* mutants (Table 4.2). The segregation patterns of the transgene from T_0 generation to T_1 generation included 3:1 (presence:absence), 1:3, 1:0, 0:1 and 1:1. Some lines which were genotyped at the T_0 generation and shown to be positive did not appear to retain the presence of the transgene within the given number of seeds germinated from those lines.
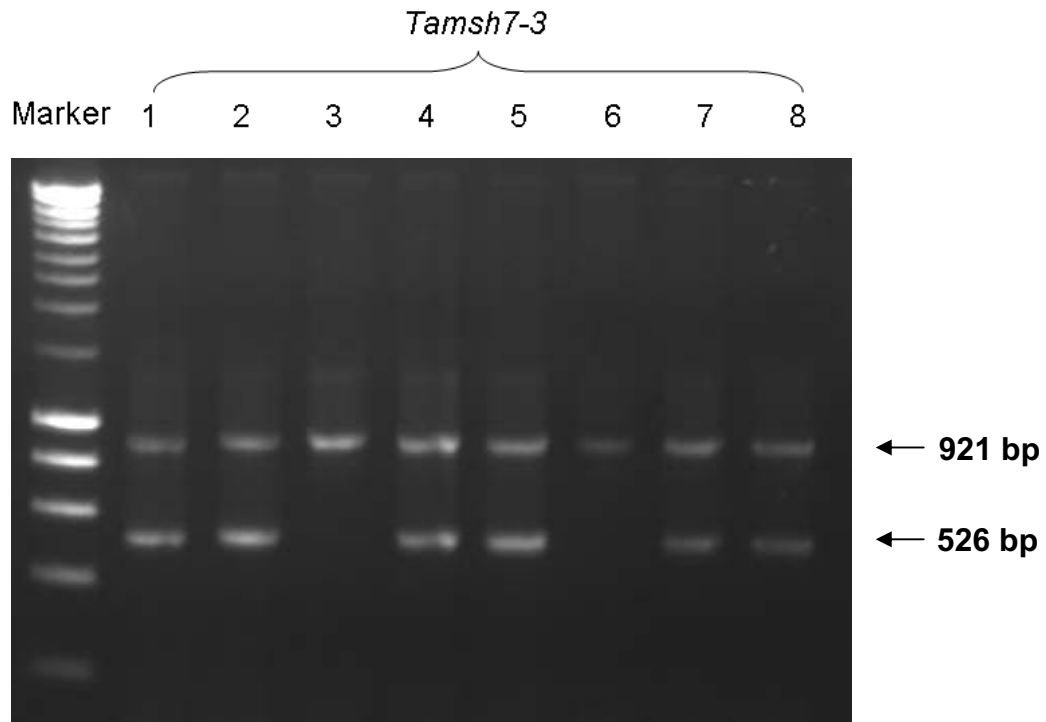
Figure 4.2 – Example of PCR products stained with ethidium bromide and separated using gel electrophoresis indicated whether plants were positive or negative for the transgene. Lane 1: 1 kb molecular marker (Bioline, U.S.A.). Lanes 2 – 9: Separated PCR products amplified from *Tamsh7-3* plants #1 to #8. A 526 bp band in the lanes 2, 3, 5, 6, 8 and 9 indicates the presence of the transgene in the corresponding plant. An absence of a 526 bp band in lanes 4 and 7 indicates that the corresponding plant did not contain the transgene. Lanes 2 to 9 all contain a 921 bp fragment (amplified using primers *TaSSRP1*_HJ05 and *TaSSRP1*_HJ13) confirming gDNA integrity.

Table 4.2 – Summary of genotyping results for transgene presence:absence in the T₁ generation of *Tamsh7* mutants from multiple independent insertion events. Various segregation patterns are presented ranging from heterozygous 3:1 patterns and unlinked loci patterns such as 1:0. The number of plants germinated is also provided in the third column.

Insertion event number	Segregation ratio	Plant germinated and analysed
Tamsh7-1	1 : 0	8
Tamsh7-2	3 : 1	12
Tamsh7-3	3 : 1	8
Tamsh7-4	1 : 1	8
Tamsh7-5	1 : 3	12
Tamsh7-6	3 : 1	12
Tamsh7-7	3 : 1	8
Tamsh7-8	0 : 1	8
Tamsh7-9	0 : 1	8

4.3.1.2 – T₁ generation *Tamsh7* mutants showed reduced *TaMSH7* transcript levels relative to wild-type

Expression analysis *via* Q-PCR revealed that expression of *TaMSH7* transcript levels were altered compared to wild-type in multiple lines generated through independent bombardment events which had retained the transgene. The levels of *TaMSH7* transcript are lower than wild-type at prophase I in the plants descendent from the insertion events *Tamsh7-1*, *Tamsh7-2*, *Tamsh7-3* and *Tamsh7-5* (Figure 4.3). However *TaMSH7* expression in plants from line *Tamsh7-4* are more similar to wild-type (Figure 4.3).
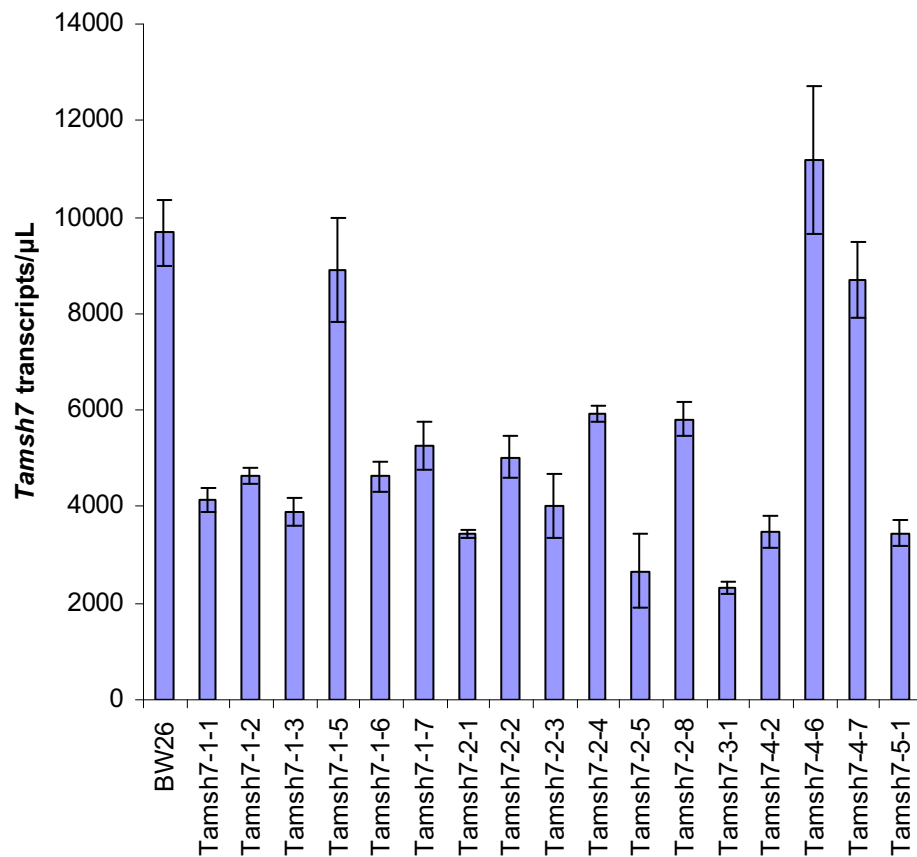
Figure 4.3 – Q-PCR expression data corresponding to the five independent insertion events examined during the T$_1$ generation of the *Tamsh7* mutants. The lines derived from insertion events *Tamsh7-1*, *Tamsh7-2*, *Tamsh7-3* and *Tamsh7-5* display reduced *TaMSH7*. Plants descendant from insertion event *Tamsh7-4* express *TaMSH7* at levels similar to wild-type.

4.3.2 – *Tamsh7* mutant analysis in the T$_2$ generation

Analysis of the T$_2$ generation was narrowed to three independent insertion events (*Tamsh7-1*, *Tamsh7-2* and *Tamsh7-3*) after the analysis of the data from the T$_1$ generation.

4.3.2.1 – Genotype analysis

Plants were scored for the presence or absence of the RNAi construct using PCR (Figure 4.4). This resulted in various segregation patterns of the transgene in the progeny of the T_2 generation (Table 4.3).
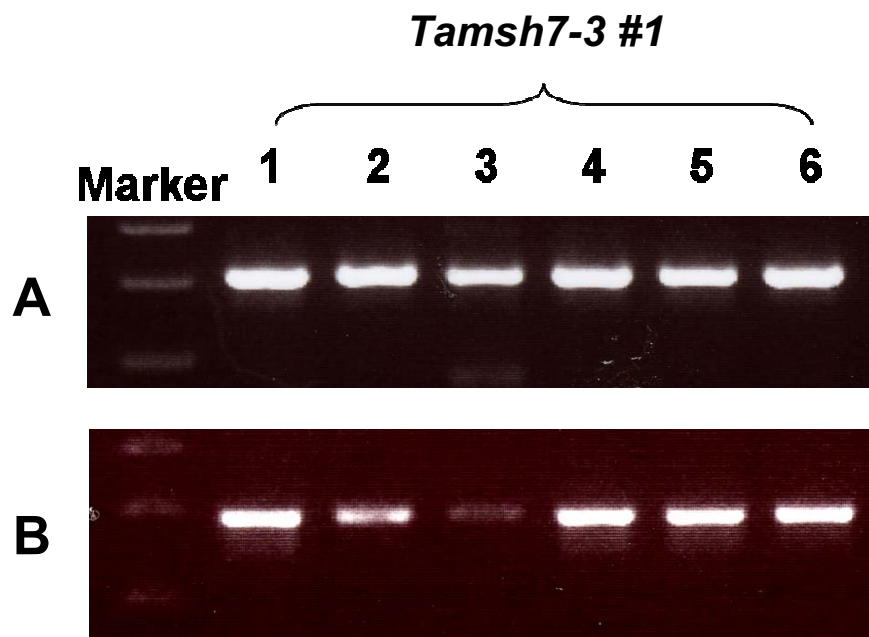
Figure 4.4 – Example of PCR products stained with ethidium bromide and separated using gel electrophoresis indicated whether plants were positive or negative for the RNAi transgene and confirmed gDNA integrity. A) Lane 1: 1 kb molecular marker (Bioline). Lanes 2 – 7: Separated PCR products amplified from *Tamsh7-3* plants. A 526 bp band indicates the presence of the transgene. B) Lane 1: 1 kb molecular marker (Bioline). Lanes 2 – 7: Separated PCR products amplified from *Tamsh7-3* plants. A 482 bp band indicates the gDNA template integrity for the reactions shown in (A).

Table 4.3 – Summary of genotyping results for the RNAi transgene presence:absence in the T_2 generation of *Tamsh7* mutants from multiple independent insertion events. Various segregation patterns are presented.

Genotype and plant	Segregation ratio (presence:absence)	Plants analysed
Tamsh7-1 #1	1:1	6
Tamsh7-1 #2	0:1	2
Tamsh7-1 #3	1:1	2
Tamsh7-1 #4	9:1	10
Tamsh7-2 # 1	10:1	11
Tamsh7-2 # 2	9:2	11
Tamsh7-2 # 3	1:0	1
Tamsh7-2 # 4	0:1	3
Tamsh7-3 #1	1:0	16
Tamsh7-3 #2	1:0	16
Tamsh7-3 #3	1:1	8
Tamsh7-3 #4	5:3	8

4.3.2.2 – *Tamsh7* plants display reduced levels of fertility

4.3.2.2.1 – Whole plant morphology

During development the *Tamsh7* mutants appeared similar to wild-type with respect to height, leaf development, seed germination frequencies and growth rates. Differences were only observed after the completion of heading and ripening commenced (Feeke's scale = 11). Grain development appeared normal at the base of the spike and towards the middle. However where embryo abortion occurred, it was prevalent in the top half of the spike, with varying levels of spike abnormalities observed. Plants from all three *Tamsh7* mutant insertion events studied at the T_2 generation (*Tamsh7-1*, *Tamsh7-2* and *Tamsh7-3*) showed primary tillers displaying relatively normal morphology through to those which had reduced fertility (Figure 4.5).

Figure 4.5 – Spike and whole plant morphology of *Tamsh7* mutants. Wild-type bread wheat spikes (A) show good grain fill and architectural integrity. *Tamsh7-1*, *Tamsh7-2* and *Tamsh7-3* mutant spikes (B & C; D & E; F & G, respectively) show variable features ranging from appearing similar to wild-type to showing lack of grain fill in addition to reduced overall spike length. General plant morphology was not affected in the *Tamsh7* mutants (H) with all plants (right) displaying vegetative growth as seen in wild-type (left). Scale bars A – G = 5 cm, H = 30 cm.

4.3.2.2.2 – Pollen viability and seed set are affected in the *Tamsh7* mutant background

Analysis of pollen viability revealed that a reduction in *TaMSH7* expression can increase the percentage of abnormal pollen cells that appear relative to the ratio observed in wild-type anthers that are at a stage of development just prior to dehiscence (Feeke's scale = 10.5.2). *Tamsh7-2* showed the most abnormal pollen grains compared to wild-type, followed by *Tamsh7-1* and then *Tamsh7-3* (Table 4.4). Normal pollen grains were large, circular and stained deep red (Figure 4.6). Pollen grains that contained any of the following characteristics were classified as abnormal: reduced size, non-spherical shape, inability to exclude the green dye. Wheat plants which did not contain the transgene in the T_2 generation but were descendents from T_1 parents who were heterozygous for the transgene showed pollen viability at wild-type levels.

Table 4.4 – The reduction of *TaMSH7* expression leads to an increased rate of pollen abortion compared to wild-type. Pollen grains from multiple plants within lines just prior to dehiscence were scored for viability based on their appearance when exposed to Alexander stain. *Tamsh7-2* shows the highest rate of pollen abortion. The total number of pollen grains counted per genotype is given in parentheses.

Genotype	% non-viable	p-value c.f. wild-type
Wild-type (BW26)	2.18% (n=504)	1.00
Tamsh7-1	25.19% (n=428)	$P < 0.05$
Tamsh7-2	43.80% (n=468)	$P < 0.05$
Tamsh7-3	7.49% (n=427)	$P > 0.05$
Tamsh7-1 fertile offspring	4.31% (n=511)	$P > 0.05$
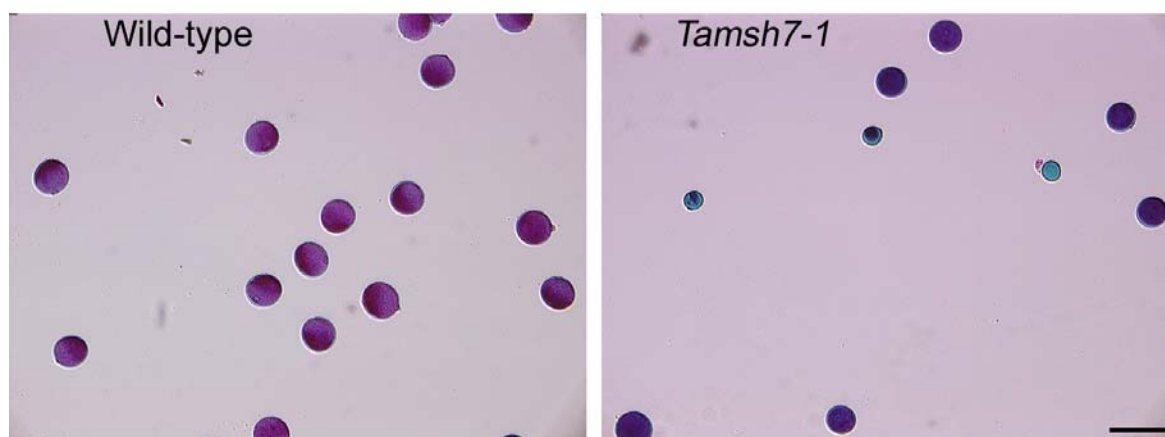
Figure 4.6 – Alexander staining reveals an increased rate of pollen abortion compared to wild-type. Wild-type pollen grains appear deep red while non-viable pollen are smaller in size, irregular in shape and the protoplasm is green in colour. Bar = 200 μm.

Seed set was also analysed in the transgenic plants relative to wild-type and found to be affected by variable degrees. *Tamsh7-1*, *Tamsh7-2* and *Tamsh7-3* showed reduced fertility at levels of $P < 0.05$, $P < 0.001$ and $P < 0.001$ respectively.

4.3.2.3 – Meiotic chromosome morphology and meiotic progression in the *Tamsh7* mutant background is altered compared to wild-type

Meiotic chromosome behaviour was monitored throughout meiosis in selected *Tamsh7* mutants and was shown to display abnormalities during prophase I and metaphase I but otherwise normal meiotic progression was observed when compared to wild-type.

4.3.2.3.1 – *Tamsh7* mutants show an increase in non-homologous interactions at meiotic metaphase I

At meiotic metaphase I in bread wheat 21 pairs of homologous chromosomes form bivalents at a frequency of 0.98 (Colas *et al.*, 2008). Chromosomes at metaphase I in the

Tamsh7-1 mutants contained an increased frequency of abnormal events relative to wild-type controls. Some univalents were observed in *Tamsh7-2* (Figure 4.7), however these are also observed in wild-type but at much lower frequencies. In contrast, *Tamsh7-1* exhibited increased non-homologous/homoeologous associations when compared to wild-type controls. These included associations between one chromosome and at least two others when aligned at the metaphase plate just prior to the first meiotic division (Figure 4.7). Other multivalent structures were also observed including the interlocking of ring bivalents. Plants segregating for the *Tamsh7-1* insertion event that lost the transgene between generations displayed a metaphase I phenotype similar to wild-type. The *Tamsh7-3* mutant appeared to be the most similar to wild-type during meiotic metaphase I.
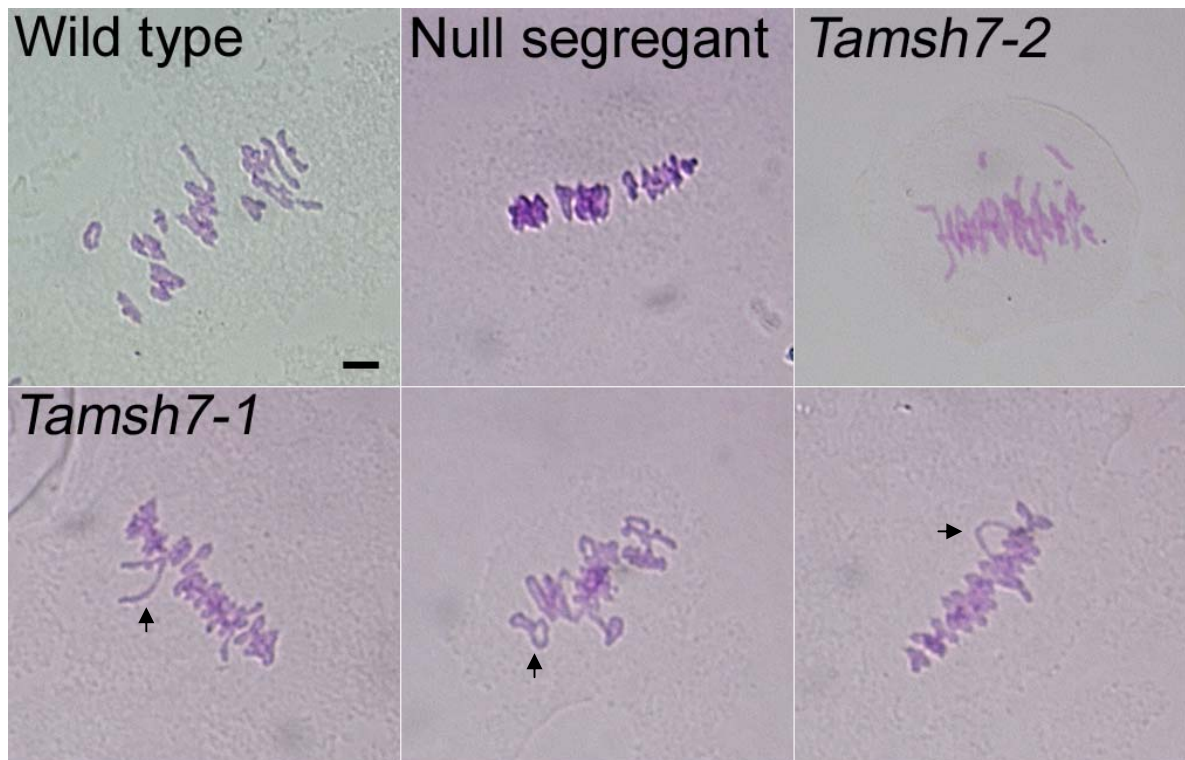
Figure 4.7 – Staining and visualisation of meiotic chromosomes at metaphase I in wild-type and *Tamsh7* mutants. 21 bivalents form in wild-type bread wheat at metaphase I, aligning on the metaphase bridge. *Tamsh7-1* mutants showed increased multivalent structures including trivalents and interlocked ring bivalents (arrows). Bar = 10 μm.

4.3.2.4 – Immuno-localisation of synaptonemal complex lateral elements

Given that multiple chromosome associations were being observed at metaphase I in some *Tamsh7* plants, prophase I was investigated using immuno-localisation. It was anticipated that additional information could be obtained through such an approach.

4.3.2.4.1 – Localisation of *Ta*ASY1 in bread wheat tracks meiotic progression in wild-type

*Ta*ASY1 localises to the axial/lateral elements of meiotic chromosomes in wild-type bread wheat (Boden *et al.*, 2008; Boden *et al.*, 2007) from late pre-meiotic interphase until

pachytene and a polyclonal antibody raised against *Ta*ASY1 specifically labels such meiocytes (Figure 4.8). Throughout this time-frame, a vivid *Ta*ASY1 signal localises only to meiotic DNA. In wild-type bread wheat ASY1 appears as punctuate foci at late pre-meiotic interphase, often with two or more nucleoli visible in addition to a tight cluster of *Ta*ASY1 signal which most likely represents the telomere bouquet (Figure 4.9A). At this stage the chromosomes appear randomly distributed throughout the entire volume of the nucleoplasm in three-dimensional space. Progressively the cell size expands and concomitantly the major nucleolus moves to the periphery of the nucleus, when *Ta*ASY1 polymerises and a thread-like signal on chromosomes replaces the punctuate signal (Figure 4.9B, C). Chromosomes align and eventually synapse (Figure 4.9D, E, F). After the 'puncate stage' of the *Ta*ASY signal but prior to complete synapsis, the ASY1 signal often shows a preferential localisation away from the centre of the nucleus but not immediately adjacent to the inner side of the nuclear envelope either. Synapsis does not occur simultaneously throughout the cell but rather slightly asynchronously in different regions. In most cases *Ta*ASY1 disassociates rapidly from the freshly synapsed regions. However the signal was seen to persist for slightly longer in some instances. In most cases any residual *Ta*ASY1 signal on the remaining synapsing/freshly synapsed regions is evenly spread throughout the nucleoplasm, with slight variations in the unloading of *Ta*ASY1 signal from chromosomes observed (Figure 4.9 H, I). Subsequently the signal is sparsely seen in the nucleoplasm and the signal moves to the inner side of the nuclear envelope and then to the major nucleolus where the signal disappears by approximately the onset of diplotene or soon after.
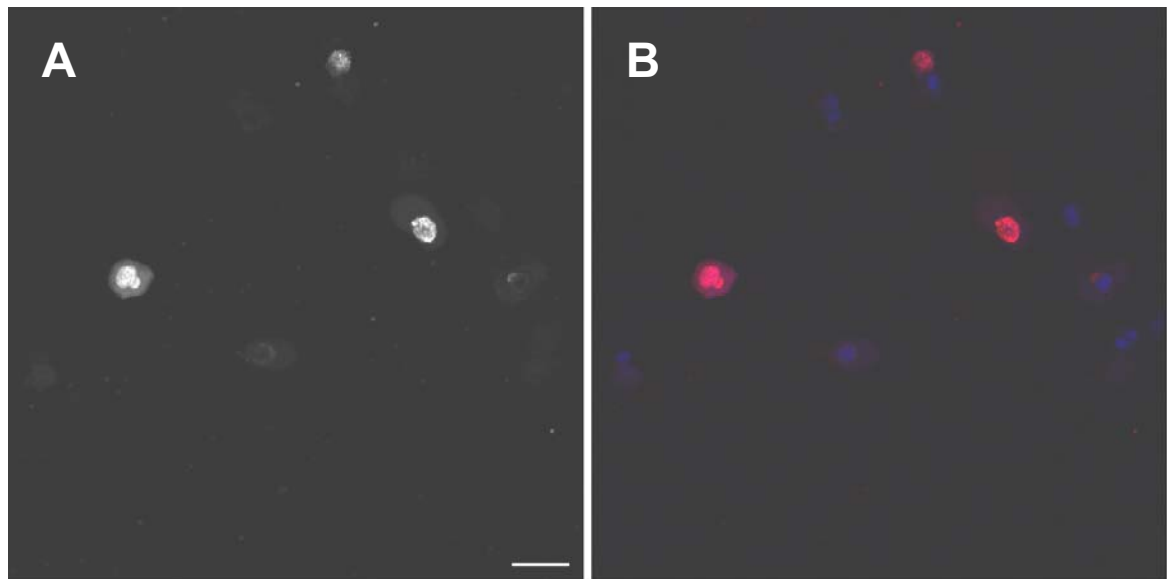
Figure 4.8 – Anti-*Ta*ASY1 specifically labels meiocytes from late pre-meiotic interphase to pachytene. *Ta*ASY1 is shown in white (A) and also false coloured merges (B) where red = anti-*Ta*ASY1 and DAPI = blue. Somatic cells remain unlabelled with respect to *Ta*ASY1 however the DNA is still stained by DAPI. Bar = 50 μm.
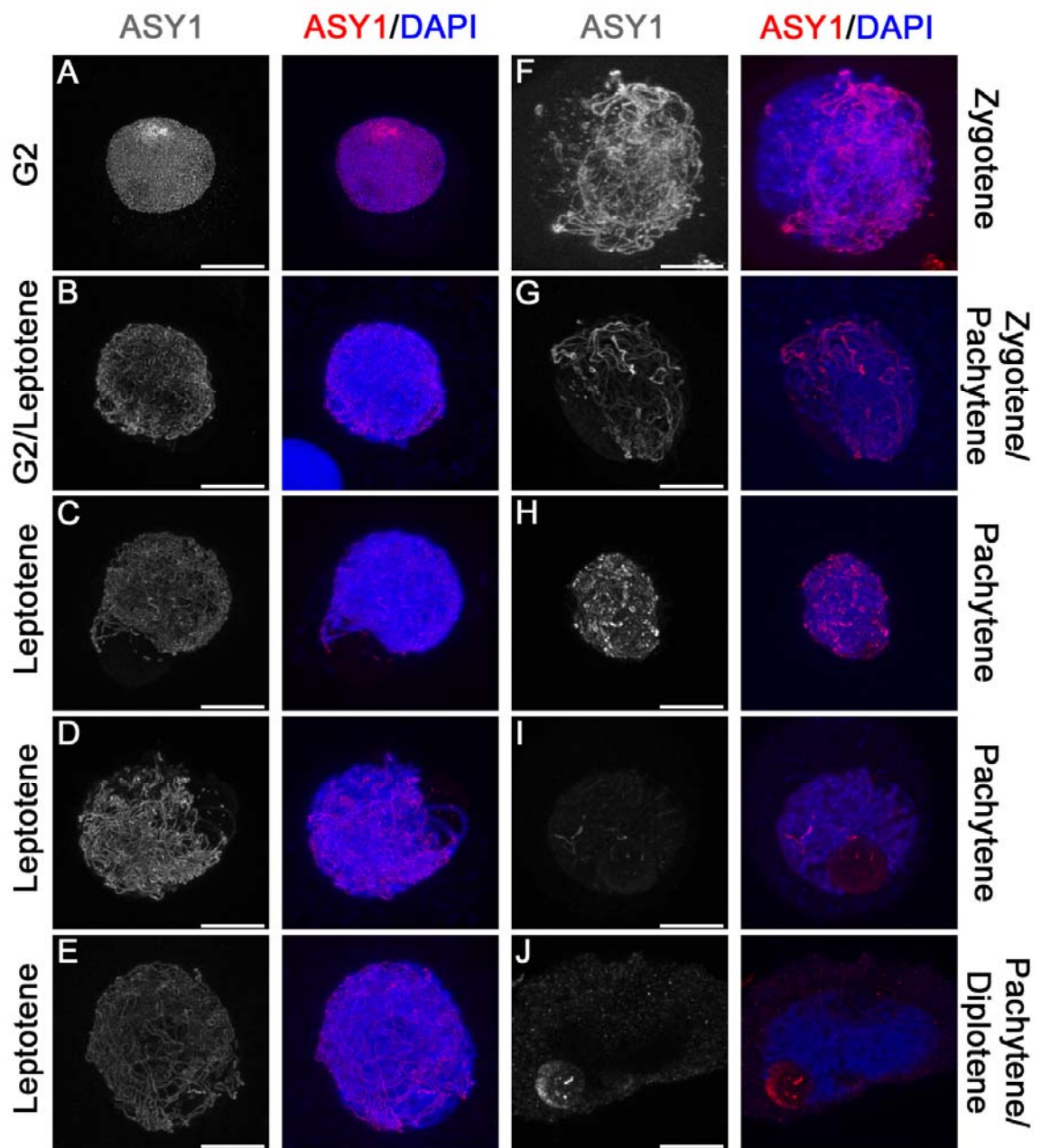
Figure 4.9 – *Ta*ASY1 localisation in wild-type tracks lateral element formation on meiotic chromosomes. (A) *Ta*ASY1 appears as punctuate foci with multiple nucleoli and the telomere bouquet present at late G2. (B – E) The major nucleolus moves to the periphery of the nucleus and the *Ta*ASY1 signal polymerises as the chromosomes roughly align. (F, G) Chromosomes synapse and (G, H) *Ta*ASY1 unloads from the chromosomes. (H, I) *Ta*ASY1 signal is almost completely absent as synapsis is complete. (J) *Ta*ASY1 signal moves to the nucleolus. White = anti-*Ta*ASY1 and red/blue merges = anti-*Ta*ASY1/DAPI respectively. Scale bar = 10 μm.

4.3.2.4.2 – Immuno-localisation of synaptonemal complex lateral elements in *Tamsh7* mutants tracks meiotic progression

The localisation of *Ta*ASY1 was analysed in the *Tamsh7-1* mutant background and compared to wild-type. The *Tamsh7-1* mutants begin meiotic prophase I much like wild-type. It was not until zygotene, where it appeared that there may have been slightly more "knobs" of ASY1 signal (Figure 4.10C) in the *Tamsh7-1* mutant. No other significant differences in *Ta*ASY1 localisation were noticed until synapsis progressed to an advanced stage where it was noted that the *Ta*ASY1 signal persisted on chromosome pairs of the mutants which were entangled (as indicated by multiple synapsed chromosomes meeting at the same X, Y and Z planes in confocal image stacks) (Figure 4.10D). When such a persistence of *Ta*ASY1 signal occurred, it did so specifically only on the chromosomes involved in the (multiple) associations. This persistence of *Ta*ASY1 signal and presumably persistence of mature synaptonemal complexes was not seen in wild-type.
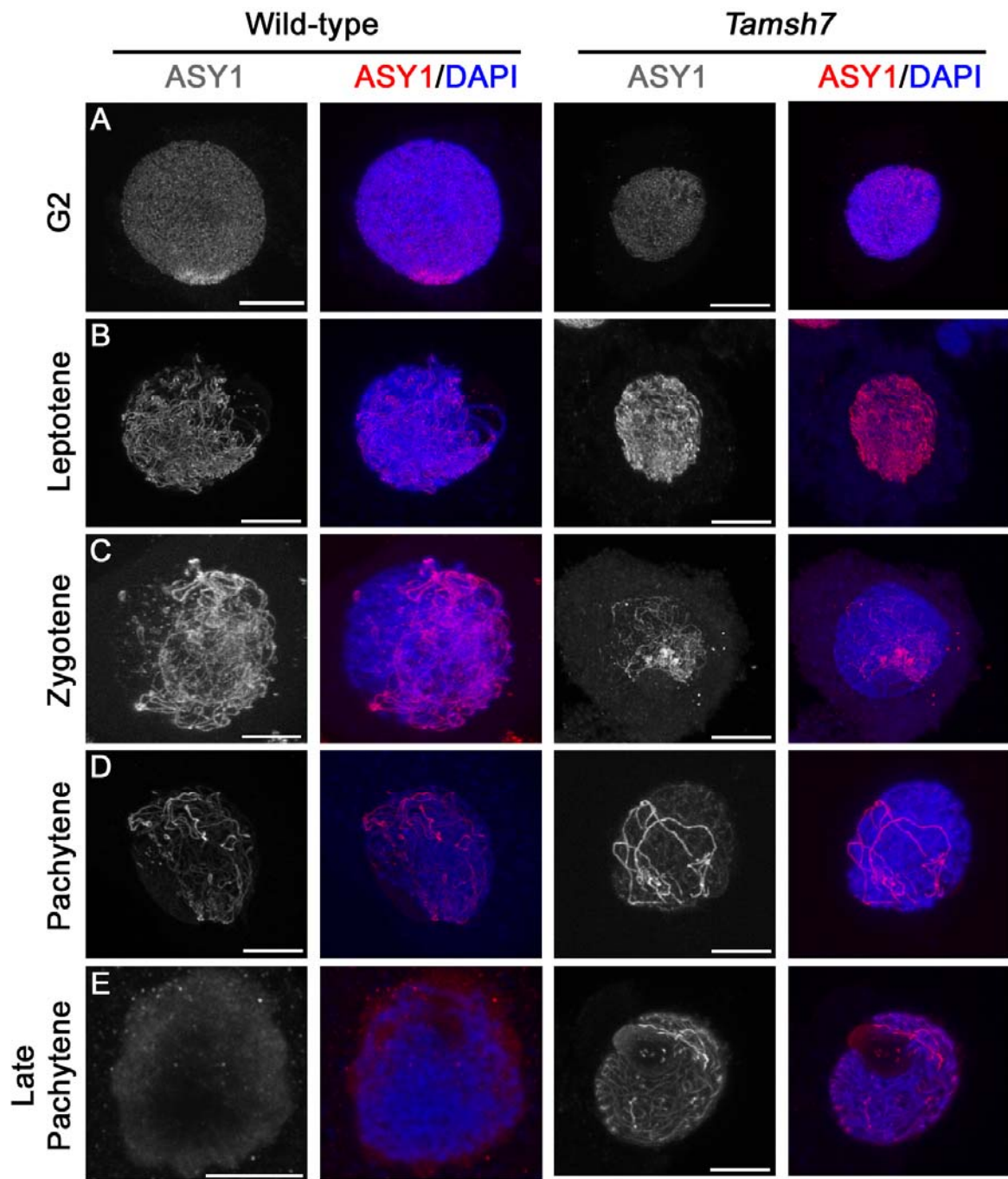
Figure 4.10 – *Ta*ASY1 localisation in the *Tamsh7-1* mutant background. G2 (A), leptotene (B) and zygotene (C) appear similar to wild-type. As pachytene progresses the *Ta*ASY1 signal is seen to persist only in regions with multiple associations (D). In late pachytene/early diplotene some *Ta*ASY1 signal continues to persist in *Tamsh7-1* compared to wild-type (E). White = anti-*Ta*ASY1 and red/blue merges = anti-*Ta*ASY1/DAPI respectively. Scale bar = 10 μm.

4.3.3 – Investigation of *TaMSH7* as a *Ph2* candidate

Given that the *Tamsh7* mutants displayed reduced levels of fertility, that meiotic chromosome behaviour appeared abnormal in several independent lines, and that *TaMSH7* resides within the *Ph2* locus, the bread wheat mutant *ph2a* was investigated using a similar strategy to that conducted with the *Tamsh7* mutants. Expression analysis of *TaMSH7* was conducted using cDNA produced from the *ph2a* mutant in addition to fluorescent immuno-localisation of *Ta*ASY1 in this mutant background.

4.3.3.1 – *TaMSH7* and *TaASY1* expression is perturbed in the *ph2a* mutant

Q-PCR analysis revealed that *TaMSH7* is not expressed in the *ph2a* mutant which lacks a region of the short arm of chromosome 3D where *TaMSH7* resides, however *TaMLH1* was expressed at levels similar to those seen in wild-type (Figure 4.11). Given the absence of *TaMSH7* expression in *ph2a* it presented the opportunity to analyse a 'pseudo *Tamsh7* mutant'. Therefore fluorescent immuno-localisation was conducted which compared *Ta*ASY1 localisation in *ph2a* mutants to wild-type in meiocytes.

     *Ta*ASY1 appeared at slightly higher levels in the *ph2a* mutant when compared to wild-type. Additionally, the spatial and temporal distribution was altered when compared to wild-type, where *Ta*ASY1 localisation was mostly restricted to chromosome axes prior to disassociation of the signal from the chromosomes. The *Ta*ASY1 signal in *ph2a* mutants persisted for longer as a diffuse stain on the meiotic chromosomes (Figure 4.12). *Ta*ASY1 also appeared more abundant in the nucleoplasm at times in the *ph2a* mutant. However, the

excess of *Ta*ASY1 in the *ph2a* mutant did not correlate with altered chromosome morphology as was seen in the *ph1b* mutant (Boden *et al.*, 2008).

The observations of a stronger *Ta*ASY1 signal in the *ph2a* mutants were supported by Q-PCR expression analysis. The data revealed increased levels of *TaASY1* transcript in the *ph2a* mutant (Figure 4.13). However, when the data was centred (the average expression value of each genotype across the respective time-course was subtracted from each data point) the *TaASY1* transcript levels between wild-type and *ph2a* share a correlation co-efficient of $R = 0.98$. This is similar to previously obtained results which found an amplification of the expression levels of *TaASY1* in the *ph1b* mutant (Boden *et al.*, 2008).
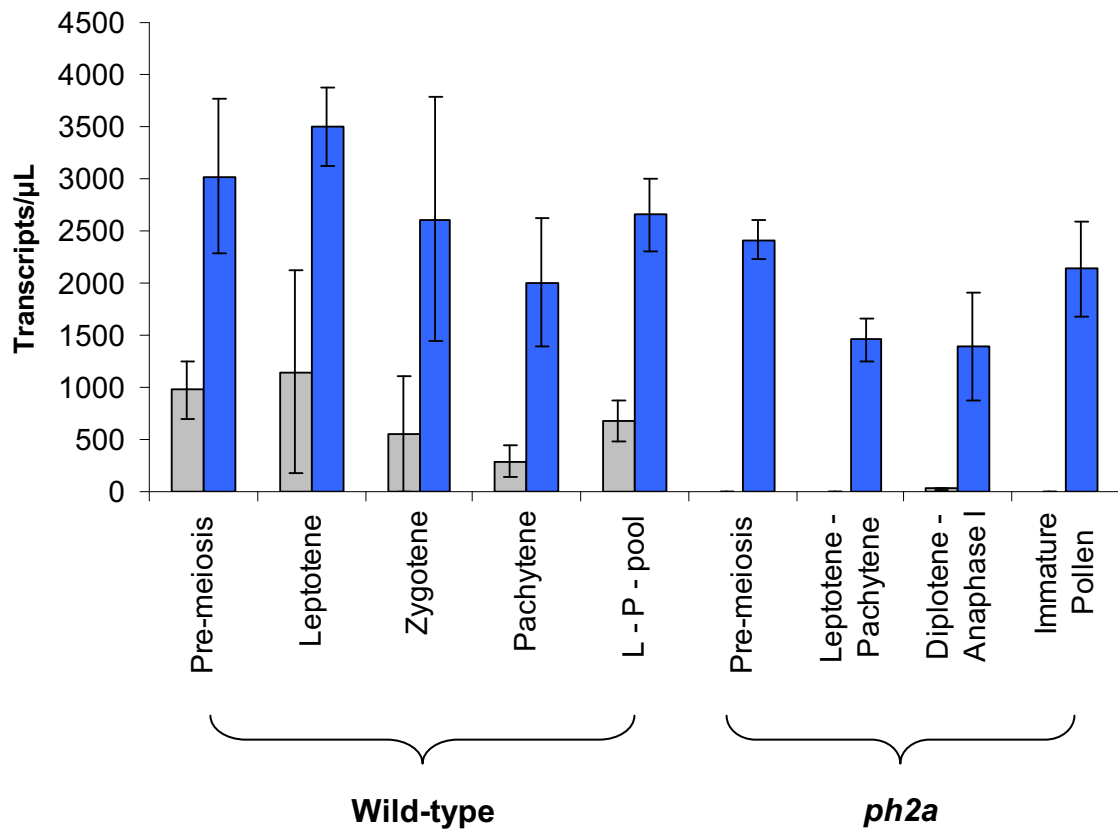
Figure 4.11 – *TaMSH7* and *TaMLH1* expression in the *ph2a* mutant. *TaMSH7* is not expressed in the X-ray-induced *ph2a* deletion mutant and *TaMLH1* is expressed similar to wild-type. L – P = leptotene to pachytene cDNA produced from equal amounts of leptotene, zygotene, pachytene RNA. Grey bars = *TaMSH7*, Blue bars = *TaMLH1*.

	Wild-type		ph2a	
	ASY1	ASY1/DAPI	ASY1	ASY1/DAPI

G2 (A)

Leptotene (B)

Zygotene (C)

Pachytene (D)

Late Pachytene (E)

Late Pachytene (F)
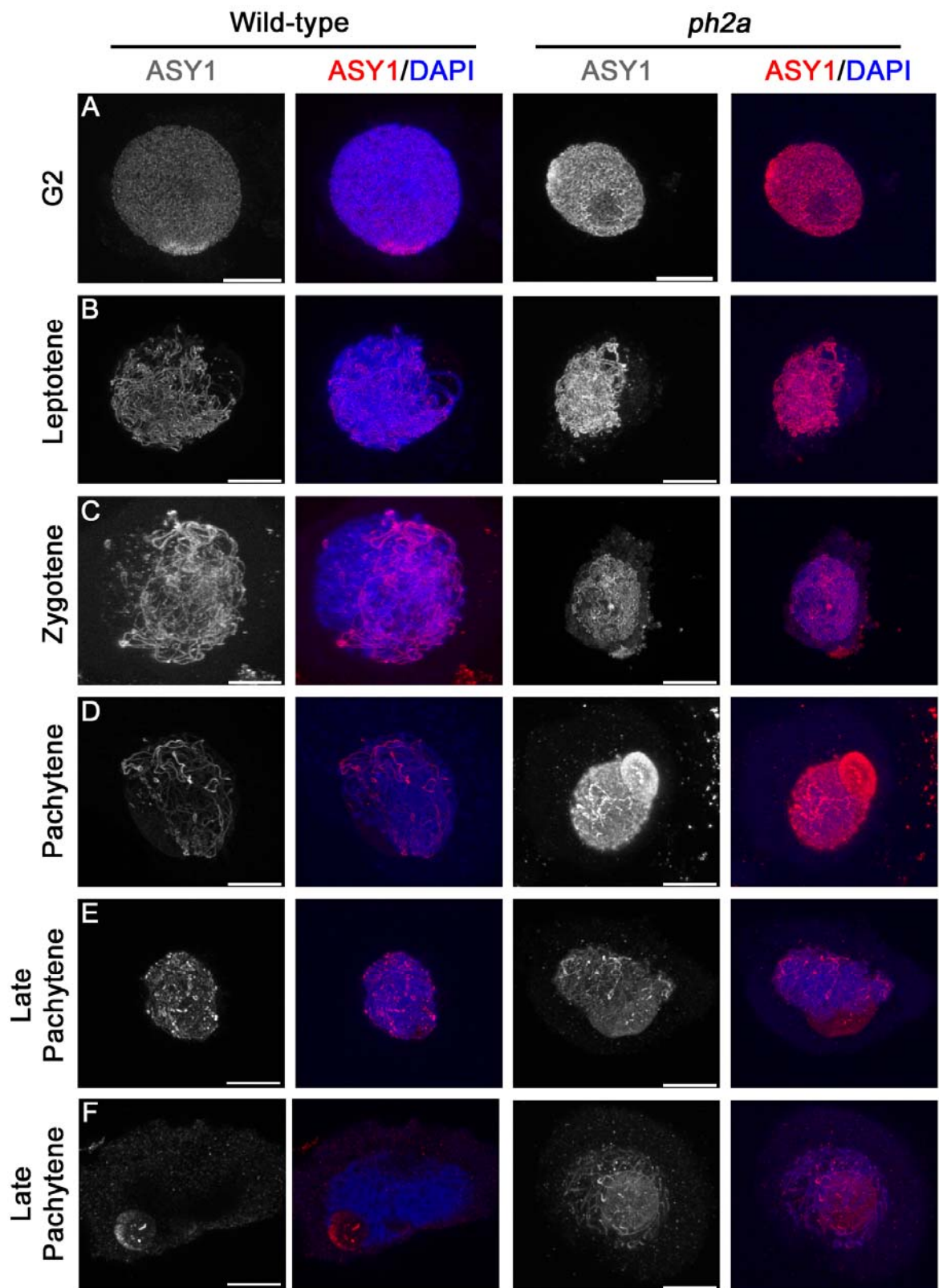
Figure 4.12 – Immuno-localisation of *Ta*ASY1 in wild-type and the *ph2a* mutant. Prophase I progresses similarly with respect to chromosome morphology and general timing of *Ta*ASY1 signal behaviour. However the general intensity of the *Ta*ASY1 signal appears stronger in *ph2a* with an excess of signal appearing around pachytene. White = anti-*Ta*ASY1 and red/blue merges = anti-*Ta*ASY1/DAPI respectively. Scale bar = 10 μm.
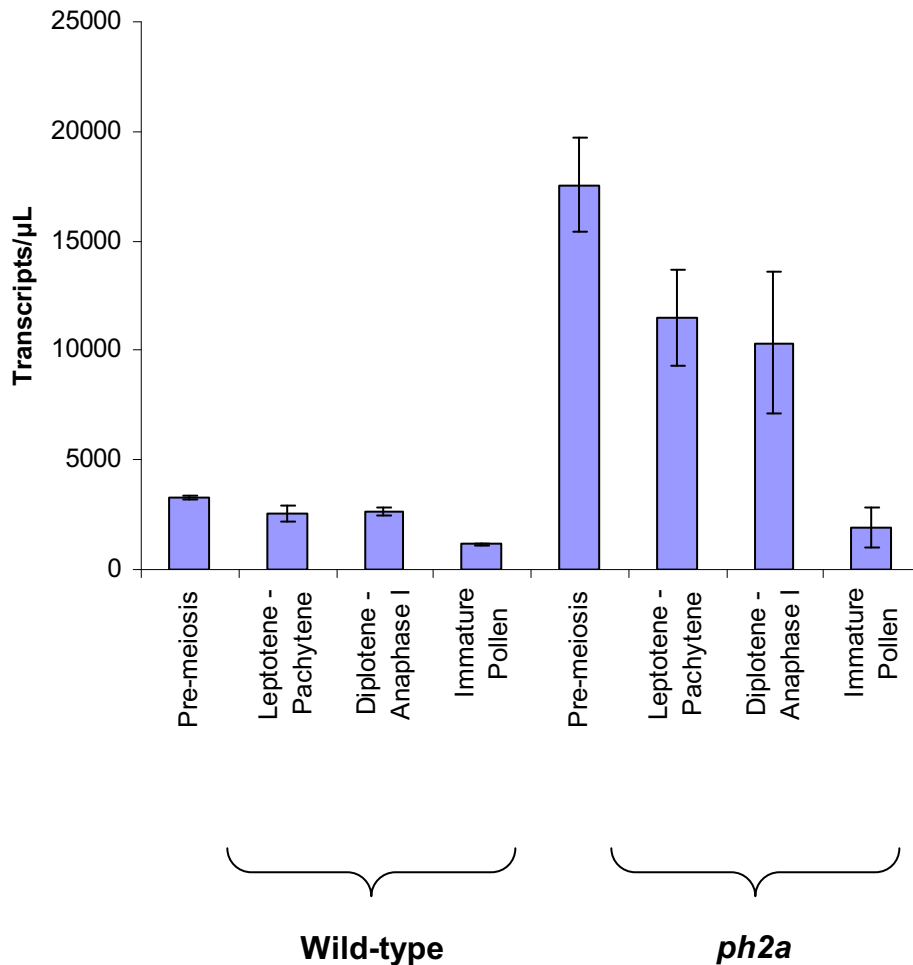
Figure 4.13 – *TaASY1* is up-regulated in the X-ray-induced *ph2a* deletion mutant compared to wild-type. *TaASY1* transcript is highest at late pre-meiotic interphase. Subsequent stages leptotene to pachytene, diplotene to anaphase I and immature pollen show a general downward trend occurring in both genotypes but a different overall level of expression is seen. The data in the two time lines have a correlation co-efficient of $R = 0.98$ when the data is centred.

4.4 – Discussion

The major goal of the research presented in this chapter was to functionally analyse the role of *TaMSH7* in bread wheat. *TaMSH7* is a gene which based on its putative function could potentially suppress homoeologous recombination events. It is known that such mechanisms do exist in bread wheat in addition to promoters of homologous pairing. The functional analysis of *TaMSH7* was performed using RNAi to reduce the levels of *TaMSH7* transcript compared to wild-type controls. While RNAi technology is a useful tool for silencing a gene of interest, it will rarely be 100% effective. Several studies including this one show that in germline tissue (at least), variable levels of transcript reduction are common (Boden *et al.*, 2008; Higgins *et al.*, 2005). Unexpected outcomes can be observed with RNAi mutants or at least, inconsistency with mutants derived through other means (Li *et al.*, 2004; Siaud *et al.*, 2004). Complications may potentially arise as it is known that there are endogenous meiotic-specific RNAi mechanisms in multiple taxonomic kingdoms (Holmes & Cohen, 2007; Nonomura *et al.*, 2007). While more ideal than RNAi technology, T-DNA insertion lines are not currently available in bread wheat due to its hexaploid nature and the problems that would be associated in obtaining mutant plants with insertions in all three homoeologous genomes.

4.4.1 – Genetic analysis of *Tamsh7* mutants

Seeds were germinated from lines that tested positive for the insertion in the T_0 generation using PCR. The T_1 generation was also genotyped. As it was necessary to increase seed numbers, no cytological analysis was performed on this generation (as cytology involves sacrificing inflorescences and therefore the seeds from that tiller). T_2 seeds were germinated from lines that carried the p*Tamsh7*-RNAi insertion. Plants were again

genotyped and closer analysis of the plants testing positive for the presence of the p*Tamsh7*-RNAi insertion was undertaken. Lines were identified that based on segregation patterns and therefore statistical probability, were likely to be homozygous. Lines that were found to have heterozygous parents were still studied as according to the theory underpinning RNAi, the RNAi phenotype is likely to be dominant. Segregation patterns and the numbers of plants analysed are suggestive of the insertion events in the three T_2 mutant lines studied being within a single loci in the genome (while being in different positions between the three independent insertion events). It is frequent that tandem arrays of the construct will insert into one position in the genome but far less frequently in multiple positions in the genome. This is not surprising given the low transformation efficiency of bread wheat when using microprojectile particle bombardment. Southern blot analysis was performed to determine the copy number present in the three *Tamsh7* mutant lines analysed. However this was unsuccessful due to the failure to produce an efficient probe (data not shown). Irrespective, the genotyping and Q-PCR results confirmed the presence and functionality of the RNAi construct.

4.4.2 – Plant morphology and fertility in the *Tamsh7* mutants

Tamsh7 mutants developed normally until ripening (Feeke's scale = 11). This is consistent with the phenotypic analysis of many meiotic mutants in Arabidopsis and wheat which show normal vegetative growth but short siliques and altered spike morphology respectively. *Tamsh7* mutants displayed reduced seed set indicating a reduction in fertility. The reduction in seed set often occurred from the top of the spike down. Residual seed set was observed from roughly the middle to the bottom of the spikes in such instances. This pattern of infertility in wheat has been noted in other meiotic mutants, specifically *ph1b* and

Taasy1 mutants (Boden *et al.*, 2008; Sears, 1977). Therefore, pollen viability was analysed. This was shown to be reduced at a statistically significant level in two of the *Tamsh7* mutant lines: *Tamsh7-1* and *Tamsh7-2*, however *Tamsh7-3* yielded numbers of aborted pollen at a frequency more similar to wild-type. The segregating plants analysed in the *Tamsh7-1* line which had lost the RNAi construct also showed pollen viability numbers similar to wild-type, suggesting that the reduction of *TaMSH7* transcript levels can lead to a decrease in fertility.

4.4.3 – *TaMSH7* expression analysis in *Tamsh7* mutants

Expression analysis using Q-PCR was conducted in *Tamsh7* mutants to identify those T_1 lines that had reduced transcript levels of *TaMSH7* when compared to wild-type. Staging of anthers from pre-meiosis to pachytene for RNA extractions generated data which showed that *TaMSH7* expression was reduced in most plants carrying the construct.

4.4.4 – Meiotic chromosome analysis in wild-type, *Tamsh7* and *ph2a* mutants

Feulgen staining of the meiocytes in the *Tamsh7* mutant backgrounds revealed abnormalities indicative of homoeologous chromosome associations occurring as multivalent structures. The nature of these chromosome associations cannot be confirmed in this study as being strictly homoeologous or non-homologous, as probes to homoeologous regions of the genome were not used. However, evidence such as the hierarchy of chromosome associations in *Brassica* and wheat species (Nicolas *et al.*, 2008; Prieto *et al.*, 2005) would suggest that when a suppressor of homoeologous pairing or promotion of homologous pairing is relaxed, the most likely associations during meiosis in

bread wheat would be between homoeologues. Some of these multivalent events can occur in wild-type as late as metaphase I (even though they are also normally resolved prior to anaphase I), however the frequencies of such events are rare (Colas *et al.*, 2008; Feldman, 1966).

Immuno-fluorescence localisation of *Ta*ASY1 in wild-type was generally reflective of the behaviour of the functional ASY1 homologue in Arabidopsis (Armstrong *et al.*, 2002). However it appears that due to the presence of homoeologues and a generally larger genome, the signal persists at times where multivalent structures can be seen between the lateral elements of multiple chromosomes suggesting that the presence of *Ta*ASY1 (and presumably its unknown counterparts) are required for the correction of these multiple associations to proceed accurately. Also, regions where the lateral elements appear to be intertwined can be seen at zygotene before this resolution occurs. Additionally, it was noted that on the same preparation/slide not every meiotic cell from pre-meiosis to pachytene (based on the DAPI signal) was immunised effectively or in the exact same manner. This most likely reflects a need for optimisation of the permeabilisation step in the protocol. However, while this was not a restrictive problem, it needs to be considered when selecting the appropriate cells for analysis.

Immuno-localisation of *Ta*ASY1 in the *Tamsh7-1* mutants revealed that *Ta*ASY1 was at times present at higher levels than in wild-type. This was typically observed as a persistent signal on synapsed chromosomes longer than at the equivalent stage in wild-type. This type of signal was seen to stem from regions of multiple associations and generally persisted along the length of the pairs (or more) of synapsed chromosomes. *Tamsh7-1* showed regions of tangled chromosomes at the same X, Y and Z planes suggestive of multiple associations which are not being corrected efficiently or at least not in the same

manner as wild-type. Furthermore the intense signal was localised only to the chromosomes with these entanglements, compared to wild-type where there was a lower intensity of signal at this later stage of correction, which was spread across many chromosomes rather than what appeared to be problematic regions. Despite this abnormality in *Ta*ASY1 behaviour, the signal still localised to chromosomes prior to synapsis and during initiation of synapsis, as is seen in wild-type. The three different independent insertion events with the *Tamsh7* RNAi lines showed variable effects. While *Tamsh7-3* appeared like wild-type, *Tamsh7-2* also appeared normal in the stages that were examined. Due to a limited amount of meiotic material, a high resolution time-course of the *Tamsh7-2* mutant could not be created.

4.4.4.1 – *TaMSH7* and *TaASY1* expression analysis in the *ph2a* mutant

Expression analysis of *TaMSH7* was conducted in the *ph2a* mutant background. Strikingly it was found that *TaMSH7* is not expressed in the *ph2a* mutant which lacks a region of 3DS. *TaMSH7* expression levels were previously analysed in this mutant and found to be reduced but still present compared to wild-type (Dong *et al.*, 2002). The time-course data presented here conflicts with the previously reported data generated *via* northern blot analysis. These discrepancies may potentially be due to non-specificity of the probes used in the previous study.

Given that upon polyploidisation in species such as bread wheat, mechanisms arise such as "cross talk" between homoeologous genes (Feldman & Levy, 2005; Griffiths *et al.*, 2006), it was anticipated that *TaMSH7* would be expressed in the *ph2a* mutant despite the deletion (Sears, 1982) of one of the three *TaMSH7* genomic copies of (Dong *et al.*, 2002). This was not the case and continues to support that *TaMSH7* might underlie the *ph2*

phenotype. It is currently unclear why the A and B genome copies of *TaMSH7* are not transcriptionally active in the *ph2a* mutant. Perhaps there is a dosage-dependent mechanism that regulates the amount of transcript produced and it is the A and B copies that are not functional even in wild-type.

Upon investigating *Ta*ASY1, expression was seen to be present in abnormally high levels during meiosis in the *ph2a* mutant based on both transcript data and immuno-localisation experiments. An abundance of protein appears to exist freely in the nucleoplasm in addition to localising to the nucleolus and at times as polycomplexes, however polycomplexes can even be seen at certain stages of prophase I in wild-type. However, these polycomplexes appear small however when compared to the size of *Ta*ASY1 polycomplexes seen in *ph1b* mutants despite the same experimental methods being used (Boden *et al.*, 2008).

The main objective of the work presented in this chapter was to determine if *TaMSH7* is required for the suppression of homoeologous recombination events. While a relatively limited "tool set" was available to determine this, *TaMSH7* has been shown to be required for fertility and normal chromosome interactions. However, at this stage it is premature to state the precise nature of the chromosomal abnormalities in these mutants and whether or not *TaMSH7* is responsible for the *Ph2* phenotype (or whether it contributes to it).

Chapter 5 – Immuno-localisation of *At*MER3 in the interfering crossover pathway

5.1 – Introduction

The previous chapter focused on aspects of the selection of recombination template during meiosis. However, another interesting facet of meiosis is the control of the frequency and positioning of crossovers/recombination between homologous chromosomes. Given the limited wheat studies of recombination along chromosomes and hence mutant/resource availability, another aspect of recombination control was analysed by moving into a model organism: *Arabidopsis thaliana*. A number of laboratories in Europe have superior resources and expertise in this model and hence a component of the work was undertaken there.

As previously discussed (see literature review), the DSBR pathway begins with a double-stranded break which leads to a crossover (CO) or a non-crossover (NCO). There are at least two types of crossovers: 1) Crossovers which do not appear adjacent to another crossover. These are known as interfering crossovers or class I COs. 2) Crossovers which are randomly positioned along chromosomes. These are known as non-interfering crossovers or class II COs. Numerous proteins have been identified in many organisms, which are essential for crossover interference. However, little is known about the pathway(s) which control the process and perhaps even more importantly, how it is that essential proteins in the pathway(s) interact with one another.

In budding yeast (*S. cerevisiae*) the ZMM epistatic group (ZIP1, ZIP2, ZIP3, ZIP4/SPO22, MSH4, MSH5 and MER3) co-ordinate the events of synaptonemal complex

formation and are essential for crossover interference (for review see Lynn *et al.*, 2007). *S. cerevisiae* MER3 is a DNA helicase that extends the DNA heteroduplex during the DSBR pathway (Mazina *et al.*, 2004). Single-end invasion intermediates and dHJs were not detected in the *mer3* mutants (Borner *et al.*, 2004), therefore building a case for MER3 playing a role which stabilises dHJ formation and also CO formation. The *mer3* mutant has reduced CO frequency but the number of NCOs is unaffected. Furthermore, the residual crossovers displayed no interference (Nakagawa & Ogawa, 1999).

Atmer3 mutants were isolated from the SALK T-DNA mutant bank (Alonso *et al.*, 2003; Mercier *et al.*, 2005). The mutant plants displayed reduced fertility and closer inspection revealed incorrect segregation of the chromosomes at the first meiotic division. In some instances sister chromatids where seen prematurely separating and also displaying incorrect bipolar orientation. Crossover formation (during the first meiotic division) in the *Atmer3* mutants was reduced by approximately 75%. The residual crossovers in an adjacent set of genetic intervals did not display interference. Based on chromatin spreads of *Atmer3* mutant meiocytes, prophase I and synapsis proceeds normally until diakinesis where it becomes apparent that there are not strictly five bivalents as in wild-type. This leads to incorrect segregation at the first meiotic division, and therefore in meiosis II when the sister chromatids separate this produces unbalanced gametes. The other abnormality based on the chromatin spreads was that the first steps of prophase up to apparently full and complete synapsis at pachytene, was that the chromatin had a 'fluffy' appearance compared to the same stages in wild-type. The biological meaning of this is not clear.

Similarly, recent characterisation of the *Atzip4* mutants showed that crossover formation was reduced by approximately 85% when compared to wild-type. When the *Atzip4* mutants were crossed with *Atmsh4* mutants, which also show a crossover reduction

of approximately 85%, the crossover level remained the same, thus demonstrating that the ZMM function of *S. cerevisiae* ZIP4 has also been conserved in Arabidopsis. In the *Atzip4* mutants, the residual crossover events that occurred in adjacent intervals on a region of chromosome I showed no interference. Interestingly, synapsis was initiated from fewer sites than wild-type levels, but synapsis was completed and mature synaptonemal complexes appeared very similar to those in wild-type. Therefore Chelysheva *et al.*, (2007) demonstrated that synapsis and class I CO formation can be uncoupled in Arabidopsis. To further understand the function of *At*MER3 in the DSBR pathway, a polyclonal antibody targeted against *At*MER3 was made (described in Vignard, 2007) and analysed in various mutant backgrounds. The results of which are presented in this chapter.

5.2 – Materials and methods

5.2.1 – Plant growth conditions and plant material

The Arabidopsis plants were grown in a temperature-controlled glasshouse at 20°C with a 16 hour photoperiod and humidity maintained at 70%. The mutants referred to in this chapter correspond to the following lines already reported in the literature: *Atmer3* – salk_045941 (Mercier *et al.*, 2005), *Atspo11* – "spo11-1-2" (Grelon *et al.*, 2001), *Atmre11* – salk_054418/"mre11-3" (Puizina *et al.*, 2004), *Atrad51*: GABI_134A01/"rad51-1" (Li *et al.*, 2004), *Atdmc1* – "dmc1-1" (Couteau *et al.*, 1999), *Atmsh5* – salk_110240/"*Atmsh5-1*" (Higgins *et al.*, 2008).

5.2.2 – Immunocytology of male *Arabidopsis thaliana* meiocytes

The following methods were adapted from Chelysheva *et al.* (2005) and Armstrong *et al.* (2002).

5.2.2.1 – Isolation and preparation of meiotic material

Slides used were boiled for 30 minutes in de-ionised water and then dried. Ten to fifteen buds measuring approximately 0.5 mm in length were isolated from at least three different inflorescences to ensure isolating the desired stages of prophase I. The buds were placed in 10 µL of digestion medium (DM) (cytohelicase 0.1 g, sucrose 0.0375 g, PVP 0.25 g, de-ionised water up to 25 mL). Anthers were then isolated from the buds in the DM and all other bud material was discarded, with the anthers centred in the solution. Anthers were incubated in the DM at 37°C for two minutes on a heating block to allow the cytohelicase to digest and weaken the callose pollen mother cell (PMC) wall (Albini, 1994). After incubation, PMCs were released from the anthers squashed in the drop of DM by tapping with a blunt rod of approximately 3 mm in diameter. Unbroken anthers were squashed with a hook-shaped needle.

10 µL of lipsol (1% in sterile de-ionised water, adjusted to pH 9 with borate buffer) was added to the drop of DM and PMCs. To release the nuclear DNA, the drop was stirred vigorously for two minutes at room temperature using the 'blunt' side of the hook-shaped needle. The spread preparations were then fixed by adding 20 µL of cold fixative, with the resulting solution spread out to approximately one inch in diameter. Fixative solution was made by dissolving 4 g of paraformaldehyde in 75 mL of sterile de-ionised water. Then 1-2 drops of 1 M KOH were added and the solution was heated at 70°C for 20 minutes, before cooling at room temperature and topped up to 100 mL with phosphate buffers to arrive at pH 7.3-7.4. The phosphate buffers were; 200 mM K_2HPO_4 ((pH 9.2) 6.97 g/200 mL of water) and 200 mM KH_2PO_4 ((pH 4.4) 5.44 g/200 mL of water).

The dried preparations were rinsed softly with sterile de-ionised water and then dried again. The dry preparations were washed in PBS-T (1 X PBS, 0.1% v/v Triton, pH 7.4) for three minutes. Excess buffer was removed by holding the slide vertical on an absorbent towel briefly.

5.2.2.2 – Immunisation of meiotic preparations

Preparations from 5.2.2.1 were then immunised with the appropriate primary antibodies (Table 5.1) at the optimal dilutions in 1 X PBS; 1% w/v BSA; 0.1% v/v Triton (PBS-T-BSA) overnight at 4 °C in a humidity chamber. The production of the *At*ASY1, *At*DMC1 and *At*MER3 antibodies are described elsewhere (Armstrong *et al.*, 2002; Chelysheva *et al.*, 2007; Vignard, 2007).

Table 5.1 – The primary antibodies used in the study. The antibodies were used at different dilutions in PBS-T-BSA. The antibodies were raised in either rabbit or rat.

Target	Dilution required	Animal immunised
*At*ASY1	1:500	Rabbit
*At*DMC1	1:20	Rabbit
*At*MER3	1:200	Rat

The following day the slides were washed three times for 15 minutes per wash in PBS-T. The meiotic preparations were then incubated with the anti-rabbit and anti-rat secondary antibody dilutions (also diluted in PBS-T-BSA – 1:100) for 1 hour at 37°C in a light-protected humidity chamber. Three 10 minute washes in PBS-T followed. A drop of approximately 15 µL of DAPI diluted in Vectashield (2 µg mL^{-1}) was applied to a cover slip, which was then placed onto the slide. Excess DAPI solution was removed by blotting with Whatman paper.

5.2.2.3 – Microscopy and image processing

All images were captured and processed as described previously (Chelysheva *et al.*, 2007).

5.3 – Results

5.3.1 – Localisation of MER3 in wild-type Arabidopsis

The nuclear distribution of *At*MER3 was analysed in wild-type Arabidopsis (ecotype Columbia-0, herein referred to as Col-0), with ASY1 used as a counter stain to track the progression of late interphase and prophase I until pachytene where ASY1 then unloads from meiotic chromosomes (*At*ASY1 behaviour is described in detail in Armstrong *et al.*, 2002). *At*MER3 was not found to be present at the very late stages of meiotic interphase where *At*ASY1 appears as punctuate foci (Figure 5.1A). The *At*MER3 signal was found to appear primarily on meiotic chromatin before synapsis initiates at an intensity slightly higher than the background signal (Figure 5.1B). By visualising the merged image of the ASY1 and MER3 signals, it is evident that *At*MER3 antibody localises along the *At*ASY1 tracks. However, the *At*MER3 foci are more prominent on regions that have recently synapsed (Figure 5.1C). This signal persists on mature synaptonemal complexes (although potentially slightly weaker).

5.3.2 – Specificity of the *At*MER3 antibody: Localisation of MER3 in the *Atmer3* mutant background

Immuno-localisation experiments with the *At*MER3 antibody in the *Atmer3* mutant background shows a background signal, however the intensity is weaker than the weakest of the *At*MER3 signals from wild-type discussed in this chapter (Figure 5.1D-F).
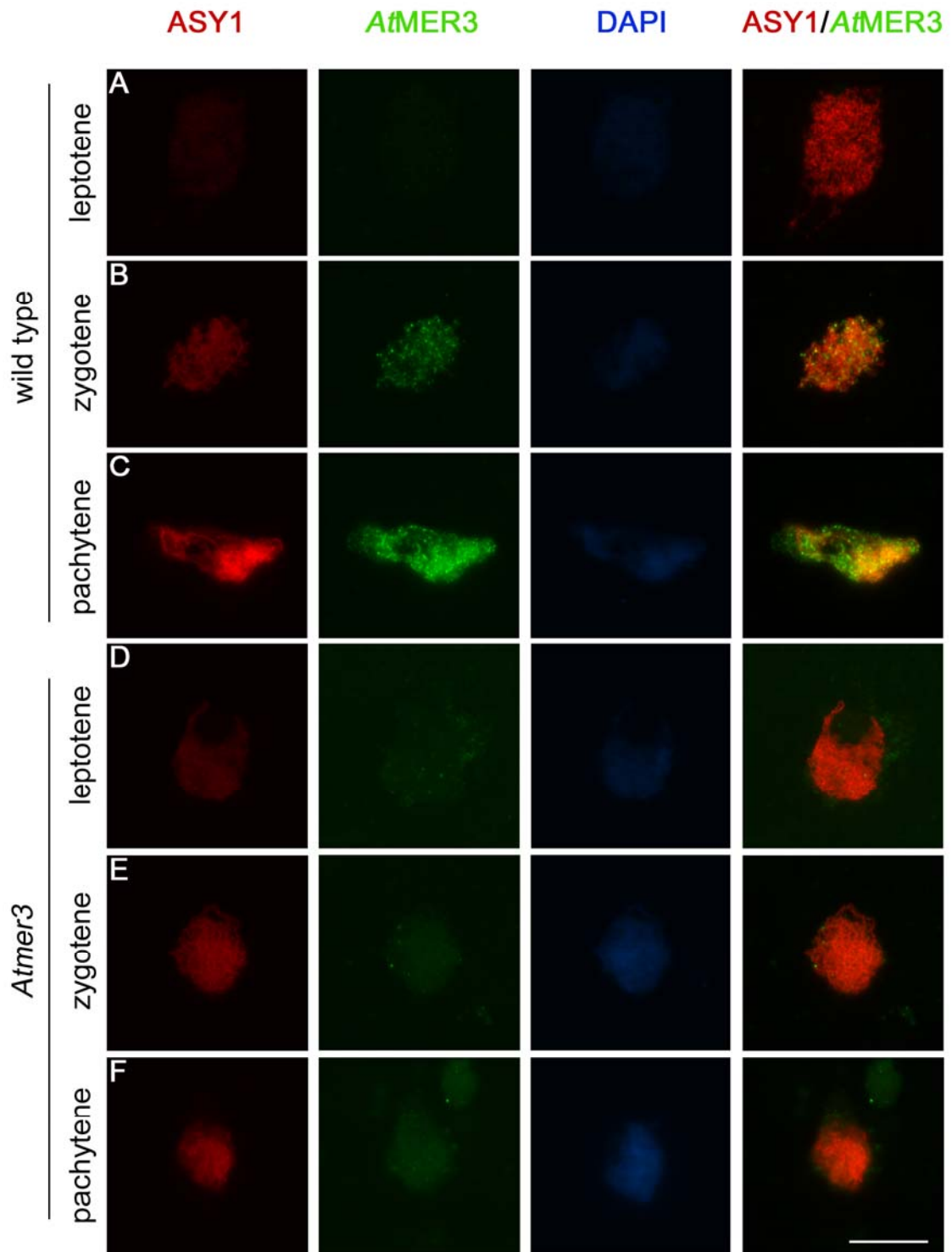
Figure 5.1 – Immunolocalisation of the *At*MER3 protein. Male meiocytes from wild-type (A-C) and the *Atmer3* mutant (D-F). Chromosomes are stained with the anti-*At*ASY1 antibody (red), the *At*MER3 antibody (green) and DAPI (blue). The *At*MER3 antibody first appears just prior to the onset of synapsis (B) and is strongest in the freshly synapsed regions of chromosomes (C). No *At*MER3 signal is detected above background levels in the *Atmer3* mutant (D-F). Scale bar = 10 μm.

5.3.3 – *At*MER3 and *At*DMC1 do not co-localise on meiotic chromosomes

*At*DMC1 is a meiosis-specific protein which localises to sites of double-strand breaks that can potentially give rise to crossovers, therefore the *At*MER3 and *At*DMC1 antibodies were used to immunise the same meiocytes to investigate whether or not they co-localise. However, co-immunolocalisation experiments found that *At*MER3 and *At*DMC1 do not co-localise during meiotic prophase I in Arabidopsis (Figure 5.2D).
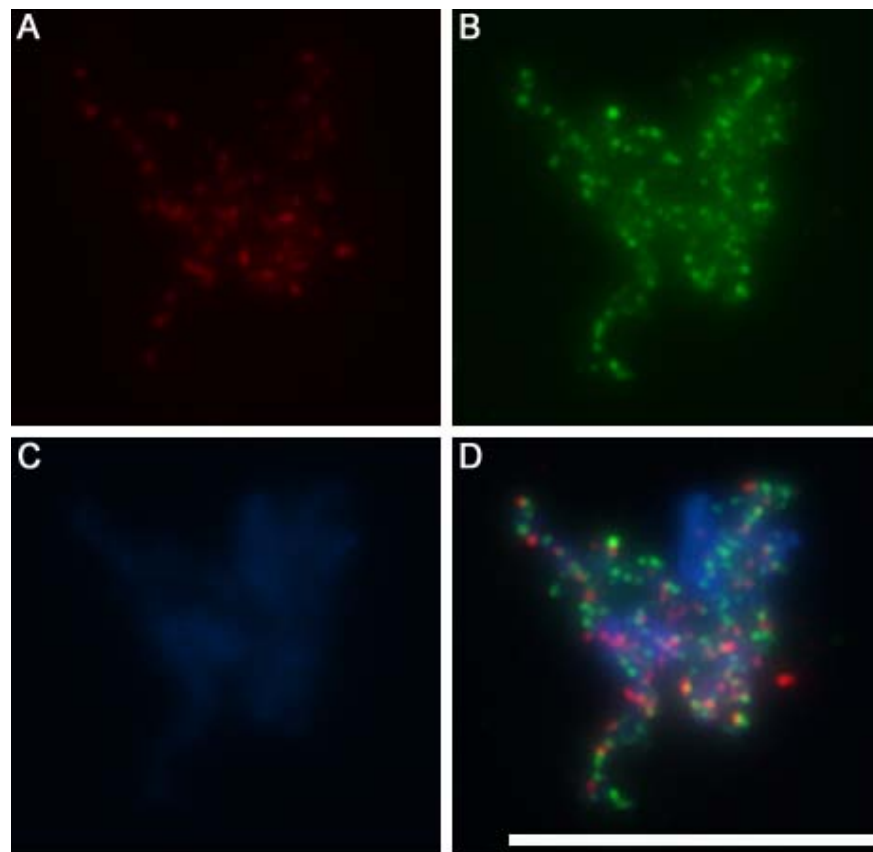
Figure 5.2 – *At*MER3 and *At*DMC1 do not co-localise. Wild-type male meiocyte stained with the *At*DMC1 antibody (A), the *At*MER3 antibody (B) and DAPI (C). The merged image (D) was constructed by overlaying A, B and C. Scale bar = 10 μm.

5.3.4 – Localisation of *At*MER3 in *Atspo11* mutants

In order to determine at what stage(s) in the double strand break repair pathway *At*MER3 acts, *At*MER3 was localised in multiple Arabidopsis meiotic mutants that have deficiencies in different stages of the DSBR pathway.

       *At*SPO11 induces double-strand breaks that are required to initiate recombination in meiosis from species as diverged as *S. cerevisiae* to Arabidopsis. *At*MER3 localisation does not appear normal in the *Atspo11* mutant background (Figure 5.3C). At a pachytene-like stage in the asynaptic *Atspo11* mutant, the *At*MER3 signal does not appear as strong as the equivalent stages in wild-type. In addition to the reduced intensity of the *At*MER3 signal, there are also *At*MER3 polycomplexes present (Figure 5.3C, indicated with white arrowheads). These results suggest that double-strand breaks produced by *At*SPO11 are required for normal loading of the *At*MER3 protein in Arabidopsis during meiotic recombination.
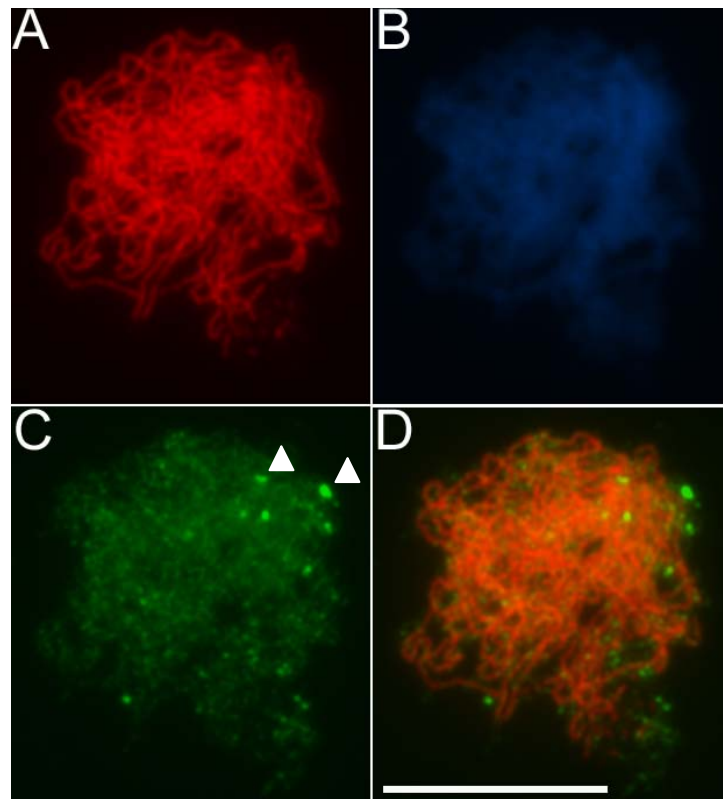
Figure 5.3 – *At*MER3 loading is perturbed in the absence of *At*SPO11. Male meiocyte stained with the *At*ASY1 antibody (A), DAPI (B) and the *At*MER3 antibody (C). The merged image (D) was created by overlaying A and C. *At*MER3 signal does not appear above background level except in the polycomplexes (indicated by arrowheads in C). Scale bar = 10 μm.

5.3.5 – Localisation of *At*MER3 in *Atmre11* mutants

The MRN complex is composed of MRE11, RAD50 and NBS1 with all three proteins indispensible for correct function of the complex. This complex is required to process *At*SPO11-induced DSBs during meiosis which in turn allows recombination events to occur. Loss of *At*MRE11 function leads to chromatin bridges and chromosome fragmentation due to lack of repair of the DSBs.

*At*MER3 localisation was attempted in the *Atmre11* background in order to determine if the localisation pattern of *At*MER3, and presumably its function also, are dependent on the DNA processing role of the MRN complex (Figure 5.4). The *At*MER3 signal appears weaker than at the equivalent stage in wild-type (based on the nature of the *At*ASY1 conformation). That is, there are no intense *At*MER3 foci as the chromatin approaches the pachytene-like stage. However, the interpretation of the results obtained for *At*MER3 localisation is not as straight forward as the other genotypes (see discussion).
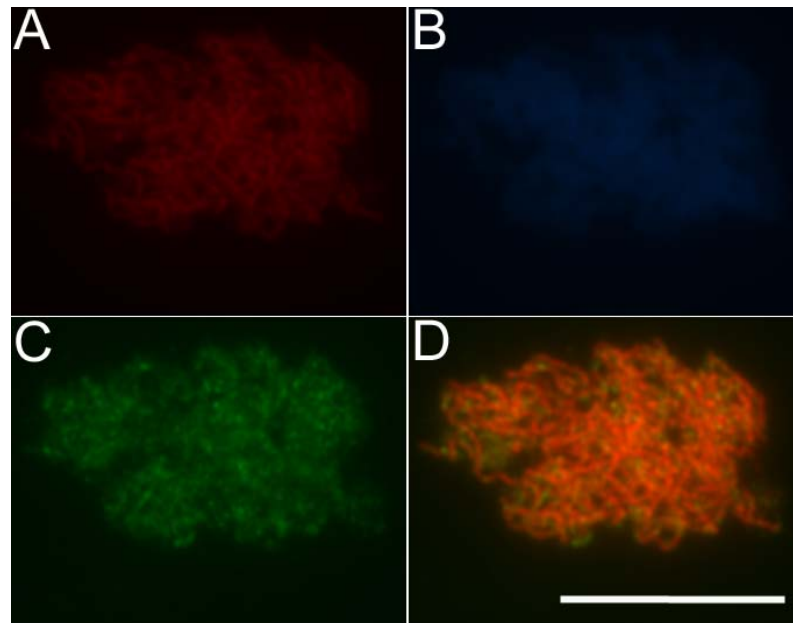
Figure 5.4 – *At*MER3 loading in the *Atmre11* mutant. Male meiocyte stained with the *At*ASY1 antibody (A), DAPI (B) and the *At*MER3 antibody (C). The merged image (D) was created by overlaying A and C. *At*MER3 signal does not appear above background level in the *Atmre11* mutant. Scale bar = 10 μm.

5.3.6 – Localisation of *At*MER3 in *Atrad51* mutants

During meiosis in Arabidopsis plants that lack a functional copy of the *At*RAD51 recombinase, chromosomes fail to synapse and become extensively fragmented (Li *et al.*,

2004). This fragmentation is *At*SPO11-dependent implying that *At*RAD51 acts in the DSBR pathway. Therefore, *At*MER3 localisation was analysed in *Atrad51* mutants.

The *At*MER3 signal in the *Atrad51* mutants is relatively normal at the pachytene-like stage. Bright *At*MER3 foci, not unlike those in wild-type with respect to both signal strength in addition to the pattern of localisation, can be seen localising along the tracks of the *At*ASY1 signal which appear thicker due to the progression of the pachytene-like stage (Figure 5.5C and D).
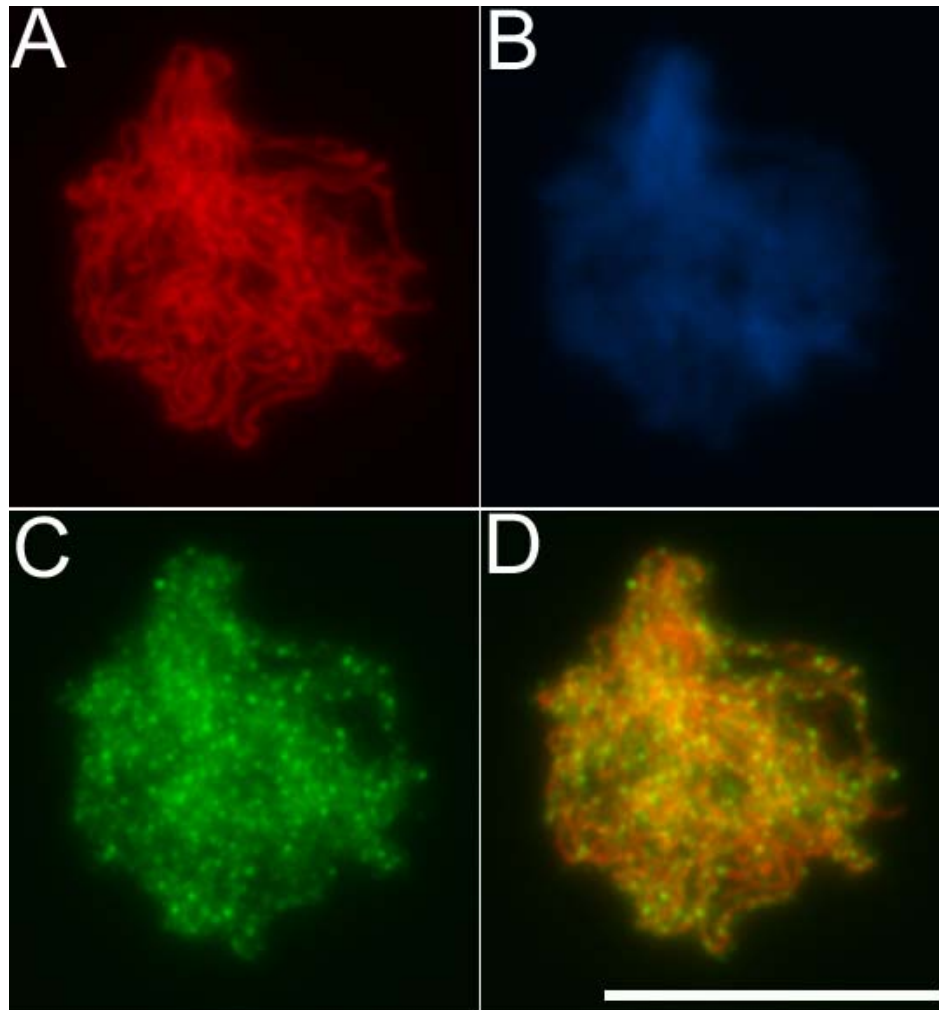
Figure 5.5 – *At*MER3 localisation is not dependent on *At*RAD51. Male meiocyte stained with the *At*ASY1 antibody (A), DAPI (B) and the *At*MER3 antibody (C). The merged image (D) was created by overlaying A and C. The *At*MER3 antibody forms foci in the pachytene-like stage in the *Atrad51* mutant much like the *At*MER3 foci in wild-type at zygotene-pachytene. Scale bar = 10 μm.

5.3.7 – Localisation of *At*MER3 in *Atdmc1* mutants

*At*DMC1 is a meiosis-specific DNA recombinase required for synapsis and bivalent formation. It is also involved in the DSBR pathway and acts at a similar stage to *At*RAD51, localising to potential sites of recombination. Results obtained were similar to that of wild-type and also the other recombinase mutant background, *Atrad51*, both spatially,

temporally and also with respect to foci intensity. There is no synapsis in the *Atdmc1* mutants, however like many meiotic mutants, it has a pachytene-like stage. It is at this stage where strong foci can be seen that localise only to meiotic chromatin as indicated by the thick and polymerised *At*ASY1 signals (Figure 5.6), indicating that *At*DMC1 is not required for normal localisation of *At*MER3.
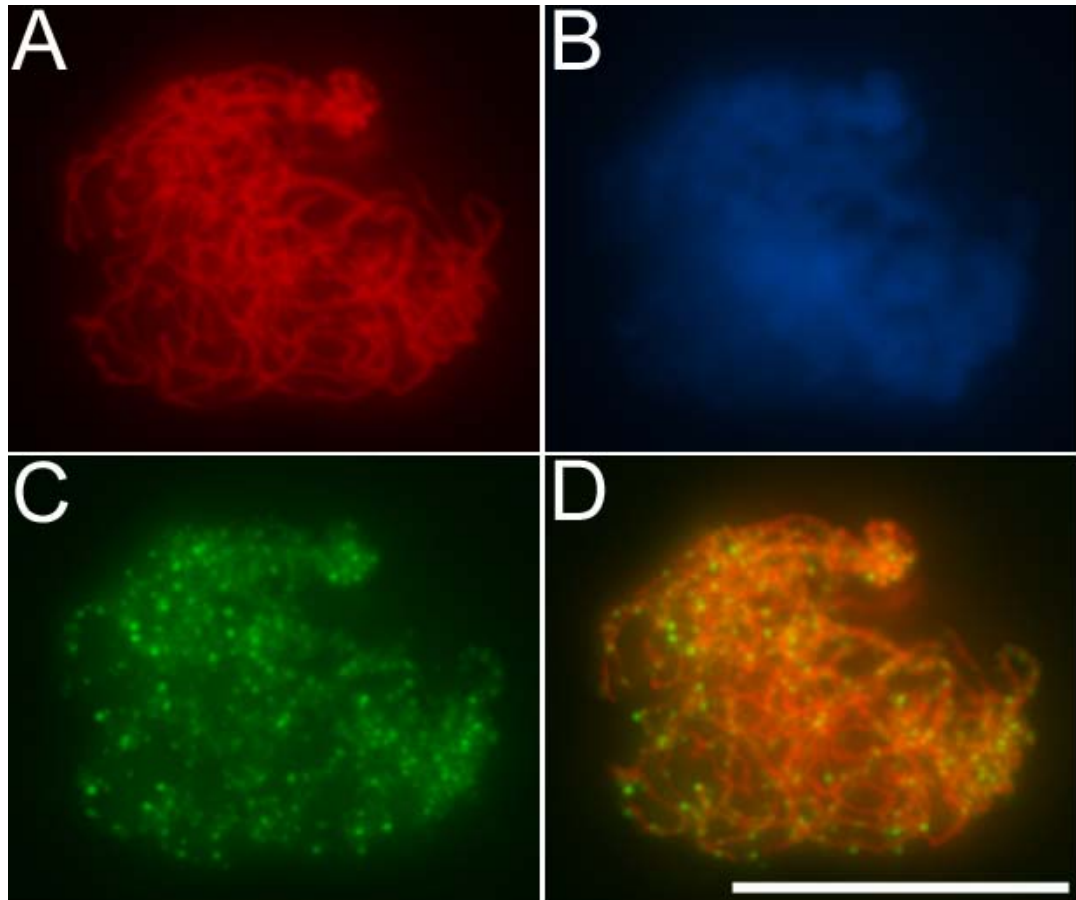
Figure 5.6 – *At*MER3 localisation is not dependent on *At*DMC1. Male meiocyte stained with the *At*ASY1 antibody (A), DAPI (B), and the *At*MER3 antibody (C). The merged image (D) was created by overlaying A and C. The *At*MER3 antibody forms foci in the pachytene-like stage in the *Atdmc1* mutant similar to the *At*MER3 foci in wild-type at zygotene-pachytene. Scale bar = 10 μm.

5.3.8 – Localisation of *At*MER3 in *Atmsh5* mutants

*At*MER3 was localised in the *Atmsh5* mutants and appears indistinguishable from *At*MER3 behaviour in wild-type (Figure 5.7). *At*MER3 signal is strongest on recently synapsed regions of DNA as indicated by the state of the *At*ASY1 signal. The primary weaker signal that appears in wild-type can also be seen on regions, where based on *At*ASY1 signal progression, synapsis has not yet been initiated (Figure 5.7).
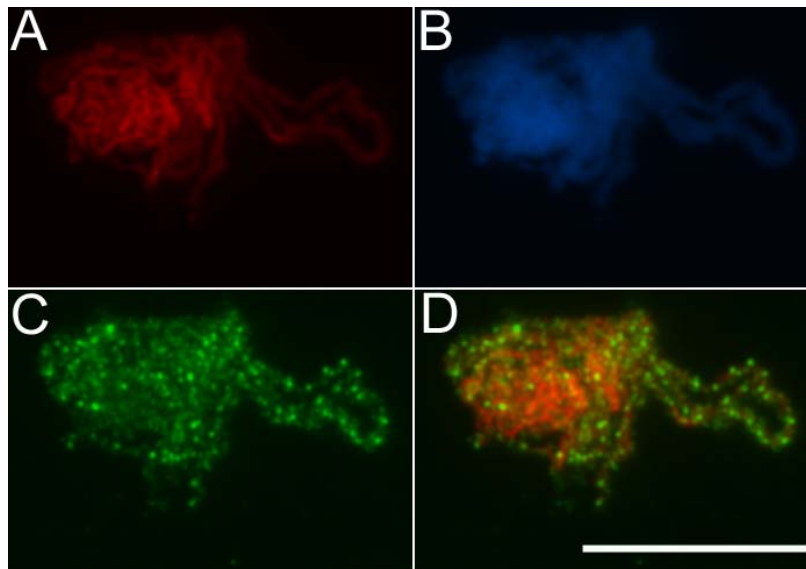
Figure 5.7 – *At*MER3 localisation is not dependent on *At*MSH5. Male meiocyte stained with the *At*ASY1 antibody (A), DAPI (B) and the *At*MER3 antibody (C). The merged image (D) was created by overlaying A and C. The *At*MER3 antibody forms foci in the synapsed regions of the chromosomes in the *Atmsh5* mutant similar to the *At*MER3 foci in wild-type at the same stage. Scale bar = 10 μm.

5.4 – Discussion

5.4.1 – Nuclear distribution of *At*MER3 in wild-type Arabidopsis meiocytes and the relationship with other meiotic proteins

*At*MER3 was previously shown to have an essential role in the maturation of class I COs during prophase I in Arabidopsis meiosis (Mercier *et al.*, 2005). Therefore, it is reasonable to expect that it would localise to chromatin during this stage of meiosis. The results of immunolocalisation experiments presented in this chapter confirm this theory. In wild-type, *At*ASY1 appears during meiotic interphase in Arabidopsis as punctuate foci which polymerise completely. Synapsis then initiates, as two linear ASY1 signals (belonging to homologous chromosomes) begin to join like a zipper. Once synapsis is complete in a

given region, the *At*ASY1 signal becomes fuzzy until it is no longer visible at the end of pachytene. The *At*MER3 signal does not appear during the G2 stage based on the *At*ASY1 signal, indicative of no requirement for *At*MER3 at this stage. This is not entirely unexpected given that the DSBR pathway has not been initiated at this stage. The *At*MER3 signal appears once the *At*ASY1 signal has completely polymerised during leptotene, presumably concurrent with or just after DSB formation. Initially the *At*MER3 signal is weak and the signal co-localises with chromatin based on DAPI and *At*ASY1 counterstains. The strongest *At*MER3 foci then appear on freshly synapsed regions of chromosomes, which is consistent with data showing links between the initiation of synapsis and crossover interference. Specifically, *S. cerevisiae sgs1* mutants display increased crossover frequency and synaptonemal initiation complex (SIC) sites, designated by ZIP3 foci (Rockmill *et al.*, 2003). Additional complementary data from *S. cerevisiae* shows that decreasing the frequency of DSBs, which are far in excess of the number of COs, does not affect ZIP3 foci formation until the DSB frequency approaches zero at which point ZIP3 foci formation rapidly decreases (*i.e.* a non-linear relationship between the DSB formation and the occurrence of ZIP3 foci) (Henderson & Keeney, 2004). This is similar to the phenomenon, if not linked to, crossover homoeostasis which maintains a given level of crossovers even in the face of miniscule DSB numbers. However, Chelysheva *et al.*, (2007) show that in Arabidopsis class I COs are not necessary for the formation of a mature synaptonemal complex in *Atzip4* mutants, therefore uncoupling the two processes. The number of SICs do decrease however in the *Atzip4* mutant background. Additionally, the numbers of SICs in many plants far exceeds the number of class I COs per meiosis (Gillies, 1985; Hasenkampf, 1984).

The signal in the *Atmer3* mutants, while present, is significantly lower than the signals of interest in wild-type Arabidopsis at equivalent stages of meiotic progression. There is also a secondary *At*MER3 signal in wild-type which does not localise to the chromatin. The equivalent signal is not seen in the *Atmer3* background suggesting that the *At*MER3 antibody is specifically binding *At*MER3 somewhere in the nucleoplasm and that the *Atmer3* allele used in this study was not binding the products of a 'leaky' *Atmer3* mutant allele. Furthermore, α-*At*MER3 was purified using the heterologously-expressed *At*MER3 in an attempt to eliminate/reduce the different classes of *At*MER3 signal reported in this study. However, when comparing results obtained using whole sera or purified α-*At*MER3, no difference was observed, therefore providing additional evidence in favour of the theory that multiple *At*MER3 signals exist.

A previous study by Vignard (2007) co-localised *At*MER3 with another meiotic protein: *At*ZYP1, a structural component of the SC, more specifically, the transverse filaments. The temporal relationship between *At*ZYP1 and *At*MER3 is interesting. Vignard (2007) co-localised *At*ZYP1 and *At*MER3 in an attempt to understand the relationship between synaptonemal complex formation and *At*MER3 function. At the beginning of zygotene when the *At*ZYP1 signals only resemble foci, the intense *At*MER3 foci have not yet appeared. However, once the *At*ZYP1 signal has begun to polymerise during mid-zygotene and the chromosomes are committed to progression of SC formation, strong *At*MER3 foci begin to appear. The *At*MER3 foci co-localise with the *At*ZYP1 signal and therefore the SC. At this time point, the appearance of the strong *At*MER3 foci begin to precede the polymerising *At*ZYP1 signal on a path which the DAPI channel indicates will be the site of future SCs. At pachytene, the *At*ZYP1 signal has polymerised along the entire length of the homologous chromosome pairs and *At*MER3 localises to the five strands of

*At*ZYP1 signal. At the end of pachytene, *At*ZYP1 begins unloading from the chromosome pairs and interestingly *At*MER3 also detaches in a very concomitant pattern. The results from Vignard (2007) and this study reveal new information about a relationship between *At*MER3 and synapsis in Arabidopsis.

5.4.2 – Interpretation of the MER3 localisation patterns and a role in crossover distribution

Based on previous findings with *S. cerevisiae* MER3 and *At*MER3, it is not an unreasonable hypothesis that *At*MER3 would appear exclusively at class I CO sites if it promotes interfering crossovers. However, perhaps if it is a suppressor of recombination events adjacent to class I COs it may be present as more than 7.8 or 9.2 foci during meiosis in Arabidopsis (the number of chiasma, the cytological reflections of crossovers, in the Wassilevskija and Col-0 backgrounds respectively). But if this were the case, would the foci be evenly spaced? This is probably an over simplification of what is a complex mechanism. The *At*MER3 foci number is far in excess of 9.2 per meiosis, indicating that *At*MER3 is not localising solely to the sites of class I COs.

5.4.3 – *At*MER3 localisation in meiotic mutant backgrounds

*At*SPO11 appears to be required for normal loading of *At*MER3 onto prophase I chromatin. Furthermore, the presence of *At*MER3 polycomplexes, seem consistent with previous observations in the literature. Polycomplexes can arise due to aberrations in chromosome morphogenesis, which is to be expected in asynaptic mutants such as *Atspo11*. Polycomplexes can also arise due to the ability of SC components to self-assemble (Zickler & Kleckner, 1999). The observations presented here with *At*MER3 localisation in the

Atspo11 mutant show consistency with these previous findings. Other recent studies that have observed polycomplexes in meiotic mutants include the research by Shinohara *et al.*, (2008) and Boden *et al.* (2008), who showed that ZIP1 forms polycomplexes in an *S. cerevisiae spo16Δ* background and that *Ta*ASY1 forms polycomplexes in the *ph1b* bread wheat pairing mutant, respectively.

The localisation of *At*MER3 in the *Atmre11* mutant has not produced excellent quality images to date as for unknown reasons the chromatin of the *Atmre11* mutant is difficult to successfully spread with the technique used. From the limited amount of data available, *At*MER3 does not appear to load normally. However, these experiments are not sufficient to reach solid conclusions.

Functional *AtRAD*51 and *AtDMC*1 are not required for temporal and spatial loading of *At*MER3. In the respective mutants, loading similar to that seen in wild-type is observed. However given that the localisation of *At*MER3 in the DSBR becomes unclear concurrently with the timing of the roles of *At*MRE11, *At*RAD51 and *At*DMC1, a possible explanation may be due to an intricate role for *At*MER3 in stabilising structures that can mature into crossover intermediates similar to *S. cerevisiae*. As *At*MER3 and *At*DMC1 do not co-localise, this suggests that possibly; 1) *At*MER3 is de-localised prior to *At*DMC1 loading. This theory is further corroborated by the difficulty associated with identifying Arabidopsis meiocytes showing *At*MER3 and *At*DMC1 signal, or 2) *At*DMC1 and *At*MER3 are on opposite sides of the DSBs. Interestingly, *At*RAD51 localises normally in the *Atmer3* mutant (Mercier *et al.*, 2005). However, despite normal localisation of the proteins in the respective experiments, it is possible that the primary antibodies are binding non-functional versions of their protein targets on the meiotic DNA. It would be interesting to know if a double mutant for *AtRAD51* and *AtDMC1* (that is, T-DNA insertions in both *AtRAD51* and

AtDMC1) would disrupt normal *At*MER3 loading onto chromatin. It is possible that *At*MER3 only requires one of the two recombinase paralogues for normal loading. However, Arabidopsis contains at least five other *RAD51* paralogues (Bleuyard *et al.*, 2005) and if two recombinases (*AtRAD51* and *AtDMC1*) were disrupted with T-DNA insertions and this did not affect *At*MER3, then the other five *RAD51* paralogues should also be targeted to be knocked out similarly to rule out their potential interactions with *At*MER3 too. An experiment of this nature would be extremely difficult and it is likely that such a mutant plant lacking all recombinases would be embryonic lethal and never reach meiosis in any case.

*At*MSH5 belongs to the ZMM epistatic group of genes and is required for normal levels of class I COs but is not necessary for completion of synapsis. MSH5 acts late in the recombination pathway in *S. cerevisiae* and interacts with MSH4 by forming a hetero-dimer. *S. cerevisiae msh5* and *msh4* mutants show very similar if not identical phenotypes. Furthermore, studies have shown that this non-redundancy of MSH4 and MSH5 and their interaction is most likely conserved in plants as illustrated by comparing the phenotypes of the *Atmsh4* and *Atmsh5* mutants (Higgins *et al.*, 2004; Higgins *et al.*, 2008). *At*MER3 localisation in the *Atmsh5* mutant appears normal. This suggests that *At*MER3 loading onto chromatin is not dependent on normal *At*MSH5 function. Therefore it will be very interesting to know if *At*MSH5 localises normally in the *Atmer3* background. If there is disrupted *At*MSH5 localisation then this would be very useful information for further dissection of the ZMM pathway, particularly as no published MER3 antibody information has been reported in any organism. If *At*MSH5 localisation was normal in the *Atmer3* background then such a result would raise even more questions about crossover

interference than those that currently exist. Irrespective, this will be a very important experiment for understanding crossover interference.

5.4.4 − *At*MER3, class I COs and the DSBR pathway

In *S. cerevisiae*, MER3 assists in stabilising structures that will potentially become crossovers. It is therefore possible that MER3 acts at the strand invasion and heteroduplex elongation stage in plants. The results presented in this chapter suggest that *At*MER3 acts in an *At*SPO11-dependent, and potentially *At*MRE11, manner. As discussed, *At*MER3 function may or may not be dependent on the recombinases, depending on if the recombinases are redundant in function where the loading of *At*MER3 is concerned. Additionally, results presented in this chapter with *At*MSH5 suggest that *At*MER3 loading is normal in the *Atmsh5* mutant. Therefore if the ZMM pathway that *At*MER3 acts in, is linear (that is, no feedback loops and it is not involved in multiple CO pathways), then the results presented here suggest that MER3 would act before *At*MSH5 (Figure 5.8). Significantly, a new member of the ZMM epistasis group was recently identified, *At*SHOC1 (Macaisne *et al.*, 2008) and it will be interesting to observe what relationship unfolds between the two genes and the other members of this group.
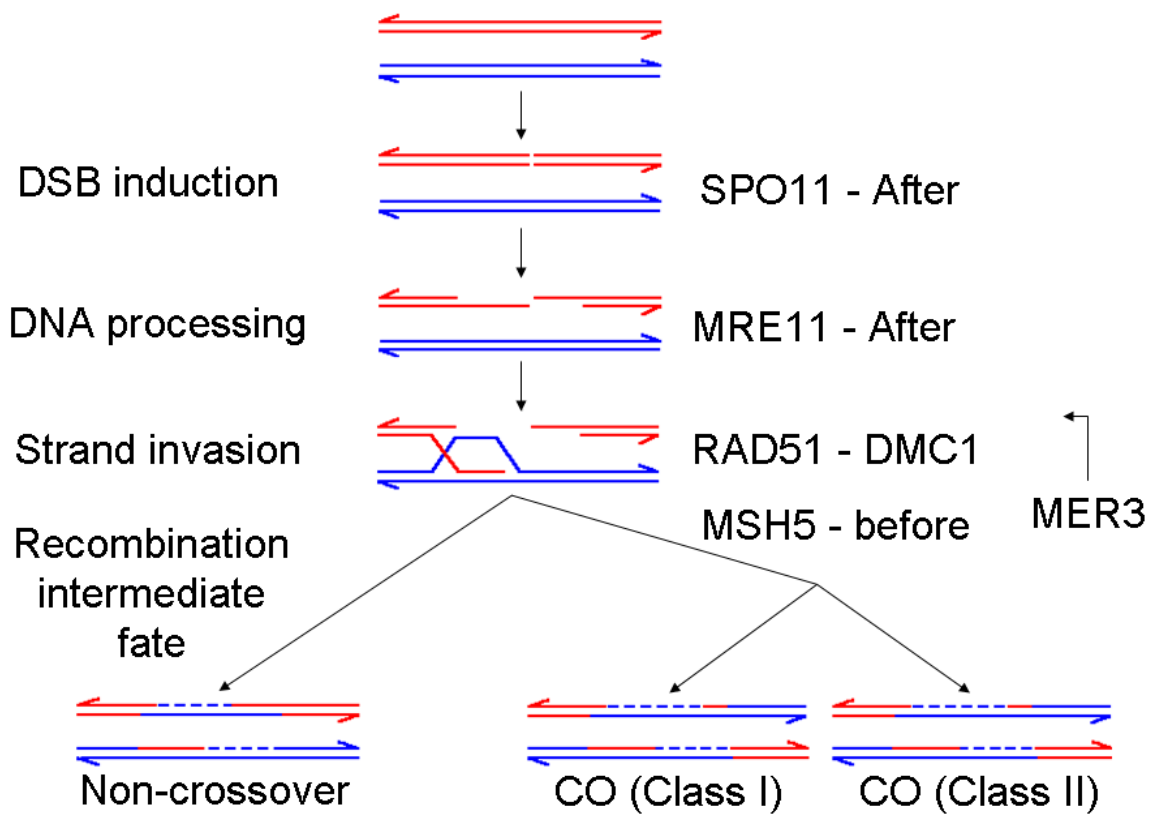
Figure 5.8 – Arabidopsis DSBR pathway with the addition of *At*MER3. *At*MER3 localises similar to wild-type in the *Atrad51*, *Atdmc1* and *Atmsh5* mutant backgrounds and is perturbed in the *Atspo11* and *Atmre11* mutant backgrounds. *At*MER3 is suggested to elicit its greatest influence at the single end invasion stage based on cytological data.

Chapter 6 – General discussion

The primary objective of this study was to identify and analyse genes involved in early meiosis in plants with a particular focus on understanding chromosome pairing in allohexaploid bread wheat. This was undertaken in multiple species using whole genome approaches and also more specific analysis of individual genes and novel transcripts with no known meiotic function.

6.1 – Transcriptomics

6.1.1 – Transcriptomics and the identification of novel meiotic genes

Available meiotic transcriptome data from rice was compared to the wheat data and identified approximately 130 similar sequences, many previously unidentified, which display meiotic regulation, suggesting possible conserved roles in meiosis. This subset of transcripts/genes forms the basis of ongoing meiotic screens with mutants for the putative homologues in other plant species. Candidate genes from the study were also mapped in bread wheat and many were found to map to chromosome group 5 which in the past has been shown to contain multiple loci involved in control of chromosome pairing (Feldman, 1966; Feldman & Mello-Sampayo, 1967; Mello-Sampayo, 1972; Riley & Chapman, 1958; Riley *et al.*, 1966; Sears & Okamoto, 1958).

Analysis of bread wheat transcript data (Chapter 3) highlighted a subset of 1,350 transcripts that were defined as being meiotically regulated. These transcripts were identified on a wheat GeneChip microarray (Affymetrix) that contained probes derived from the publicly available EST databases limited up to 2004. Consequently this chip does

not represent the entire wheat transcriptome. Rice was shown to have in excess of 7,000 transcripts that were defined as being meiotically-regulated using a chip that represents an entire (or very close to entire) transcriptome. However, this discrepancy is large and may not only be due to sequence availability. The rice dataset contains a pooled meiotic stage which means that the stages post-prophase I for which the wheat dataset had a very high resolution, was absent. Therefore the transcriptional program which occurs after prophase I, is also included in the rice dataset.

Interestingly, while bread wheat had 1,350 meiotically-regulated transcripts and rice had more than 7,000 meiotically-regulated transcripts, there appears to be approximately 130 transcripts that make up the core cereal meiotic transcriptome. However, the true figure is probably slightly more due to the incomplete sequencing of the bread wheat genome. Furthermore, proteins which have a conserved tertiary structure but diverged primary structures are also likely to exist between species and therefore increase the figure of transcripts/proteins which are in the core cereal meiotic transcriptome. Even more intriguing is that it has been reported that between *S. cerevisiae* and *S. pombe* there is a core meiotic transcriptome of slightly less than 100 genes (Mata *et al.*, 2002). Given this relatively low number it was suggested that the regulation of gene expression during meiosis may have arisen after the divergence of the two species (Mata *et al.*, 2002). However, given the similar number of meiotically-regulated transcripts between wheat and rice, perhaps the core meiome is composed of a relatively small number of genes.

6.1.2 – Transcriptomics future directions

A small number of selected transcripts from bread wheat had their putative homologue identified in Arabidopsis and mutants for the respective genes were isolated (data not

presented). PCR-based genotyping identified homozygous mutants, heterozygous plants and plants null for the mutations, for many of the lines. No genes were suspected to have a meiotic function based on tetrad analysis or metaphase I visualisation.

A larger reverse genetic screen was also set up with the putative Arabidopsis homologues of the wheat transcripts within the 1,350 meiotically regulated transcripts from chapter three. Uncharacterised genes were selected which had one clear homologue in Arabidopsis based on BLAST analysis. However despite isolating approximately 25 lines with reduced fertility and dead pollen grains, none of them where affected during meiosis (*personal communication* and major contributions from Dr Raphaël Mercier and the L'Institut National de la Recherche Agronomique, France). This suggests multiple things: 1) that it is becoming increasingly harder to find novel genes involved in meiosis with reverse genetic screens as perhaps almost all of the genes with roles in meiosis are known; 2) that the methodology of how genes are selected from transcriptomic data for screens is extremely important as chance identification of new meiotic genes is small; and 3) that new means of identifying meiotic defects must be considered/developed. Screening for short silique length can identify genes involved in fertility, however this can miss subtle meiotic phenotypes.

Undoubtedly as technology advances and the sequences of more genomes such as bread wheat become available, so will follow new possibilities and major advances. This will further enhance the existing capabilities of conducting more comprehensive comparative transcriptomics across taxonomic kingdoms. A small, additional piece of research which was not presented in the experimental chapters here, was a comparison between the core meiotic yeast transcriptome (84 transcripts) (Mata *et al.*, 2002) and the core cereal meiotic transcriptome as defined in chapter two (129 transcripts). A total of five

transcripts were identified that were common between the two data sets. A B-type cyclin involved in cell cycle progression (CLB3), a protein involved in cytokinesis (CDC5), two proteins associated with the anaphase-promoting complex (CDC27 and CDH1) and a component of autophagosomes and vesicles (ATG8). When redundancy was included (that is, an additional eight yeast genes which hit to the same rice transcripts), four more yeast B-type cyclins were identified, three proteins linked to the anaphase-promoting complex and a protein kinase involved in calcium signalling. The general theme in the functions of these eight to thirteen proteins is a role in signalling and cell cycle progression. The BLAST algorithm used for this analysis was a tBLASTx. Therefore it focuses on amino acid sequence similarities and not tertiary structures of proteins. So while it appears the conserved proteins are signalling proteins, future studies may reveal the conservation of the mechanical themes in meiosis. This is supported when considering that *Ta*ASY1 displays poor sequence similarity to HOP1 from *S. cerevisiae* despite being a functional homologue, and that *At*ZYP1 (which is a structural component of the synaptonemal complex) has functional similarity to ZIP1 from *S. cerevisiae* despite no significant sequence similarity (Boden *et al.*, 2008; Boden *et al.*, 2007; Higgins *et al.*, 2005).

In years to come it may be possible in bread wheat to explore the technique of DNA microarrays (as opposed to expression arrays). Recently an extremely powerful study in *S. cerevisiae* shed light on many aspects of early meiosis using this approach (Chen *et al.*, 2008). The research focused on recombination throughout the *S. cerevisiae* genome and confirmed various sets of genetic data relating to various facets of meiosis. Some of the aspects investigated included the measurement of repression of COs near telomeres and centromeres, and the link between CO interference and CO homeostasis (the phenomenon where a decrease in DSBs does not reduce the number of COs). Research such as this will

undoubtedly form an integral component of future meiotic experimentation (not just in bread wheat).

6.2 – MER3

6.2.1 – A mechanism controlling the decision to form class I crossovers

There has been a great deal of work investigating the formation of class I COs in various organisms ranging from *S. cerevisiae* to Arabidopsis. Despite these efforts, little is known about the decision making process involved in the formation of class I COs. *At*MER3 is essential for the formation of class I COs in Arabidopsis (Mercier *et al.*, 2005). Therefore an *At*MER3 antibody was produced (Vignard, 2007) and used in immuno-localisation experiments in an effort to determine its spatial and temporal localisation and where precisely in the DSBR pathway the protein exerts its influence.

*At*MER3 foci were observed at a frequency far higher than the number of COs per meiosis. Therefore this may suggest that *At*MER3 is involved in the pathway which converts unstable interactions between homologous chromatids into intermediates that can potentially form class I COs. However, the high foci count suggests that *At*MER3 is not directly involved in the 'decision' to form a class I CO, which agrees with yeast *zmm* mutant data (reviewed in Bishop & Zickler, 2004).

It was found that SPO11 is required for normal MER3 loading. While MRE11 also appears to be required, the clarity of the results in the *Atmre11* background were not as vivid as those that were obtained in other genotypes and replication of *At*MER3 loading in the *Atmre11* mutant background is needed. *AtRAD51*, *AtDMC1* and *AtMSH5* are not required for normal loading of MER3. This suggests that MER3 is upstream of these

proteins in the DSBR pathway or perhaps not dependent on one of these proteins for normal loading and possibly function.

A major gap in the knowledge about class I COs is precisely what "measures" distance along chromosomes, which governs the physical distance over which interference acts. A substrate sequestration model has been suggested (Snowden *et al.*, 2004), however given that the number of *At*MSH4 and *At*MSH5 foci far exceed the number of crossovers (Higgins *et al.*, 2004; Higgins *et al.*, 2008), such a stoichiometric phenomenon is unlikely. Proposals based on scarce information discuss the possibility that CO interference could be mediated by a polymerising signal, however it is not clear how a signal could measure distance. A mechanical model for CO interference can explain how these distance-dependent events occur, where redistribution of mechanical stress can be the medium for a "mechanism" which suppresses COs occurring directly adjacent to another CO (Borner *et al.*, 2004). It is also speculated that the redistribution of mechanical stress which causes buckling of the homologues could promote nucleation of the SC (Borner *et al.*, 2004), thereby creating a physical/mechanical link between the SC and the ZMM proteins in some species.

6.2.2 – Unanswered questions and future directions for MER3 research in Arabidopsis

There are a number of experimental approaches that could yield valuable data for understanding the ZMM epistasis group and its role in CO interference. The application and benefits gained from cytology in meiotic research are significant. Building upon the existing suite of tools can only help our understanding of CO interference move forward. One of the most useful experiments in the short term would be to localise all of the ZMM

proteins in the collection of *zmm* mutant backgrounds using the available ZMM antibodies. The matrix of data that would be generated could then be built on as the collection of antibodies (and potentially mutants) increase and therefore guide future experimentation and models of CO interference.

An additional cytological-based approach would be to count the number of intense *At*MER3 foci on synapsed regions in wild-type Arabidopsis. This number could be compared to the foci numbers of other meiotic proteins that appear to localise in a similar temporal manner to *At*MER3. This information could offer clues as to whether *At*MER3 is up- or down-stream of the proteins of interest. However, this experimental approach assumes that the two (or more) proteins are part of the same linear meiotic DSB repair pathway. Some of the candidates to be counted and compared to *At*MER3 include *At*DMC1 and the other ZMM proteins, *At*MSH4 and *At*MSH5 for which co-localisation would also be valuable. Interestingly, different intensities of *At*MER3 signal were consistently observed in wild-type and do not appear to be artifacts or background. Neither of these signals appeared in the *Atmer3* mutants at the equivalent stages of meiosis suggesting that there are at least two true 'types' of *At*MER3 signal. The strongest foci which occur on the freshly synapsed regions form the most practical foci to count until additional information is gained to determine what the lower intensity signals represent. The weaker *At*MER3 signal which appears to exist in the nucleoplasm (based on ASY1 and DAPI signal) in high numbers may in fact be localising to DNA which is neither compact nor juxtaposed to axial elements. This may suggest that MER3 has a role which links chromatin conformation, SC formation and interfering crossovers.

Recent tools developed with markers encoding different "coloured" fluorescent proteins distributed throughout the genome utilising the *qrt* mutant in Arabidopsis (Francis

et al., 2007) will make CO interference studies more rapid and also provide the opportunity for greater statistical significance. By analysing the fluorescent tetrads which "stick together" in the *Atqrt* mutant, the products of thousands of meioses can be analysed using microscopy, and statistical models about CO interference can be built with the resulting data for given loci. This tool will prove useful for additional studies given that while *AtMER3* and *AtMSH4*/*AtMSH5* are all required for CO interference, the number of residual chiasmata in the respective mutant backgrounds are slightly different (Higgins *et al.*, 2004; Higgins *et al.*, 2008; Mercier *et al.*, 2005).

As plant meiocyte accessibility is relatively easy, and as meiotic chromosomes in plants are often easy to visualise due to their size, cytology is often favoured over other techniques given that it is a vivid means of observing cellular events. However, biochemical assays such as yeast 2-hybrids or pull-downs are certainly required to complement cytological and genetic data. Furthermore, these assays are likely to provide information that may have never been identified through other means. One final consideration is that if the mechanical model of CO interference is correct, then this phenomenon will still need to be better understood, in addition to the genes/proteins that are known to be required for this process.

6.3   – *TaMSH7*

6.3.1 – The role of *Ta*MSH7 in chromosome pairing

TaMSH7 is a candidate meiotic gene previously suggested (Dong *et al.*, 2002; Lloyd *et al.*, 2007) to underlie the phenotype noticed in the absence of *Ph2* (Prieto *et al.*, 2005; Sears, 1982; Wall *et al.*, 1971a). When considering that loss of function of MMR genes has

increased homoeologous recombination in other species (Emmanuel *et al.*, 2006; Li *et al.*, 2006; Trouiller *et al.*, 2006) and that *TaMSH7* maps to the *Ph2* locus, it is fair to conclude that of all the other identified candidates within this locus, *TaMSH7* is a strong candidate.

RNAi-induced *Tamsh7* mutants were created and analysed to determine if reduced *TaMSH7* levels would have a meiotic effect. Three lines were analysed in the T_2 generation and variable levels of fertility and *TaMSH7* expression were observed. Reduction of *TaMSH7* transcript levels can be linked to abnormal chromosome associations at metaphase I in some of the mutants but not all. The abnormal chromosome interactions are an interesting observation given that some of the older wheat deletion mutants are relatively normal at metaphase I when self-pollinating (*ph2a* for example, data not shown). The true effect of the mutations will not be seen until metaphase I is analysed in inter-specific hybrids that are created using these mutants. However, the abnormal metaphase I spreads seen in chapter four suggests that the phenotype produced in an inter-specific hybrid carrying the *TaMSH7*-RNAi transgene could potentially lead to more extreme phenotypes than those previously observed with hybrids lacking *Ph2*.

The abnormal chromosome structures seen at metaphase in line *Tamsh7-1* may have also been reflected with immuno-localisation of *Ta*ASY1 staining the lateral elements in a local, brighter and more persistent manner than what was observed in wild-type. These structures appear to be precursors to multivalents (that were seen at metaphase I) which *Ta*MSH7 is normally involved in resolving. It is reasonable to assume that the abnormal structures seen in *Tamsh7-1* are homoeologous chromosome interactions, given the hierarchy of chromosome interactions that exist in bread wheat and other plants (Nicolas *et al.*, 2008; Prieto *et al.*, 2005). However this needs to be confirmed experimentally *via* a

technique such as fluorescent *in situ* hybridisation or genetic/karyoptypic analysis which can identify the nature of chromosome rearrangements.

TaMSH7 expression analysis was conducted in the *ph2a* mutant background. Surprisingly this revealed that *TaMSH7* is not expressed in anthers analysed from pre-meiosis to immature pollen in the *ph2a* mutant. This is interesting because it conflicts with data generated previously which interrogated *TaMSH7* expression using northern blot analysis that showed *TaMSH7* expression levels were reduced but still present in the *ph2a* mutant (Dong *et al.*, 2002). Expression of *Ta*ASY1 was found to be dramatically higher in *ph2a* when compared to wild-type. This was an unexpected finding and is similar to the finding reported by Boden *et al.*, (2008) when examining *Ta*ASY1 in the *ph1b* background. While there is a link when comparing the expression of *TaASY1* in these two wheat mutants, normal chromatin conformation was observed in the *ph2a* background. Interestingly, while both *ph1b* and *ph2a* display abnormal ASY1 regulation, very few meiotic mutants in Arabidopsis have reported disrupted ASY1 behaviour (Chelysheva *et al.*, 2005; Mercier *et al.*, 2003). As additional meiotic mutants are developed for wheat, it will be important to determine if genes such as *TaASY1* are adversely affected. If so, this would suggest that there is a major difference in the pairing pathway of polyploid wheat when compared to diploid Arabidopsis.

6.3.2 – MSH7 future directions

A future direction with *TaMSH7* should centre on investigating the levels of synapsis in the *Tamsh7* mutants, especially given the research reported in the *ph2b* wheat mutant and other species that have examined MMR genes (Baker *et al.*, 1995; Baker *et al.*, 1996; Martinez *et al.*, 2001). This would require a ZYP1 antibody to be studied in wild-type wheat as well as

the *Tamsh7* and *ph2* mutants. While electron microscopy could be used for studying SC formation, immuno-fluorescence microscopy can provide temporal information about multiple proteins that play a role in the unique events of prophase I.

While not reported in the experimental chapters of this thesis, *Ta*ZYP1 localisation was attempted in wild-type bread wheat and the *Tamsh7* mutants using different antibodies and techniques kindly contributed by Dr Glyn Jenkins (Aberystwyth University, Wales) and Professor Chris Franklin (University of Birmingham, England). However, all attempts were generally unsuccessful despite the success with anti-*At*ASY1 in fluorescence-based immuno-localisations conducted. This suggests that amino acid sequence similarity or structural similarity is not at a level high enough to promote binding to the *TaZYP1* epitopes. This is despite the fact that the region of amino acids the *At*ZYP1 antibody was raised against shows a strong similarity between wheat and Arabidopsis. An antibody raised against *Ta*MSH7 is currently being completed to complement the *ph2a* expression analysis conducted with the *TaMSH7* transcript. This will provide additional data about the mode of action of *Ta*MSH7 when analysed spatially and temporally in wild-type bread wheat, and various mutants that are now available.

An additional approach in furthering our understanding of *TaMSH7* could focus on map-based cloning, in order to reduce the size of the *Ph2* locus (which is estimated to be as large as 80 Mbp) (Sutton *et al.*, 2003). Such experimentation would take approximately two years, where the EMS-induced *ph2* mutant (*ph2b*) could be crossed with wild-type bread wheat of a different cultivar. Recombination events could then be mapped and scored for presence or absence of the *ph2* phenotype in a subsequent inter-specific cross.

6.3.3 – A model for chromosome pairing in bread wheat

Ph1 promotes a form of specialised feedback loop where more or less simultaneous differentiation occurs at favourable sites between homologous chromosomes (Colas *et al.*, 2008). However, "rogue" recombination events can be provoked during meiosis, possibly due to DSBs forming and DSBR machinery assembling at other fortuitously-accessible regions (Kleckner, 1996). *Ph2* has been shown to be a suppressor of such rogue chromosome associations at meiosis in bread wheat. Data presented here does not directly conflict with that theory however it does suggest an unexpected form of regulation of other components of meiotic machinery which would presumably lie upstream of this correction mechanism. This may be in the form of a suppression mechanism of the earlier meiotic machinery upon completion of the *Ph2* function: that is, the correction of mis-paired chromosomes in mid-late prophase I (Figure 6.1). There have also been reports which highlight links/similarities between *Ph2* and the 'missing' pachytene checkpoint in plants (Martinez-Perez & Moore, 2008; Martinez *et al.*, 2001). Recent work linking meiotic chromosome axis morphology, sister chromatid cohesion and recombination, and interference in various species also provides additional information which can help link the processes in bread wheat meiosis (Martinez-Perez *et al.*, 2008; Nabeshima *et al.*, 2004; Storlazzi *et al.*, 2008). The suggested model presented in this thesis incorporates the observation of increased *TaASY1* transcript in the *ph2a* background.

6.4 – The bigger picture

Additional gene discovery will most likely continue to fuel new findings in meiosis research for at least another decade or more. This will build on current knowledge and the mechanisms which control such events as recombination frequency and positioning.

Understanding the mechanical aspects of early meiosis will comprise equal importance as candidate gene approaches in the future. Specifically from a bread wheat viewpoint, there is great academic interest in understanding how the *ph* mutants work. Through furthering that knowledge, the cereal meiosis community will then understand more comprehensively how *Tamsh7* and *Taasy1* mutants differ from wild-type. Importantly, it will then also be known if they can induce subtle amounts of homeologous recombination with a higher level of genomic stability than is currently offered with the *ph1b* mutant. The altruistic goals of the 'Able laboratory' are to increase introgression of alien chromatin in cereal breeding programmes in a controlled manner. If this can be achieved in bread wheat, then the rapid development of agronomically superior cereal varieties will go some way in being able to meet increasing global food demands.
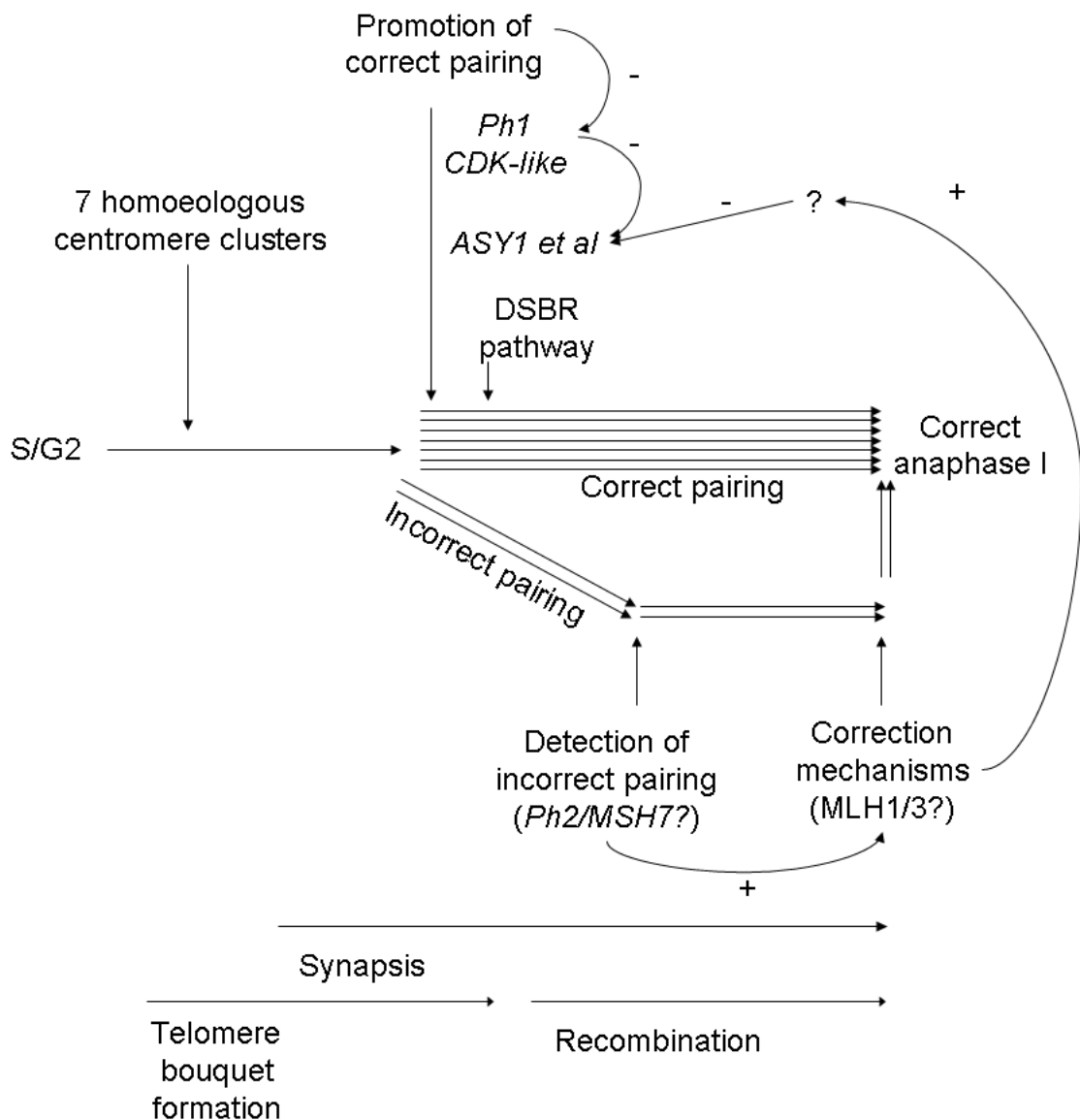
Figure 6.1 – A model for meiotic chromosome pairing in bread wheat based on literature and new information derived in this research. The major effect on correct chromosome associations is exerted by *Ph1* (Martinez-Perez et al., 2001) and its downstream targets (e.g. suppression of excessive ASY1 levels (Boden *et al.*, 2008)). Not all homologues are paired correctly and mechanisms are required to resolve these erroneous associations (Colas *et al.*, 2008) (e.g. *Ph2*) in addition to an appropriate amount of time, provided by *Ph1* (Bennett *et al.*, 1974; Dover & Riley, 1972; Gillies, 1987). This recruits a repair mechanism and it is upon repair and/or failure to detect any more mis-paired chromosomes that the remodelling machinery no longer acts to align homologous chromsomes and the transition into diplotene commences.

References

Abranches R, Beven AF, Aragon-Alcaide L, Shaw PJ (1998) Transcription sites are not correlated with chromosome territories in wheat nuclei. *J Cell Biol* **143:** 5-12

Ade J, Belzile F, Philippe H, Doutriaux MP (1999) Four mismatch repair paralogues coexist in *Arabidopsis thaliana*: *AtMSH2*, *AtMSH3*, *AtMSH6-1* and *AtMSH6-2*. *Mol Gen Genet* **262:** 239-249

Al-Kaff N, Knight E, Bertin I, Foote T, Hart N, Griffiths S, Moore G (2007) Detailed dissection of the chromosomal region containing the *Ph1* locus in wheat *Triticum aestivum*: With deletion mutants and expression profiling. *Annals Of Botany* **101:** 863-872

Albini SM (1994) A karyotype of the *Arabidopsis thaliana* genome derived from synaptonemal complex analysis at prophase I of meiosis. *Plant J* **5:** 665-672

Allers T, Lichten M (2001) Intermediates of yeast meiotic recombination contain heteroduplex DNA. *Mol Cell* **8:** 225-231

Alonso JM, Stepanova AN, Leisse TJ, Kim CJ, Chen HM, Shinn P, Stevenson DK, Zimmerman J, Barajas P, Cheuk R *et al.* (2003) Genome-wide insertional mutagenesis of *Arabidopsis thaliana*. *Science* **301:** 653-657

Andrews J, Bouffard GG, Cheadle C, Lu JN, Becker KG, Oliver B (2000) Gene discovery using computational and microarray analysis of transcription in the *Drosophila melanogaster* testis. *Genome Res* **10:** 2030-2043

Arabidopsis Genome Initiative (2000) Analysis of the genome sequence of the flowering plant *Arabidopsis thaliana*. *Nature* **408:** 796-815

Armstrong SJ, Caryl AP, Jones GH, Franklin FCH (2002) Asy1, a protein required for meiotic chromosome synapsis, localizes to axis-associated chromatin in Arabidopsis and Brassica. *J Cell Sci* **115:** 3645-3655

Armstrong SJ, Franklin FCH, Jones GH (2001) Nucleolus-associated telomere clustering and pairing precede meiotic chromosome synapsis in *Arabidopsis thaliana*. *J Cell Sci* **114:** 4207-4217

Attia T, Robbelen G (1986) Meiotic pairing in haploids and amphidiploids of spontaneous versus synthetic origin in rape, *Brassica napus* L. *Can J Genet Cytol* **28:** 330-334

Baker SM, Bronner CE, Zhang L, Plug AW, Robatzek M, Warren G, Elliott EA, Yu JA, Ashley T, Arnheim N *et al.* (1995) Male-mice defective in the DNA mismatch repair gene *PMS2* exhibit abnormal chromosome synapsis in meiosis. *Cell* **82:** 309-319

Baker SM, Plug AW, Prolla TA, Bronner CE, Harris AC, Yao X, Christie DM, Monell C, Arnheim N, Bradley A *et al.* (1996) Involvement of mouse MLH1 in DNA mismatch repair and meiotic crossing over. *Nat Genet* **13:** 336-342

Ban C, Yang W (1998) Crystal structure and ATPase activity of MutL: Implications for DNA repair and mutagenesis. *Cell* **95:** 541-552

Bartel DP (2004) MicroRNAs: Genomics, biogenesis, mechanism, and function. *Cell* **116:** 281-297

Bennett MD, Dover GA, Riley R (1974) Meiotic duration in wheat genotypes with and without homoeologous meiotic chromosome pairing. *Proc R Soc Biol Sci Ser B* **187:** 191-207

Berchowitz LE, Francis KE, Bey AL, Copenhaver GP (2007) The role of *At*MUS81 in interference-insensitive crossovers in *A. thaliana*. *Plos Genetics* **3:** 1355-1364

Bishop DK, Nikolski Y, Oshiro J, Chon J, Shinohara M, Chen X (1999) High copy number suppression of the meiotic arrest caused by a *dmc1* mutation: REC114 imposes an early recombination block and RAD54 promotes a DMC1-independent DSB repair pathway. *Genes Cells* **4:** 425-443

Bishop DK, Zickler D (2004) Early decision: Meiotic crossover interference prior to stable strand exchange and synapsis. *Cell* **117:** 9-15

Bleuyard JY, Gallego ME, Savigny F, White CI (2005) Differing requirements for the Arabidopsis Rad51 paralogs in meiosis and DNA repair. *Plant J* **41:** 533-545

Bleuyard JY, Gallego ME, White CI (2004) Meiotic defects in the *Arabidopsis* rad50 mutant point to conservation of the MRX complex function in early stages of meiotic recombination. *Chromosoma* **113:** 197-203

Boden SA, Langridge P, Spangenberg G, Able JA (2008) *Ta*ASY1 promotes homologous chromosome interactions and is affected by deletion of *Ph1*. *Plant J* **57:** 487-497

Boden SA, Shadiac N, Tucker EJ, Langridge P, Able JA (2007) Expression and functional analysis of *Ta*ASY1 during meiosis of bread wheat (*Triticum aestivum*). *BMC Mol Biol* **8**

Borner GV, Kleckner N, Hunter N (2004) Crossover/noncrossover differentiation, synaptonemal complex formation, and regulatory surveillance at the leptotene/zygotene transition of meiosis. *Cell* **117:** 29-45

Boyes DC, Zayed AM, Ascenzi R, McCaskill AJ, Hoffman NE, Davis KR, Gorlach J (2001) Growth stage-based phenotypic analysis of Arabidopsis: A model for high throughput functional genomics in plants. *Plant Cell* **13:** 1499-1510

Brown MS (1954) A comparison of pachytene and metaphase pairing in species hybrids of *Gossypium*. *Genetics* **39:** 962-963

Canales RD, Luo YL, Willey JC, Austermiller B, Barbacioru CC, Boysen C, Hunkapiller K, Jensen RV, Knight CR, Lee KY *et al.* (2006) Evaluation of DNA microarray results with quantitative gene expression platforms. *Nat Biotechnol* **24:** 1115-1122

Caryl AP, Armstrong SJ, Jones GH, Franklin FCH (2000) A homologue of the yeast *HOP1* gene is inactivated in the Arabidopsis meiotic mutant *asy1*. *Chromosoma* **109:** 62-71

Ceoloni C, Donini P (1993) Combining mutations for the 2 homoeologous pairing suppressor genes *Ph1* and *Ph2* in common wheat and in hybrids with alien *Triticeae*. *Genome* **36:** 377-386

Chelysheva L, Diallo S, Vezon D, Gendrot G, Vrielynck N, Belcram K, Rocques N, Marquez-Lema A, Bhatt AM, Horlow C *et al.* (2005) *At*REC8 and *At*SCC3 are essential to the monopolar orientation of the kinetochores during meiosis. *J Cell Sci* **118:** 4621-4632

Chelysheva L, Gendrot G, Vezon D, Doutriaux MP, Mercier R, Grelon M (2007) Zip4/Spo22 is required for class I CO formation but not for synapsis completion in *Arabidopsis thaliana*. *Plos Genetics* **3:** 802-813

Chen SY, Tsubouchi T, Rockmill B, Sandler JS, Richards DR, Vader G, Hochwagen A, Roeder GS, Fung JC (2008) Global analysis of the meiotic crossover landscape. *Dev Cell* **15:** 401-415

Chu S, DeRisi J, Eisen M, Mulholland J, Botstein D, Brown PO, Herskowitz I (1998) The transcriptional program of sporulation in budding yeast. *Science* **282:** 699-705

Chuaqui RF, Bonner RF, Best CJM, Gillespie JW, Flaig MJ, Hewitt SM, Phillips JL, Krizman DB, Tangrea MA, Ahram M *et al.* (2002) Post-analysis follow-up and validation of microarray experiments. *Nat Genet* **32:** 509-514

Colas I, Shaw P, Prieto P, Wanous M, Spielmeyer W, Mago R, Moore G (2008) Effective chromosome pairing requires chromatin remodeling at the onset of meiosis. *Proc Natl Acad Sci U S A* **105:** 6075-6080

Copenhaver GP, Housworth EA, Stahl FW (2002) Crossover interference in Arabidopsis. *Genetics* **160:** 1631-1639

Couteau F, Belzile F, Horlow C, Grandjean O, Vezon D, Doutriaux MP (1999) Random chromosome segregation without meiotic arrest in both male and female meiocytes of a dmc1 mutant of Arabidopsis. *Plant Cell* **11:** 1623-1634

Crismani W, Baumann U, Sutton T, Shirley N, Webster T, Spangenberg G, Langridge P, Able JA (2006) Microarray expression analysis of meiosis and microsporogenesis in hexaploid bread wheat. *BMC Genomics* **7**

Culligan KM, Hays JB (2000) Arabidopsis MutS homologs-*At*MSH2, *At*MSH3, *At*MSH6, and a novel *At*MSH7-form three distinct protein heterodimers with different specificities for mismatched DNA. *Plant Cell* **12:** 991-1002

Culligan KM, Meyer-Gauen G, Lyons-Weiler J, Hays JB (2000) Evolutionary origin, diversification and specialization of eukaryotic MutS homolog mismatch repair proteins. *Nucleic Acids Res* **28:** 463-471

Czechowski T, Stitt M, Altmann T, Udvardi MK, Scheible WR (2005) Genome-wide identification and testing of superior reference genes for transcript normalization in Arabidopsis. *Plant Physiology* **139:** 5-17

Dallas PB, Gottardo NG, Firth MJ, Beesley AH, Hoffmann K, Terry PA, Freitas JR, Boag JM, Cummings AJ, Kees UR (2005) Gene expression levels assessed by oligonucleotide microarray analysis and quantitative real-time RT-PCR - how well do they correlate? *Bmc Genomics* **6**

de la Fuente A, Brazhnik P, Mendes P (2002) Linking the genes: inferring quantitative gene networks from microarray data. *Trends In Genetics* **18:** 395-398

De Muyt A, Vezon D, Gendrot G, Gallois JL, Stevens R, Grelon M (2007) *At*PRD1 is required for meiotic double strand break formation in *Arabidopsis thaliana*. *Embo Journal* **26:** 4126-4137

Dong CM, Thomas S, Becker D, Lorz H, Whitford R, Sutton T, Able JA, Langridge P (2005) WM5: Isolation and characterisation of a gene expressed during early meiosis and shoot meristem development in wheat. *Funct Plant Biol* **32:** 249-258

Dong CM, Whitford R, Langridge P (2002) A DNA mismatch repair gene links to the *Ph2* locus in wheat. *Genome* **45:** 116-124

Dover GA, Riley R (1972) Prevention of pairing of homoeologous meiotic chromosomes of wheat by an activity of supernumeracy chromosomes of *Aegilops*. *Nature* **240:** 159-161

Driscoll C (1972) Genetic suppression of homologous chromosome pairing in hexaploid wheat. *Can J Genet Cytol* **14:** 39-42

Driscoll CJ (1973) Minor genes affecting homoeologous pairing in hybrids between wheat and related genera. *Genetics* **74:** 566

Drouaud J, Camilleri C, Bourguignon PY, Canaguier A, Berard A, Vezon D, Giancola S, Brunel D, Colot V, Prum B *et al.* (2006) Variation in crossing-over rates across chromosome 4 of *Arabidopsis thaliana* reveals the presence of meiotic recombination "hot spots". *Genome Res* **16:** 106-114

Dvorak J (1976) The relationship between the genome of *Triticum urartu* and the A and B genomes of *T. aestivum*. *Can J Genet Cytol* **18:** 371–377

Dvorak J (1988) Genome analysis in the *Triticum-aegilops* alliance. *9th International Wheat Genetics Symposium***:** 8-11

Egel-mitani M, Olson LW, Egel R (1982) Meiosis in *Aspergillus nidulans* - another example for lacking synaptonemal complexes in the absence of crossover interference. *Hereditas* **97:** 179-187

Eisen MB, Spellman PT, Brown PO, Botstein D (1998) Cluster analysis and display of genome-wide expression patterns. *Proc Natl Acad Sci U S A* **95:** 14863-14868

Emmanuel E, Yehuda E, Melamed-Bessudo C, Avivi-Ragolsky N, Levy AA (2006) The role of *AtMSH2* in homologous recombination in *Arabidopsis thaliana*. *EMBO Rep* **7:** 100-105

Etienne W, Meyer MH, Peppers J, Meyer RA (2004) Comparison of mRNA gene expression by RT-PCR and DNA microarray. *BioTechniques* **36:** 618-620, 622, 624-626

Feldman M (1966) The effect of chromosome 5A, 5B and 5D on chromosome pairing in *Triticum aestivum*. . *Proc Natl Acad Sci U S A* **55:** 1447-1453

Feldman M (1968) Regulation of somatic association and meiotic pairing in common wheat. *Proc 3rd Int Wheat Genet Symp*: 169-178

Feldman M, Levy AA (2005) Allopolyploidy - a shaping force in the evolution of wheat genomes. *Cytogenet Genome Res* **109:** 250-258

Feldman M, Mello-Sampayo T (1967) Suppression of homoeologous pairing in hybrids of polyploid wheats x *Triticum speltoides*. *Can J Genet Cytol* **9:** 307-313

Francis D (2007) The plant cell cycle - 15 years on. *New Phytol* **174:** 261-278

Francis KE, Lam SY, Harrison BD, Bey AL, Berchowitz LE, Copenhaver GP (2007) Pollen tetrad-based visual assay for meiotic recombination in Arabidopsis. *Proc Natl Acad Sci U S A* **104:** 3913–3918

Franklin AE, McElver J, Sunjevaric I, Rothstein R, Bowen B, Cande WZ (1999) Three-dimensional microscopy of the Rad51 recombination protein during meiotic prophase. *Plant Cell* **11:** 809-824

Gale MD, Devos KM (1998) Comparative genetics in the grasses. *Proc Natl Acad Sci U S A* **95:** 1971-1974

Gauthier FM, McGinnis RC (1968) The meiotic behaviour of a nullihaploid plant in *Avena sativa* L. *Can J Genet Cytol* **10:** 186–189

Gillies CB (1985) An electron-microscopic study of synaptonemal complex formation at zygotene in rye. *Chromosoma* **92:** 165-175

Gillies CB (1987) The effect of the *Ph1* gene allele on synaptonemal complex formation in *Triticum aestivum* x *T. kotschyi* hybrids. *Theor Appl Genet* **74:** 430-438

Giorgi B (1978) A homoeologous pairing mutant isolated in *Triticum durum* cv. Cappelli. *Mutant Breed Newslett* **11:** 4-5

Goff SA, Ricke D, Lan TH, Presting G, Wang RL, Dunn M, Glazebrook J, Sessions A, Oeller P, Varma H *et al.* (2002) A draft sequence of the rice genome (*Oryza sativa* L. ssp japonica). *Science* **296:** 92-100

Grasser K, Krohn NM, Lichota J, Stemmer C (2000) Chromatin-associated HMG1, HMGI/Y and SSRP1 proteins of higher plants. *Physiol Plant* **110:** 427-435

Grelon M, Vezon D, Gendrot G, Pelletier G (2001) *At*SPO11-1 is necessary for efficient meiotic recombination in plants. *Embo Journal* **20:** 589-600

Griffiths S, Sharp R, Foote TN, Bertin I, Wanous M, Reader S, Colas I, Moore G (2006) Molecular characterization of *Ph1* as a major chromosome pairing locus in polyploid wheat. *Nature* **439:** 749-752

Hannon GJ (2002) RNA interference. *Nature* **418:** 244-251

Hasenkampf CA (1984) Synaptonemal complex formation in pollen mother cells of *Tradescantia*. *Chromosoma* **90:** 275-284

Henderson KA, Keeney S (2004) Tying synaptonemal complex initiation to the formation and programmed repair of DNA double-strand breaks. *Proc Natl Acad Sci U S A* **101:** 4519-4524

Higgins JD, Armstrong SJ, Franklin FCH, Jones GH (2004) The Arabidopsis MutS homolog *At*MSH4 functions at an early step in recombination: evidence for two classes of recombination in Arabidopsis. *Genes Dev* **18:** 2557-2570

Higgins JD, Sanchez-Moran E, Armstrong SJ, Jones GH, Franklin FCH (2005) The Arabidopsis synaptonemal complex protein ZYP1 is required for chromosome synapsis and normal fidelity of crossing over. *Genes Dev* **19:** 2488-2500

Higgins JD, Vignard J, Mercier R, Pugh AG, Franklin FCH, Jones GH (2008) *At*MSH5 partners *At*MSH4 in the class I meiotic crossover pathway in *Arabidopsis thaliana*, but is not required for synapsis. *Plant J* **55:** 28-39

Hollingsworth NM, Brill SJ (2004) The Mus81 solution to resolution: generating meiotic crossovers without Holliday junctions. *Genes Dev* **18:** 117-125

Holm PB (1986) Chromosome pairing and chiasma formation in allohexaploid wheat, *Triticum aestivum* analyzed by spreading of meiotic nuclei. *Carlsberg Research Communications* **51:** 239-294

Holm PB (1988) Chromosome pairing and synaptonemal complex formation in hexaploid wheat, nullisomic for chromosome 5B. *Carlsberg Research Communications* **53:** 91-110

Holmes RJ, Cohen PE (2007) Small RNAs and RNAi pathways in meiotic prophase I. *Chromosome Res* **15:** 653-665

Huang S, Spielmeyer W, Lagudah ES, Munns R (2008) Comparative mapping of HKT genes in wheat, barley, and rice, key determinants of Na^+ transport, and salt tolerance. *J Exp Bot* **59:** 927-937

Jackson N, Sanchez-Moran E, Buckling E, Armstrong SJ, Jones GH, Franklin FCH (2006) Reduced meiotic crossovers and delayed prophase I progression in *At*MLH3-deficient Arabidopsis. *Embo Journal* **25:** 1315-1323

Jantsch V, Pasierbek P, Mueller MM, Schweizer D, Jantsch M, Loidl J (2004) Targeted gene knockout reveals a role in meiotic recombination for ZHP-3, a zip3-related protein in Caenorhabditis elegans. *Mol Cell Biol* **24:** 7998-8006

Jardim SN (2007) Comparative genomics of grasses tolerant to aluminum. *Genet Mol Res* **6:** 1178-1189

Jenczewski E, Eber F, Grimaud A, Huet S, Lucas MO, Monod H, Chevre AM (2003) *PrBn*, a major gene controlling homeologous pairing in oilseed rape (*Brassica napus*) haploids. *Genetics* **164:** 645-653

Ji YF, Zhao XP, Paterson AH, Price HJ, Stelly DM (2007) Integrative mapping of *Gossypium hirsutum* L. by meiotic fluorescent *in situ* hybridization of a tandemly repetitive sequence (B77). *Genetics* **176:** 115-123

Joseph I, Lustig AJ (2007) Telomeres in meiotic recombination: The Yeast Side Story. *Cell Mol Life Sci* **64:** 125-130

Kawaura K, Mochida K, Ogihara Y (2008) Genome-wide analysis for identification of salt-responsive genes in common wheat. *Funct Integr Genomics* **8:** 277-286

Keeney S (2001) Mechanism and control of meiotic recombination initiation. In *Current Topics in Developmental Biology* **52:** 1-53

Kim SK, Lund J, Kiraly M, Duke K, Jiang M, Stuart JM, Eizinger A, Wylie BN, Davidson GS (2001) A gene expression map for *Caenorhabditis elegans*. *Science* **293:** 2087-2092

Kleckner N (1996) Meiosis: How could it work? *Proc Natl Acad Sci U S A* **93:** 8167-8174

Kononen J, Bubendorf L, Kallioniemi A, Barlund M, Schraml P, Leighton S, Torhorst J, Mihatsch MJ, Sauter G, Kallioniemi OP (1998) Tissue microarrays for high-throughput molecular profiling of tumor specimens. *Nature Medicine* **4:** 844-847

Lamers MH, Perrakis A, Enzlin JH, Winterwerp HHK, de Wind N, Sixma TK (2000) The crystal structure of DNA mismatch repair protein MutS binding to a G/T mismatch. *Nature* **407:** 711-717

Lander ES, Linton LM, Birren B, Nusbaum C, Zody MC, Baldwin J, Devon K, Dewar K, Doyle M, FitzHugh W *et al.* (2001) Initial sequencing and analysis of the human genome. *Nature* **409:** 860-921

Large E (1954) Growth stages in cereals: Illustration of the Feeke's scale. *Pl Path* **3:** 128–129

Leflon M, Eber F, Letanneur JC, Chelysheva L, Coriton O, Huteau V, Ryder CD, Barker G, Jenczewski E, Chevre AM (2006) Pairing and recombination at meiosis of *Brassica rapa* (AA) x *Brassica napus* (AACC) hybrids. *Theor Appl Genet* **113:** 1467-1480

Levy J (1994) Sequencing The Yeast Genome - An International Achievement. *Yeast* **10:** 1689-1706

Li LL, Jean M, Belzile F (2006) The impact of sequence divergence and DNA mismatch repair on homeologous recombination in Arabidopsis. *Plant J* **45:** 908-916

Li WX, Chen CB, Markmann-Mulisch U, Timofejeva L, Schmelzer E, Ma H, Reiss B (2004) The Arabidopsis *AtRAD51* gene is dispensable for vegetative development but required for meiosis. *Proc Natl Acad Sci U S A* **101:** 10596-10601

Liu ZQ, Adamczyk K, Manzanares-Dauleux M, Eber F, Lucas MO, Delourme R, Chevre AM, Jenczewski E (2006) Mapping *PrBn* and other quantitative trait loci responsible for the control of homeologous chromosome pairing in oilseed rape (*Brassica napus* L.) haploids. *Genetics* **174:** 1583-1596

Lloyd AH, Milligan AS, Langridge P, Able JA (2007) *TaMSH7*: A cereal mismatch repair gene that affects fertility in transgenic barley (*Hordeum vulgare* L.). *BMC Plant Biol* **7**

Lynn A, Soucek R, Borner GV (2007) ZMM proteins during meiosis: Crossover artists at work. *Chromosome Res* **15:** 591-605

Macaisne N, Novatchkova M, Peirera L, Vezon D, Jolivet S, Froger N, Chelysheva L, Grelon M, Mercier R (2008) SHOC1, an XPF endonuclease-related protein, is essential for the formation of class I meiotic crossovers. *Curr Biol* **18:** 1432-1437

Maleck K, Levine A, Eulgem T, Morgan A, Schmid J, Lawton KA, Dangl JL, Dietrich RA (2000) The transcriptome of *Arabidopsis thaliana* during systemic acquired resistance. *Nat Genet* **26:** 403-410

Martinez-Perez E, Mara Schvarzstein E, Barroso C, Lightfoot J, Dernburg AF, Villeneuve AM (2008) Crossovers trigger a remodeling of meiotic chromosome axis composition that is linked to two-step loss of sister chromatid cohesion. *Genes Dev* **22:** 2886-2901

Martinez-Perez E, Moore G (2008) To check or not to check? The application of meiotic studies to plant breeding. *Curr Opin Plant Biol* **11:** 222-227

Martinez-Perez E, Shaw P, Moore G (2001) The *Ph1* locus is needed to ensure specific somatic and meiotic centromere association. *Nature* **411:** 204-207

Martinez M, Cunado N, Carcelen N, Romero C (2001) The *Ph1* and *Ph2* loci play different roles in the synaptic behaviour of hexaploid wheat *Triticum aestivum. Theor Appl Genet* **103:** 398-405

Masterson J (1994) Stomatal size in fossil plants - evidence for polyploidy in majority of angiosperms. *Science* **264:** 421-424

Mata J, Lyne R, Burns G, Bahler J (2002) The transcriptional program of meiosis and sporulation in fission yeast. *Nat Genet* **32:** 143-147

Mazina OM, Mazin AV, Nakagawa T, Kolodner RD, Kowalczykowski SC (2004) Saccharomyces cerevisiae MER3 helicase stimulates 3 '-5 ' Heteroduplex extension by Rad51: Implications for crossover control in meiotic recombination. *Cell* **117:** 47-56

McLeish J, Snoad B (1958) *Looking at chromosomes*: Macmillan and company limited. pp 48-69.

Mello-Sampayo T (1971) Genetic regulation of meiotic chromosome pairing by chromosome 3D of *Triticum aestivum. Nat New Biol* **230:** 22-23

Mello-Sampayo T (1972) Compensated monosomic 5B-trisomic 5A plants in tetraploid wheat. *Can J Genet Cytol* **14:** 463-475

Mello-Sampayo T, Canas A (1973) Suppressors of meiotic chromosome pairing in common wheat. *Proc 4th Int Wheat Genet Symp* **Mo. Agric. Exp. Stn., Columbia:** 706-713

Mercier R, Armstrong SJ, Horlow C, Jackson NP, Makaroff CA, Vezon D, Pelletier G, Jones GH, Franklin FCH (2003) The meiotic protein SWI1 is required for axial element formation and recombination initiation in Arabidopsis. *Development* **130:** 3309-3318

Mercier R, Grelon M (2008) Meiosis in plants: ten years of gene discovery. *Cytogenet Genome Res* **120:** 281-290

Mercier R, Grelon M, Vezon D, Horlow C, Pelletier G (2001) How to characterize meiotic functions in plants? *Biochimie* **83:** 1023-1028

Mercier R, Jolivet S, Vezon D, Huppe E, Chelysheva L, Giovanni M, Nogue F, Doutriaux MP, Horlow C, Grelon M *et al.* (2005) Two meiotic crossover classes cohabit in Arabidopsis: One is dependent on MER3, whereas the other one is not. *Curr Biol* **15:** 692-701

Mette MF, Aufsatz W, van der Winden J, Matzke MA, Matzke AJM (2000) Transcriptional silencing and promoter methylation triggered by double-stranded RNA. *Embo Journal* **19:** 5194-5201

Meyer GF (1960) The fine structure of spermatocyte nuclei of *Drosophila melanogasta. Proc Eur Reg Conf Electron Micros* **2:** 951-954

Moolhuijzen P, Dunn DS, Bellgard M, Carter M, Jia J, Kong X, Gill BS, Feuillet C, Breen J, Appels R (2007) Wheat genome structure and function: genome sequence data and the International Wheat Genome Sequencing Consortium. *Aust J Agric Res* **58:** 470-475

Nabeshima K, Villeneuve AM, Hillers KJ (2004) Chromosome-wide regulation of meiotic crossover formation in *Caenorhabditis elegans* requires properly assembled chromosome axes. *Genetics* **168:** 1275-1292

Nakagawa T, Ogawa H (1999) The Saccharomyces cerevisiae MER3 gene, encoding a novel helicase-like protein, is required for crossover control in meiosis. *Embo Journal* **18:** 5714-5723

Namekawa SH, Iwabata K, Sugawara H, Hamada FN, Koshiyama A, Chiku H, Kamada T, Sakaguchi K (2005) Knockdown of *LIM15/DMC1* in the mushroom *Coprinus cinereus* by double-stranded RNA-mediated gene silencing. *Microbiology* **151:** 3669-3678

Napoli C, Lemieux C, Jorgensen R (1990) Introduction of a chimeric chalcone synthase gene into petunia results in reversible co-suppression of homologous genes in trans. *Plant Cell* **2:** 279-289

Nicolas SD, Leflon M, Liu Z, Eber F, Chelysheva L, Coriton O, Chevre AM, Jenczewski E (2008) Chromosome 'speed dating' during meiosis of polyploid Brassica hybrids and haploids. *Cytogenet Genome Res* **120:** 331-338

Nonomura KI, Morohoshi A, Nakano M, Eiguchi M, Miyao A, Hirochika H, Kurata N (2007) A germ cell-specific gene of the ARGONAUTE family is essential for the progression of premeiotic mitosis and meiosis during sporogenesis in rice. *Plant Cell* **19:** 2583-2594

Nonomura KI, Nakano M, Eiguchi M, Suzuki T, Kurata N (2006) PAIR2 is essential for homologous chromosome synapsis in rice meiosis I. *J Cell Sci* **119:** 217-225

Nonomura KI, Nakano M, Murata K, Miyoshi K, Eiguchi M, Miyao A, Hirochika H, Kurata N (2004) An insertional mutation in the rice PAIR2 gene, the ortholog of Arabidopsis ASY1, results in a defect in homologous chromosome pairing during meiosis. *Molecular Genetics And Genomics* **271:** 121-129

Obmolova G, Ban C, Hsieh P, Yang W (2000) Crystal structures of mismatch repair protein MutS and its complex with a substrate DNA. *Nature* **407:** 703-710

Okamoto M (1957) Asynaptic effect of chromosome V. *Wheat Inf Serv* **5:** 6

Olson LW, Eden U, Egel-Mitani M, Egel R (1978) Asynaptic meiosis in fission yeast? *Hereditas* **89:** 189–199

Pang ALY, Johnson W, Ravindranath N, Dym M, Rennert OM, Chan WY (2006) Expression profiling of purified male germ cells: stage-specific expression patterns related to meiosis and postmeiotic development. *Physiol Genomics* **24:** 75-85

Pastinen T, Kurg A, Metspalu A, Peltonen L, Syvanen AC (1997) Minisequencing: A specific tool for DNA analysis and diagnostics on oligonucleotide arrays. *Genome Res* **7:** 606-614

Pastinen T, Raitio M, Lindroos K, Tainola P, Peltonen L, Syvanen AC (2000) A system for specific, high-throughput genotyping by allele-specific primer extension on microarrays. *Genome Res* **10:** 1031-1042

Paux E, Roger D, Badaeva E, Gay G, Bernard M, Sourdille P, Feuillet C (2006) Characterizing the composition and evolution of homoeologous genomes in hexaploid wheat through BAC-end sequencing on chromosome 3B. *Plant J* **48:** 463-474

Paux E, Sourdille P, Salse J, Saintenac C, Choulet F, Leroy P, Korol A, Michalak M, Kianian S, Spielmeyer W *et al.* (2008) A physical map of the 1-gigabase bread wheat chromosome 3B. *Science* **322:** 101-104

Pawlowski WP, Golubovskaya IN, Timofejeva L, Meeley RB, Sheridan WF, Cande WZ (2004) Coordination of meiotic recombination, pairing, and synapsis by PHS1. *Science* **303:** 89-92

Pellegrineschi A, Noguera LM, Skovmand B, Brito RM, Velazquez L, Salgado MM, Hernandez R, Warburton M, Hoisington D (2002) Identification of highly transformable wheat genotypes for mass production of fertile transgenic plants. *Genome* **45:** 421-430

Prieto P, Moore G, Reader S (2005) Control of conformation changes associated with homologue recognition during meiosis. *Theor Appl Genet* **111:** 505-510

Primig M, Williams RM, Winzeler EA, Tevzadze GG, Conway AR, Hwang SY, Davis RW, Esposito RE (2000) The core meiotic transcriptome in budding yeasts. *Nat Genet* **26:** 415-423

Puizina J, Siroky J, Mokros P, Schweizer D, Riha K (2004) Mre11 deficiency in Arabidopsis is associated with chromosomal instability in somatic cells and Spo11-dependent genome fragmentation during meiosis. *Plant Cell* **16:** 1968-1978

Quarrie SA, Steed A, Calestani C, Semikhodskii A, Lebreton C, Chinoy C, Steele N, Pljevljakusic D, Waterman E, Weyen J *et al.* (2005) A high-density genetic map of hexaploid wheat (*Triticum aestivum* L.) from the cross Chinese Spring X SQ1 and its use to compare QTLs for grain yield across a range of environments. *Theor Appl Genet* **110:** 865-880

Rajhathy T, Thomas H (1972) Genetic control of chromosome pairing in hexaploid oats. *Nature New Biol* **239:** 217–219

Rasmussen SW (1973) Ultrastructural studies of spermatogenesis in *Drosophila melanogaster*. *Meigen Z Zellforsch Mikrosk Anat* **140:** 125–144

Redon R, Ishikawa S, Fitch KR, Feuk L, Perry GH, Andrews TD, Fiegler H, Shapero MH, Carson AR, Chen WW *et al.* (2006) Global variation in copy number in the human genome. *Nature* **444:** 444-454

Reinke V, Smith HE, Nance J, Wang J, Van Doren C, Begley R, Jones SJM, Davis EB, Scherer S, Ward S *et al.* (2000) A global profile of germline gene expression in *C. elegans*. *Mol Cell* **6:** 605-616

Reyesvaldes MH, Stelly DM (1995) A maximum-likelihood algorithm for genome mapping of cytogenetic loci from meiotic configuration data. *Proc Natl Acad Sci U S A* **92:** 9824-9828

Riley R, Chapman C, Kimber G (1960) Position of the gene determining the diploid-like meiotic behaviour of wheat. *Nature* **186:** 259-260

Riley R, Chapman V (1958) Genetic control of the cytologically diploid behaviour of hexaploid wheat. *Nature* **182:** 713-715

Riley R, Chapman V, Young R, Belfield A (1966) Control of meiotic chromosome pairing by the chromosomes of homoeologous group 5 of *Triticum aestivum*. . *Nature* **212:** 1475-1477

Rockett JC, Hellmann GM (2004) Confinning microarray data - is it really necessary? *Genomics* **83:** 541-549

Rockmill B, Fung JC, Branda SS, Roeder GS (2003) The Sgs1 helicase regulates chromosome synapsis and meiotic crossing over. *Curr Biol* **13:** 1954-1962

Ross KJ, Fransz P, Armstrong SJ, Vizir I, Mulligan B, Franklin FCH, Jones GH (1997) Cytological characterization of four meiotic mutants of Arabidopsis isolated from T-DNA-transformed lines. *Chromosome Res* **5:** 551-559

Ross KJ, Fransz P, Jones GH (1996) A light microscopic atlas of meiosis in *Arabidopsis thaliana*. *Chromosome Res* **4:** 507-516

Rubin-Bejerano I, Sagee S, Friedman O, Pnueli L, Kassir Y (2004) The in vivo activity of Ime1, the key transcriptional activator of meiosis-specific genes in *Saccharomyces cerevisiae*, is inhibited by the cyclic AMP protein kinase A signal pathway through the glycogen synthase kinase 3-beta homolog Rim11. *Mol Cell Biol* **24:** 6967-6979

Samson SF, Brunaud V, Balzergue S, Dubreucq B, Lepiniec L, Pelletier G, Caboche M, A. L (2002) FLAGdb/FST: a database of mapped flanking insertion sites (FSTs) of *Arabidopsis thaliana* T-DNA transformants. *Nucleic Acids Res* **30:** 94-97

Sanchez-Moran E, Benavente E, Orellana J (2001) Analysis of karyotypic stability of *homoeologous pairing* (*ph*) mutants in allopolyploid wheats. *Chromosoma* **110:** 371-377

Schena M (2003) *Microarray analysis*: Wiley-Liss.

Schena M, Shalon D, Davis RW, Brown PO (1995) Quantitative monitoring of gene expression patterns with a complementary DNA microarray. *Science* **270:** 467-470

Schena M, Shalon D, Heller R, Chai A, Brown PO, Davis RW (1996) Parallel human genome analysis: Microarray-based expression monitoring of 1000 genes. *Proc Natl Acad Sci U S A* **93:** 10614-10619

Schlecht U, Demougin P, Koch R, Hermida L, Wiederkehr C, Descombes P, Pineau C, Jegou B, Primig M (2004) Expression profiling of mammalian male meiosis and

gametogenesis identifies novel candidate genes for roles in the regulation of fertility. *Mol Biol Cell* **15:** 1031-1043

Schlecht U, Primig M (2003) Mining meiosis and gametogenesis with DNA microarrays. *Reproduction* **125:** 447-456

Schmid M, Davison TS, Henz SR, Pape UJ, Demar M, Vingron M, Scholkopf B, Weigel D, Lohmann JU (2005) A gene expression map of *Arabidopsis thaliana* development. *Nat Genet* **37:** 501-506

Sears E (1954) The aneuploids of common wheat. *Mo Agric Exp Stn Res Bull 572***:** 1-58

Sears E (1976) Genetic control of chromosome pairing in wheat. *Annu Rev Genet* **10:** 31-51

Sears E (1977) An induced mutant with homoeologous pairing in common wheat. *Can J Genet Cytol* **19:** 585–593

Sears E, Okamoto M (1958) Intergenomic chromosome relationships in hexaploid wheat. *Int Proc 10th Int Cong Genet* **2:** 258-259

Sears ER (1982) A wheat mutation conditioning an intermediate level of homoeologous chromosome pairing. *Can J Genet Cytol* **24:** 715-719

Sessions A, Burke E, Presting G, Aux G, McElver J, Patton D, Dietrich B, Ho P, Bacwaden J, Ko C *et al.* (2002) A high-throughput Arabidopsis reverse genetics system. *Plant Cell* **14:** 2985-2994

Shinohara M, Oh SD, Hunter N, Shinohara A (2008) Crossover assurance and crossover interference are distinctly regulated by the ZMM proteins during yeast meiosis. *Nat Genet* **40:** 299-309

Shippy R, Sendera TJ, Lockner R, Palaniappan C, Kaysser-Kranich T, Watts G, Alsobrook J (2004) Performance evaluation of commercial short-oligonucleotide microarrays and the impact of noise in making cross-platform correlations. *BMC Genomics* **5**

Siaud N, Dray E, Gy I, Gerard E, Takvorian N, Doutriaux MP (2004) Brca2 is involved in meiosis in Arabidopsis thaliana as suggested by its interaction with Dmc1. *Embo Journal* **23:** 1392-1401

Smyth GK, Speed T (2003) Normalization of cDNA microarray data. *Methods* **31:** 265-273

Snowden T, Acharya S, Butz C, Berardini M, Fishel R (2004) hMSH4-hMSH5 recognizes Holliday junctions and forms a meiosis-specific sliding clamp that embraces homologous chromosomes. *Mol Cell* **15:** 437-451

Sorrells ME, La Rota M, Bermudez-Kandianis CE, Greene RA, Kantety R, Munkvold JD, Miftahudin, Mahmoud A, Ma XF, Gustafson PJ *et al.* (2003) Comparative DNA sequence analysis of wheat and rice genomes. *Genome Res* **13:** 1818-1827

Stacey NJ, Kuromori T, Azumi Y, Roberts G, Breuer C, Wada T, Maxwell A, Roberts K, Sugimoto-Shirasu K (2006) Arabidopsis SPO11-2 functions with SPO11-1 in meiotic recombination. *Plant J* **48:** 206-216

Storlazzi A, Tesse S, Ruprich-Robert G, Gargano S, Poggeler S, Kleckner N, Zickler D (2008) Coupling meiotic chromosome axis integrity to recombination. *Genes Dev* **22:** 796-809

Sutton T, Whitford R, Baumann U, Dong CM, Able JA, Langridge P (2003) The *Ph2* pairing homoeologous locus of wheat (*Triticum aestivum*): identification of candidate meiotic genes using a comparative genetics approach. *Plant J* **36:** 443-456

Szostak JW, Orrweaver TL, Rothstein RJ, Stahl FW (1983) The double-strand break repair model for recombination. *Cell* **33:** 25-35

Tan PK, Downey TJ, Spitznagel EL, Xu P, Fu D, Dimitrov DS, Lempicki RA, Raaka BM, Cam MC (2003) Evaluation of gene expression measurements from commercial microarray platforms. *Nucleic Acids Res* **31:** 5676-5684

The *C. elegans* Sequencing Consortium (1998) Genome sequence of the nematode *C. elegans*: A platform for investigating biology. *Science* **282:** 2012-2018

Thomas CL, Jones L, Baulcombe DC, Maule AJ (2001) Size constraints for targeting post-transcriptional gene silencing and for RNA-directed methylation in *Nicotiana benthamiana* using a potato virus X vector. *Plant J* **25:** 417-425

Tolia NH, Joshua-Tor L (2007) Slicer and the Argonautes. *Nat Chem Biol* **3:** 36-43

Trojak-Goluch A, Berbeć A (2003) Cytological investigations of the interspecific hybrids of *Nicotiana tabacum* L. × *N. glauca* Grah. *J Appl Genet* **44:** 45-54

Trojak-Goluch A, Berbeć A (2007) Meiosis and fertility in interspecific hybrids of *Nicotiana tabacum* L. x *N. glauca* Grah. and their derivatives. *Plant Breed* **126:** 201-206

Trouiller B, Schaefer DG, Charlot F, Nogué F (2006) MSH2 is essential for the preservation of genome integrity and prevents homeologous recombination in the moss Physcomitrella patens. *Nucleic Acids Res* **34:** 232-242

Tsubouchi H, Roeder GS (2003) The importance of genetic recombination for fidelity of chromosome pairing in meiosis. *Dev Cell* **5:** 915-925

Udall JA, Quijada PA, Osborn TC (2005) Detection of chromosomal rearrangements derived from homeologous recombination in four mapping populations of *Brassica napus* L. *Genetics* **169:** 967-979

Vafaie-Tabar M, Chandrashekaran S (2007) Meiosis in a triploid hybrid of *Gossypium*: high frequency of secondary bipolar spindles at metaphase II. *J Genet* **86:** 45-49

van't Veer LJ, Dai HY, van de Vijver MJ, He YDD, Hart AAM, Mao M, Peterse HL, van der Kooy K, Marton MJ, Witteveen AT *et al.* (2002) Gene expression profiling predicts clinical outcome of breast cancer. *Nature* **415:** 530-536

van de Vijver MJ, He YD, van't Veer LJ, Dai H, Hart AAM, Voskuil DW, Schreiber GJ, Peterse JL, Roberts C, Marton MJ *et al.* (2002) A gene-expression signature as a predictor of survival in breast cancer. *N Engl J Med* **347:** 1999-2009

van Heemst D, Kafer E, John T, Heyting C, van Aalderen M, Zickler D (2001) BimD/SPO76 is at the interface of cell cycle progression, chromosome morphogenesis, and recombination. *Proc Natl Acad Sci U S A* **98:** 6267-6272

Vignard J (2007) Etude de fonctions clés de la recombinaison meiotique chez *Arabidopsis thaliana*. *PhD thesis***:** L'Université de Paris-Sud XI

Vignard J, Siwiec T, Chelysheva L, Vrielynck N, Gonord F, Armstrong SJ, Schlogelhofer P, Mercier R (2007) The interplay of RecA-related proteins and the MND1-HOP2 complex during meiosis in Arabidopsis thaliana. *Plos Genetics* **3:** 1894-1906

Wall AM, Riley R, Chapman C (1971a) Wheat mutants permitting homoeologous meiotic chromosome pairing. *Genet Res, Camb* **18:** 311-328

Wall AM, Riley R, Gale MD (1971b) The position of a locus on chromosome 5B of *Triticum aestivum* affecting homoeologous meiotic pairing. *Genet Res Camb* **18:** 329-339

Wan YF, Poole RL, Huttly AK, Toscano-Underwood C, Feeney K, Welham S, Gooding MJ, Mills C, Edwards KJ, Shewry PR *et al.* (2008) Transcriptome analysis of grain development in hexaploid wheat. *BMC Genomics* **9**

Wassenegger M, Heimes S, Riedel L, Sanger HL (1994) RNA-directed *de novo* methylation of genomic sequences in plants. *Cell* **76:** 567-576

Winter D, Vinegar, B, Nahal, H, Ammar, R, Wilson, GV, Provart, NJ (2007) An "Electronic Fluorescent Pictograph" browser for exploring and analyzing large-scale biological data sets. *Plos One* **2:** e718

Wu SY, Culligan K, Lamers M, Hays J (2003) Dissimilar mispair-recognition spectra of Arabidopsis DNA-mismatch-repair proteins MSH2.MSH6 (MutS alpha) and MSH2.MSH7 (MutS gamma). *Nucleic Acids Res* **31:** 6027-6034

Yu J, Hu SN, Wang J, Wong GKS, Li SG, Liu B, Deng YJ, Dai L, Zhou Y, Zhang XQ *et al.* (2002) A draft sequence of the rice genome (*Oryza sativa* L. ssp indica). *Science* **296:** 79-92

Zickler D, Kleckner N (1998) The leptotene-zygotene transition of meiosis. *Annu Rev Genet* **32:** 619-697

Zickler D, Kleckner N (1999) Meiotic chromosomes: Integrating structure and function. *Annu Rev Genet* **33:** 603-754

Zilberman D, Cao XF, Jacobsen SE (2003) ARGONAUTE4 control of locus-specific siRNA accumulation and DNA and histone methylation. *Science* **299:** 716-719

Appendix A

BLASTx results using 129 rice sequences as the queries against the non-redundant database. The annotations of the 129 rice sequences also represent the 125 wheat sequences based on analysis discussed in the Chapter 3 Addendum.

Blast Search Results:

database: nr   26/09/2008

QUERY	Length (bp)	Database match	EXP	Putative ID
consensus:Rice:OsAffx.19544.1.S1_x_at; tigr|9640.m00715;	2973	ref|NP_0010065922.1|	0	dehydration-responsive protein-related
consensus:Rice:Os.20348.1.S1_at; gb|AK066417.1;	2581	ref|NP_0010057376.1|	0	NIK1 (NSP-INTERACTING KINASE 1
consensus:Rice:OsAffx.3315.1.S1_s_at; tigr|9631.m02431;	1509	ref|NP_0010060447.1|	7.00E-83	unknown protein
consensus:Rice:Os.54526.1.S1_at; gb|AK105520.1;	1450	ref|NP_0010049387.1|	2.00E-96	polygalacturonase, putative / pectinase
consensus:Rice:Os.2319.1.S2_at; gb|AF134807.2;	3922	ref|NP_0010063545.1|	e-111	dihydroflavonol 4-reductase family / dihydrokaempferol 4-reductase family
consensus:Rice:Os.6101.1.S1_at; gb|AK106302.1;	1842	ref|NP_0010052244.1|	7.00E-87	Probable UDP-glucosyl transferase
consensus:Rice:Os.35425.1.S1_at; gb|AK067556.1;	2624	ref|NP_0010044732.1|	0	ATPase, coupled to transmembrane movement of substances
consensus:Rice:OsAffx.28544.2.S1_x_at; tigr|9635.m02165;	1290	ref|NP_0010059449.1|	e-132	chalcone synthase family protein
consensus:Rice:Os.33605.2.S1_x_at; gb|AK069643.1;	1452	ref|NP_0010043999.1|	3.00E-22	zinc finger (C3HC4-type RING finger) family protein
consensus:Rice:Os.55120.1.S1_at; gb|AK107521.1;	1750	ref|NP_0010053872.1|	2.00E-91	PAZ domain-containing protein / piwi domain-containing protein
consensus:Rice:Os.17268.1.S1_at; gb|AK104878.1;	1354	ref|NP_0010063624.1|	6.00E-99	putative peroxisomal membrane carrier protein

Consensus	Value	RefSeq	E-value	Description
consensus:Rice:OsAffx.16813.1.S1_x_at; tigr|9636.m00286;	3498	ref|NP_001060926.1	0	CYP703/CYP703A2 (CYTOCHROME P450, FAMILY 703, SUBFAMILY A, POLYPEPTIDE 2)
consensus:Rice:OsAffx.16983.1.S1_at; tigr|9636.m01363;	1002	no link		No hits above cut off
consensus:Rice:Os.52786.1.S1_at; gb|AK069250.1;	1361	ref|NP_001062210.1	2.00E-60	unnamed protein product
consensus:Rice:OsAffx.28096.1.S1_at; tigr|9634.m04281;	1926	ref|NP_001058232.1	e-166	unknown protein
consensus:Rice:Os.9496.1.S1_at; gb|AK064038.1;	1307	ref|NP_001065487.1	7.00E-51	cinnamoyl-CoA reductase-related
consensus:Rice:Os.19331.1.S1_at; gb|AK071286.1;	1610	ref|NP_001055921.1	1.00E-120	MtN21 nodulin protein-like
consensus:Rice:Os.34647.1.S1_at; gb|AK070644.1;	2176	ref|NP_001056404.1	0	MAP kinase
consensus:Rice:Os.54800.1.S1_at; gb|AK106792.1;	2366	ref|NP_001058033.1	0	ABC transporter family protein
consensus:Rice:Os.52091.1.S1_at; gb|AK064698.1;	1807	ref|NP_974827.1	e-127	pectinacetylesterase family protein
consensus:Rice:Os.11558.1.S1_at; gb|AK101508.1;	1620	ref|NP_001042703.1	1.00E-60	peroxidase, putative
consensus:Rice:Os.56988.1.S1_at; gb|AK110695.1;	952	ref|NP_001051269.1	5.00E-50	minor allergen
consensus:Rice:Os.2550.1.S1_at; gb|AK109476.1;	2165	ref|NP_001064930.1	4.00E-72	unknown protein
consensus:Rice:Os.15696.1.S1_a_at; gb|AB081464.1;	1901	ref|NP_001047562.1	e-179	BETA-VPE (vacuolar processing enzyme beta); cysteine-type endopeptidase
consensus:Rice:Os.9955.1.S1_a_at; gb|AK068737.1;	1914	ref|NP_001042602.1	0	ATSK11 (Arabidopsis thaliana SHAGGY-related kinase 11);
consensus:Rice:OsAffx.7832.1.S1_at; tigr|9640.m03777;	1521	ref|NP_001067112.1	1.00E-51	unknown protein
consensus:Rice:Os.46304.1.S1_a_at; gb|CB668496;	837	no link		No hits above cut off
consensus:Rice:Os.54831.1.S1_at; gb|AK106857.1;	789	no link		No hits above cut off
consensus:Rice:OsAffx.29643.1.S1_at; tigr|9636.m04407;	429	ref|NP_001062420.1	1.00E-10	A9 protein precursor-like

consensus	ref|NP accession	E-value	Description	
consensus:Rice:Os.35089.1.S1_at; gb|AK069013.1;	ref|NP_001053131.1|	6.00E-48	CDC48-interacting UBX-domain protein	1262
consensus:Rice:Os.56156.1.S1_at; gb|AK109467.1;	ref|NP_001051964.1|	e-116	MATE efflux family protein	1597
consensus:Rice:Os.31518.1.S1_at; gb|AK107209.1;	ref|NP_001042758.1|	0	Cyclin-B1-3 (G2/mitotic-specific cyclin-B1-3)	1725
consensus:Rice:OsAffx.13955.1.S1_x_at; tigr|9632.m02290;	ref|NP_001052437.1|	e-174	4-coumarate--CoA ligase family protein / 4-coumaroyl-CoA synthase family protein	1668
consensus:Rice:Os.10860.2.S1_at; gb|AK069437.1;	ref|NP_001053351.1|	0	YSL7 (YELLOW STRIPE LIKE 7)	2127
consensus:Rice:Os.45920.1.S1_at; gb|CR281284;	ref|NP_001048679.1|	0	tubulin beta-8	1720
consensus:Rice:Os.54989.1.S1_at; gb|AK107258.1;	ref|NP_001062795.1|	4.00E-88	UBIQUITIN-CONJUGATING ENZYME 25	1620
consensus:Rice:Os.5124.1.S1_at; gb|AK070411.1;	ref|NP_001056382.1|	0	EMBRYO DEFECTIVE 2742	2540
consensus:Rice:Os.16882.1.S1_at; gb|AK121304.1;	ref|NP_001061466.1|	1.00E-47	peptidyl-prolyl cis-trans isomerase	3305
consensus:Rice:OsAffx.27333.1.S1_at; tigr|9633.m04302;	ref|NP_001044073.1|	e-128	choline kinase, putative	1059
consensus:Rice:Os.5873.1.S1_at; gb|AK100301.1;	ref|NP_001053779.1|	2.00E-34	Pspzf zinc finger protein-like	1523
consensus:Rice:Os.12268.1.S1_at; gb|AF049889.1;	ref|NP_001048259.1|	e-117	ethylene-forming enzyme	3119
consensus:Rice:OsAffx.17435.1.S1_at; gb|NM_188999.1;	ref|NP_001062236.1|	e-111	dihydroflavonol 4-reductase family / dihydrokaempferol 4-reductase family	1035
consensus:Rice:Os.470.1.S1_s_at; gb|AK121722.1;	ref|NP_001043541.1|	0	PLEIOTROPIC DRUG RESISTANCE 12	4839
consensus:Rice:Os.11107.1.S1_at; gb|AK100744.1;	ref|NP_171649.1|	2.00E-97	UDP-glucoronosyl/UDP-glucosyl transferase family protein	1890
consensus:Rice:Os.13973.3.S1_at; gb|AK060575.1;	ref|NP_001055303.1|	e-108	protein phosphatase 2C, putative	1931
consensus:Rice:Os.3422.1.S1_at; gb|AK063598.1;	ref|NP_001051822.1|	0	actin 7	1711
consensus:Rice:Os.46383.2.A1_s_at; gb|CB652033;	ref|NP_001047825.1|	2.00E-68	phosphoribulokinase precursor	838

Consensus ID	Score	Accession	E-value	Description
consensus:Rice:Os.8511.1.S1_s_at; gb|AK100972.1;	1744	ref|NP_001051991.1|	2.00E-91	cytochrome P450, family 93
consensus:Rice:Os.28096.1.S1_at; gb|AK060834.1;	1759	ref|NP_001055991.1|	e-155	CALRETICULIN 3; calcium ion binding
consensus:Rice:Os.38001.1.A1_at; gb|AK073434.1;	2291	ref|NP_001048588.1|	e-133	leucine-rich repeat family protein
consensus:Rice:Os.11219.1.S1_at; gb|BP184466;	1744	ref|NP_001044754.1|	2.00E-42	Histone H2B
consensus:Rice:Os.46325.1.A1_at; gb|AK120658.1;	1947	ref|NP_001042129.1|	e-147	zinc finger (C3HC4-type RING finger) family
consensus:Rice:Os.4731.1.A1_s_at; gb|CB661833;	1358	gb|EAY96137.1|	1.00E-50	unknown protein
consensus:Rice:Os.18877.1.S1_at; gb|AK060336.1;	1167	ref|NP_001055547.1|	e-109	ISOPENTENYL DIPHOSPHATE ISOMERASE 1
consensus:Rice:Os.15571.1.S1_at; gb|AK063753.1;	1482	ref|NP_001067285.1|	e-159	pyruvate dehydrogenase E1 beta subunit
consensus:Rice:Os.9110.1.S1_at; gb|AK071305.1;	1755	ref|NP_001063681.1|	e-160	thioesterase family protein
consensus:Rice:Os.18206.1.S1_at; gb|AK062929.1;	635	ref|NP_001044595.1|	3.00E-43	60S ribosomal protein L30
consensus:Rice:OsAffx.15017.1.S1_at; tigr|9633.m03610;	2094	ref|NP_187577.1|	0	putative minichromosome maintenance (MCM) protein
consensus:Rice:Os.2241.1.S1_a_at; gb|AK059818.1;	1184	ref|NP_001044339.1|	5.00E-36	Glutathione S-transferase
consensus:Rice:Os.17881.1.S1_at; gb|AK100467.1;	2537	ref|NP_001062612.1|	0	coatomer protein complex, subunit alpha, putative
consensus:Rice:Os.18583.1.S1_at; gb|AK073783.1;	2092	ref|NP_001042118.1|	e-116	hypothetical protein
consensus:Rice:Os.14415.1.S1_a_at; gb|AK072689.1;	3169	ref|NP_001050995.1|	0	LOX5; lipoxygenase
consensus:Rice:Os.21075.1.S1_at; gb|AK110878.1;	1982	ref|NP_001066285.1|	e-179	putative growth regulator protein
consensus:Rice:Os.53929.1.S1_s_at; gb|AK100884.1;	2053	ref|NP_001055220.1|	0	NADH dehydrogenase
consensus:Rice:Os.4421.1.S1_at; gb|AK102494.1;	2226	ref|NP_001056550.1|	0	SKU5 (skewed 5); copper ion binding

| Consensus	Number	Accession	E-value	Description
consensus:Rice:Os.11631.1.S1_at; gb|AK120783.1;	2021	ref|NP_001057353.1	e-113	aspartyl protease family protein
consensus:Rice:OsAffx.17580.1.S1_at; tigr|9637.m00423;	1266	ref|NP_001062648.1	e-138	CDC20.1; signal transducer
consensus:Rice:Os.372.1.S1_a_at; gb|AY078072.1;	1961	ref|NP_001053132.1	0	glucose-6-phosphate 1-dehydrogenase
consensus:Rice:Os.28409.5.S1_at; gb|AK104167.1;	1224	no link	9.00E-179	Arabidopsis thaliana chloroplast DNA
consensus:Rice:Os.38299.1.S1_at; gb|AK102668.1;	1461	ref|NP_001058750.1	3.00E-100	protein phosphatase 2C family protein
consensus:Rice:Os.49778.1.S1_at; gb|AB109238.1;	2180	ref|NP_001063610.1	e-174	Asynapsis 1 (ASY1)
consensus:Rice:Os.18189.1.S1_at; gb|AK073256.1;	1278	ref|NP_001047974.1	1.00E-71	Chromatin structure-remodeling complex protein BSH (Protein bushy) - (SNF5 homolog)
consensus:Rice:Os.18395.1.S1_s_at; gb|AK062516.1;	769	ref|NP_001057346.1	1.00E-27	gibberellin-responsive protein, putative
consensus:Rice:Os.8647.1.S1_at; gb|AK120851.1;	2630	ref|NP_001046976.1	2.00E-35	unknown protein
consensus:Rice:Os.51150.1.S1_s_at; gb|AK061163.1;	1329	ref|NP_001058014.1	4.00E-44	putative ethylene responsive element
consensus:Rice:OsAffx.24019.1.S1_x_at; tigr|9629.m07214;	3426	ref|NP_001045457.1	0	ATMLH1 (ARABIDOPSIS THALIANA MUTL-HOMOLOGUE 1)
consensus:Rice:OsAffx.11847.1.S1_at; tigr|9629.m07373;	831	ref|NP_001054459.1	e-104	inorganic diphosphatase/ pyrophosphatase
consensus:Rice:Os.35685.1.S1_at; gb|AK066300.1;	2681	ref|NP_001044387.1	0	glycosyl hydrolase family 3 protein
consensus:Rice:Os.15548.1.S1_at; gb|AK111670.1;	1752	ref|NP_001061119.1	e-170	transducin family protein / WD-40 repeat family protein
consensus:Rice:Os.27371.1.A1_at; gb|AK065263.1;	2052	ref|NP_001056967.1	e-171	beta-glucuronidase
consensus:Rice:Os.15551.1.S1_at; gb|AK059480.1;	1369	gb|AAP88334.1	3.00E-78	unknown protein
consensus:Rice:OsAffx.15881.1.S1_at; tigr|9634.m04026;	2178	ref|NP_001058099.1	0	HOBBIT (cell division cycle protein 27)
consensus:Rice:Os.49195.1.S1_at; gb|AK103138.1;	2084	ref|NP_001049413.1	0	glycosyl hydrolase family 17 protein / beta-1,3-glucanase, putative

consensus:Rice:Os.54997.1.S1_at; gb|AK107276.1;	947	refNP_001051116.1		No hits above cut off
consensus:Rice:Os.5187.1.S1_at; gb|AK062162.1;	1115	refNP_001060690.1	2.00E-59	unknown protein
consensus:Rice:Os.27969.1.S1_at; gb|AK064894.1;	890	refNP_001057309.1	7.00E-35	Nudix hydrolase 21, chloroplast precursor
consensus:Rice:Os.53771.1.A1_at; gb|AK099930.1;	4185	refNP_001062645.1	0	nucleotide binding
consensus:Rice:Os.16956.1.S1_s_at; gb|AK103608.1;	2859	refNP_001043256.1	0	early-responsive to dehydration protein-related / ERD protein-related
consensus:Rice:Os.54158.1.S1_at; gb|AK102230.1;	2844	refNP_001056445.1	e-158	putative transposase
consensus:Rice:Os.9121.1.S1_at; gb|AK073973.1;	2957	refNP_199003.1|	e-109	POLA3/POLA4; DNA primase
consensus:Rice:Os.8979.1.S1_at; gb|AK111523.1;	1914	refNP_001064441.1	e-143	kelch repeat-containing F-box family protein
consensus:Rice:Os.51962.1.S1_at; gb|AK064417.1;	2399	refNP_001064187.1	8.00E-84	unknown protein
consensus:Rice:Os.7893.1.S1_at; gb|AK066658.1;	878	refNP_001063869.1	2.00E-30	HIGH MOBILITY GROUP B 3
consensus:Rice:Os.536.1.S1_at; gb|AK099949.1;	1436	refNP_001042042.1	3.00E-82	short-chain dehydrogenase/reductase (SDR) family protein
consensus:Rice:Os.27991.1.S1_at; gb|AK101995.1;	1745	refNP_001062946.1	e-109	HISTONE ACETYLTRANSFERASE OF THE GNAT FAMILY 2
consensus:Rice:Os.19344.1.S1_at; gb|AK068184.1;	887	refNP_001043469.1	e-31	unknown protein
consensus:Rice:Os.7698.1.S1_at; gb|AK121169.1;	744	refNP_001061171.1	8.00E-58	ATG8C (AUTOPHAGY 8C); microtubule binding
consensus:Rice:Os.9100.1.S3_at; gb|AK068222.1;	5300	refNP_001119390.1	0	binding
consensus:Rice:OsAffx.31710.1.S1_x_at; tigr|9640.m01173;	2199	refNP_201182.1|	0	DIACYLGLYCEROL KINASE 2
consensus:Rice:Os.48636.1.S1_at; gb|AK069638.1;	3449	refNP_001062293.1		No hits above cut off
consensus:Rice:OsAffx.6894.1.S1_x_at; tigr|9638.m03344;	411	refNP_001065071.1	2.00E-26	unknown protein

consensus:Rice:Os.24111.2.S1_at; gb|AK108209.1;	1051	ref|NP_001056519.1	3.00E-33	unknown protein
consensus:Rice:Os.2613.1.S1_at; gb|AF309381.1;	1250	ref|NP_001066398.1	3.00E-34	GLUTATHIONE S-TRANSFERASE 18
consensus:Rice:OsAffx.16824.1.S1_at; tigr|9636.m00365;	1556	ref|NP_001060962.1	e-139	serine/threonine-specific protein kinase-like protein
consensus:Rice:Os.10930.1.S1_at; gb|BI806747;	551	ref|NP_001047483.1	8.00E-33	phenylalanine ammonia-lyase
consensus:Rice:Os.25639.1.S1_at; gb|AK100844.1;	2227	ref|NP_001052535.1	e-178	ROTAMASE FKBP 1
consensus:Rice:Os.8463.1.S2_at; gb|AK066026.1;	4160	ref|NP_001056347.1	3.00E-88	kinase-related
consensus:Rice:Os.11668.1.S1_at; gb|AK073626.1;	991	ref|NP_001049891.1	5.00E-60	TENA/THI-4 family protein
consensus:Rice:Os.40181.2.S1_s_at; gb|NM_191744.1;	597	ref|NP_001044060.1	3.00E-83	AtRABG3a
consensus:Rice:Os.25486.1.S1_at; gb|AK103291.1;	2050	ref|NP_001044365.1	2.00E-85	unknown protein
consensus:Rice:Os.25687.1.S1_x_at; gb|AK068993.1;	2498	ref|NP_001047484.1	0	phenylalanine ammonia-lyase, putative
consensus:Rice:OsAffx.11501.1.S1_x_at; tigr|9629.m04531;	1614	ref|NP_001043779.1	2.00E-62	exonuclease-related
consensus:Rice:Os.54493.1.S1_at; gb|AK105344.1;	1608	ref|NP_001057315.1	e-155	calmodulin-binding heat-shock protein
consensus:Rice:Os.6756.1.S1_at; gb|AK072565.1;	1298	ref|NP_001062767.1	9.00E-54	unknown protein
consensus:Rice:Os.32736.1.S1_at; gb|AK103085.1;	1229	ref|NP_001051453.1	e-102	fatty acid hydroxylase-like protein
consensus:Rice:Os.12974.1.S1_at; gb|AK121422.1;	3231	ref|NP_001067910.1	0	MCM2-related protein
consensus:Rice:Os.11407.1.S1_at; gb|AK106044.1;	2198	ref|NP_001054218.1	e-142	ATPAO3 (POLYAMINE OXIDASE 3); oxidoreductase
consensus:Rice:Os.24751.1.S1_at; gb|AK071844.1;	1473	ref|NP_001059405.1	5.00E-91	S-adenosylmethionine carrier
consensus:Rice:Os.7111.1.S1_x_at; gb|AK106228.1;	460	ref|NP_001047085.1		No hits above cut off

consensus		ref	E-value	Description
consensus:Rice:Os.37571.1.S1_at; gb|AK063639.1;	1001	ref|NP_0010062070.1|		No hits above cut off
consensus:Rice:Os.49084.1.S1_at; gb|AK064752.1;	1885	ref|NP_0010057133.1|	e-166	putative NADH dehydrogenase
consensus:Rice:Os.27818.1.S1_at; gb|AK073491.1;	2110	ref|NP_0010061433.1|	e-53	WRKY4 (WRKY DNA-binding protein 4); transcription factor
consensus:Rice:Os.25780.1.S1_s_at; gb|AK067751.1;	2640	ref|NP_0010054078.1|	3.00E-50	zinc finger (C3HC4-type RING finger) family protein
consensus:Rice:Os.53107.1.S1_at; gb|AK070852.1;	1188	ref|NP_0010046689.1|	3.00E-43	unknown protein
consensus:Rice:Os.4660.1.S1_s_at; gb|AK066494.1;	559	ref|NP_0010049319.1|		No hits above cut off
consensus:Rice:OsAffx.26540.1.S1_s_at; tigr|9632.m04809;	588	ref|NP_0010047768.1|	7.00E-24	RHA3B (RING-H2 finger A3B); protein binding / zinc ion binding
consensus:Rice:Os.8207.1.S1_at; gb|CB096959;	2696	ref|NP_0010050457.1|	0	tRNA-splicing endonuclease positive effector-related
consensus:Rice:Os.10258.1.S1_at; gb|AK072446.1;	2890	ref|NP_0010045208.1|	e-48	CPR5 (CONSTITUTIVE EXPRESSION OF PR GENES 5)
consensus:Rice:Os.5655.1.S1_at; gb|AK101293.1;	1387	ref|NP_0010050402.1|	e-132	inosine-uridine preferring nucleoside hydrolase family protein

Appendix B

Genomic DNA was extracted from a set of 21 nullisomic-tetrasomic wheat plants and wild-type (cv. Chinese Spring), digested and then blotted onto a nylon membrane by Margaret Pallotta (ACPFG, Adelaide, Australia). The resulting autoradiographs from Southern blot hybridisations with various radioactively labelled probes indicate on which chromosome(s) a particular transcript/gene is located by the absence of a band in the appropriate nullisomic line. The target transcripts/probes for each autoradiograph are written below the appropriate figure. Not all transcripts mapped (and reported in Chapter 3 Addendum) are shown. Red circles indicate absence of a band.
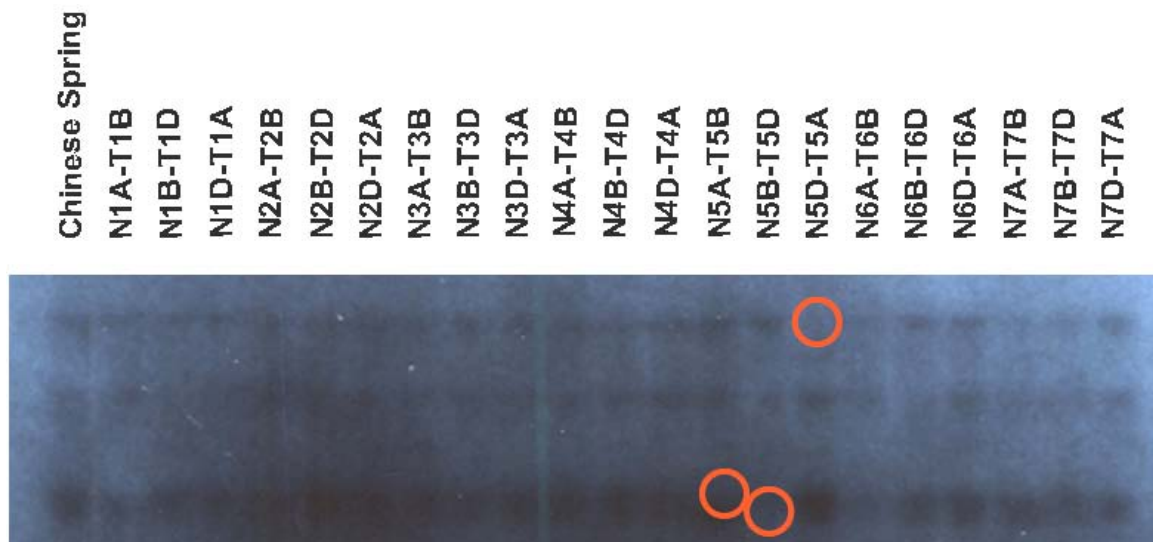
TaMSH6

TaRAD51C
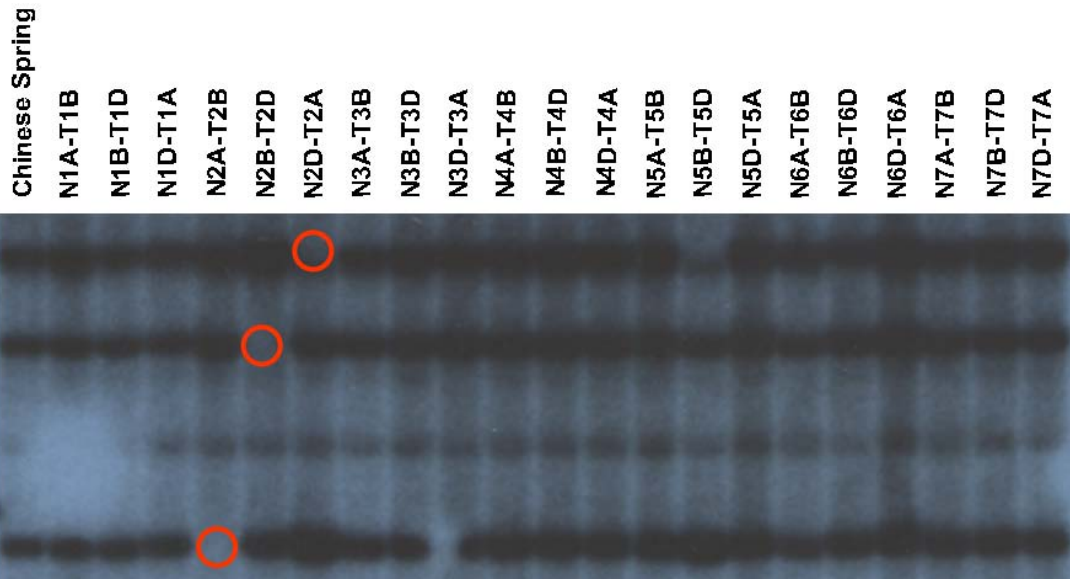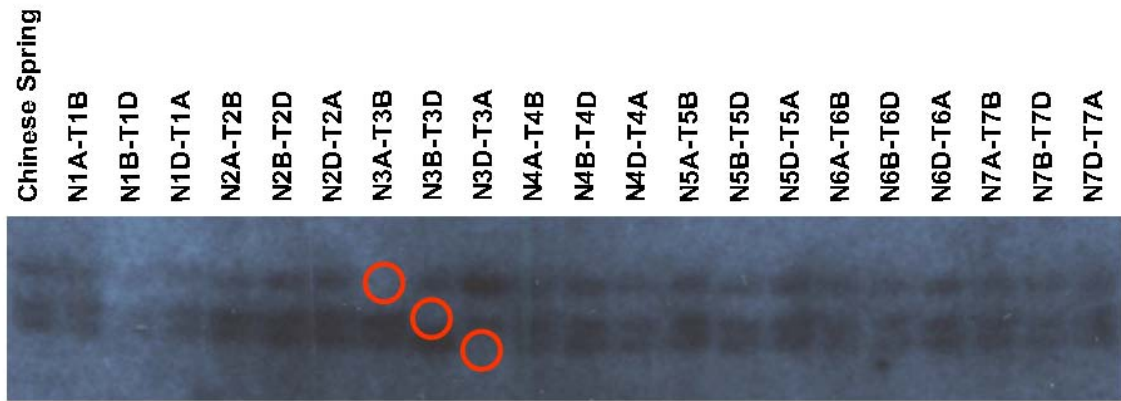
TaWMC3

TaWMC4

TaWMC5

TaWMC6

Appendix C

Author declaration permitting the use of the publication, Crismani *et al.* (2006) Microarray expression analysis of meiosis and microsporogenesis in hexaploid bread wheat. *BMC Genomics* 7, in this thesis.

I the undersigned give permission for the paper;

Crismani W, Baumann U, Sutton T, Shirley N, Webster T, Spangenberg G, Langridge P, Able JA (2006) Microarray expression analysis of meiosis and microsporogenesis in hexaploid bread wheat. *BMC Genomics* **7**

to be included in the thesis of Wayne Matthew Crismani for the academic program, Ph.D

in Sciences at the University of Adelaide, Australia.

The statement of contributions below is sourced directly from the relevant publication.

Authors' contributions

WC conducted the research, analyzed the data and drafted the manuscript.

UB and TS designed the research, analyzed the data and drafted the manuscript.

NS, TW and GS contributed analytical tools and analyzed the data.

PL designed the research and drafted the manuscript.

JAA designed and conducted the research, analyzed the data and drafted the manuscript.

All authors read and approved the final manuscript.

Appendix D

<u>RE: Looking at Chromosomes by McLeish, J. and Snoad, B, use of 1 figure</u>

It is our policy to grant permission free of charge to students who are looking to quote excerpts from our titles for strictly academic purposes. This is subject to the following conditions:

- Your work must be of a entirely academic nature; no commercial publication of the work at hand is allowed;

- You must acknowledge our edition directly below the reproduced material as follows : «author/editor, title, year of publication, publisher (as it appears on our copyright page) reproduced with permission of Palgrave Macmillan. This material may not be copied or reproduced without permission from Palgrave Macmillan»

Your thesis may be reproduced through academic aggregators but should it become eligible for commercial publication at a later stage, you will need to re-apply for our permission.

Best wishes

Lauren Russell
Rights Assistant
Palgrave Macmillan
Houndmills
Basingstoke
Hampshire
RG21 6XS
+44 (0)1256 329242 Ext. 3518
fax +44(0)1256 353774